ISBN 978-82-326-6937-0 (printed ver.)
ISBN 978-82-326-5327-0 (electronic ver.)
ISSN 1503-8181 (printed ver.)
ISSN 2703-8084 (electronic ver.)

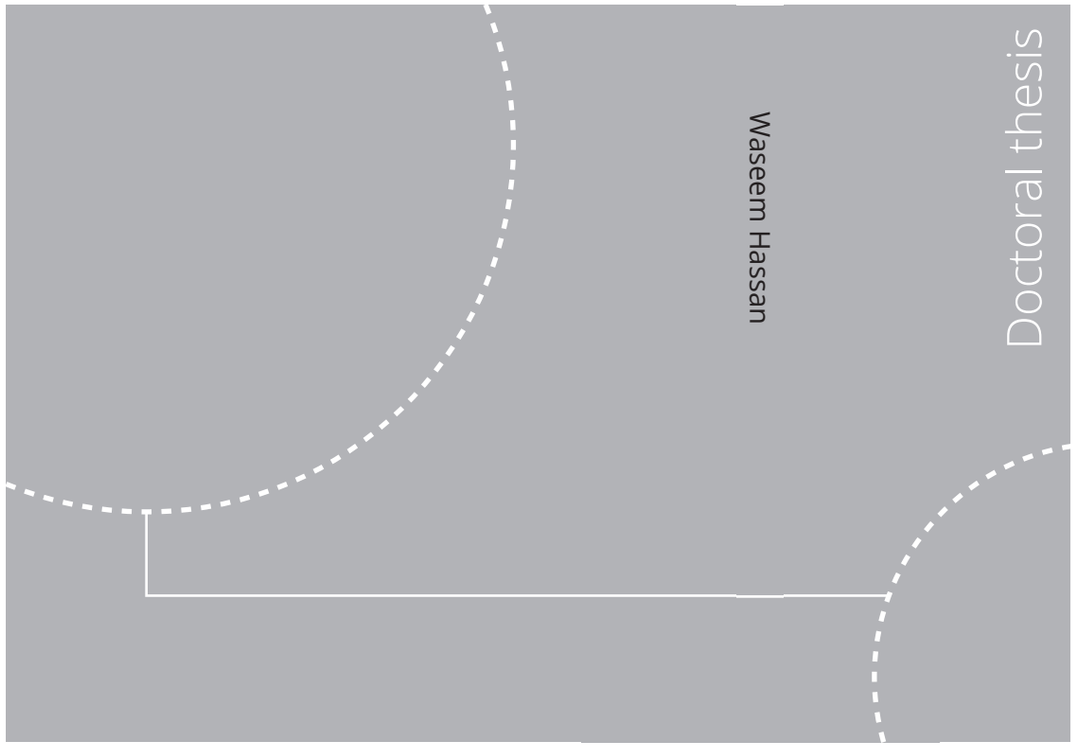

Doctoral theses at NTNU, 2021:259

Waseem Hassan

Fish on the net

Acoustic Doppler telemetry and remote monitoring of individual fish in aquaculture

NTNU
Norwegian University of
Science and Technology
Thesis for the degree of
Philosophiae Doctor
Faculty of Information Technology
and Electrical Engineering
Department of Engineering Cybernetics

NTNU
Norwegian University of
Science and Technology

Doctoral theses at NTNU, 2021:259

NTNU

NTNU
Norwegian University of
Science and Technology

Waseem Hassan

Fish on the net

Acoustic Doppler telemetry and remote monitoring of individual fish in aquaculture

Thesis for the degree of Philosophiae Doctor

Trondheim, September 2021

Norwegian University of Science and Technology
Faculty of Information Technology
and Electrical Engineering
Department of Engineering Cybernetics

NTNU
Norwegian University of
Science and Technology

NTNU
Norwegian University of Science and Technology

Thesis for the degree of Philosophiae Doctor

Faculty of Information Technology
and Electrical Engineering
Department of Engineering Cybernetics

ISBN 978-82-326-6937-0 (printed ver.)
ISBN 978-82-326-5327-0 (electronic ver.)
ISSN 1503-8181 (printed ver.)
ISSN 2703-8084 (electronic ver.)

ITK-report: 2021-4-W

2021:259 Waseem Hassan

Printed by Skipnes Kommunikasjon AS

Summary

The two main contributions of this thesis are the Internet of Fish (IoF) concept and a novel fish swimming speed measurement principle. The IoF concept is a reliable communication protocol which could relay acoustic telemetry data over long distances at very low power consumption in real-time. The speed computation algorithm provides a novel and robust approach for measuring instantaneous swimming speed of individual fish by using Doppler analysis. The methods developed in this study were tested in commercial scale marine farms for Atlantic salmon (*Salmo salar* L.) production, however they could also be applied for other species farmed in marine environment and even in scientific studies of wild fish.

Norway is the world's largest producer of farmed Atlantic salmon and a global leader in marine farming. An important goal for the Norwegian farming industry is to have sustained growth with an improved fish welfare and environmental footprint. This could be achieved via novel technological solutions such as the Precision Fish Farming (PFF) concept. Whereas technology is innovating different aspects of farm management operations, monitoring fish underwater poses unique challenges due to lack of direct observations. This is further exacerbated by the recently growing number of more exposed farming sites.

Acoustic biotelemetry has been reliably used for individual fish monitoring in the underwater environment. Basic building blocks of an acoustic telemetry system are a transmitter tag and one or more matched receivers for receiving and decoding telemetry data sent by the tag. Commercially available telemetry receivers are normally logging receivers and provide no real-time support to the telemetry data. Cabled and existing wireless or cellular protocols are often used to address the problem of real-time support. However, such solutions suffer from the issues of limited coverage area and offer poor energy efficiency, respectively. This was addressed by establishing the IoF concept in this study. The IoF provides long range, low power real-time support to the telemetry receivers. The IoF concept was realised by developing a dedicated surface communication module and was

also extended for real-time fish positioning. A Quality of Service (QoS) of more than 90% proved the IoF concept as a reliable communication protocol.

Fish swimming is an important indicator of fish behaviour, growth and energy expenditure. It becomes more relevant for assessing fish welfare at exposed farming sites where fish might face strong currents. Currently, there exists no solution for quantifying swimming speed of individual free-ranging fish. A novel method for measuring free-ranging individual fish swimming speed using Doppler analysis was developed and demonstrated in a commercial scale fish farm. The method is elegant in the sense that the speed measurement can be piggybacked onto the existing Pulse Position Modulation (PPM) signal sent by a tag. In essence, this means that the new speed measurement data value could be extracted from the existing acoustic carrier wave without significantly modifying the telemetry system. Although requiring significant signal processing capacity in the acoustic receiver, it remains much easier to expand a receiver with additional resources with respect to computational capacity and energy. The proposed speed measurement algorithm was tested via a series of experiments ranging from emulated motions in a lab to a marine farm with fish tagged with acoustic transmitter inside a fully stocked commercial sea cage. A relative rms error of less than 10% of the overall speed range was achieved in all the experimental stages, affirming that the proposed method is promising and could be used for *in-situ* swimming speed measurement of an individual free-ranging fish.

Preface

This thesis is submitted in partial fulfilment of the requirements for the degree of Philosophiae Doctor (Ph.D.) at NTNU - the Norwegian University of Science and Technology. This work has been performed at the department of Engineering Cybernetics (ITK) under the supervision of Associate Professor Jo Arve Alfredsen and Associate Professor Martin Føre and was undertaken from 2017 to 2020. Funding has been provided by the Norwegian Research Council through the Centre for research-based innovation in Exposed Aquaculture Technology (grant number 237790) led by SINTEF Ocean with NTNU as cooperating partner and in parts by the "CycLus" R&D project (CycLus NTF36/37).

Acknowledgements

First and foremost, I am extremely grateful to ALLAH (*SWT*) for giving me the courage and strength to complete this thesis and my doctoral studies. I would like to express my deepest appreciation for my supervisors Jo Arve Alfredsen and Martin Føre, for their constructive criticism, support, advise and for keeping me motivated at the times when things were not going as planned. I am also thankful to all of my colleagues and friends at the Department of Engineering Cybernetics, especially Leif Erik Andersson and Kristbjörg Edda Jónsdóttir, for the discussions, coffee breaks, playing klask and social activities. It would have been impossible to spend four years without my dear friends in Trondheim. The time we spent together in making meals, playing games, watching movies and going for walks is memorable. Many thanks to Usman Shoukat and Marie Curtet. I must also thank Muhammad Abdullah bin Azhar, for his invaluable friendship and for always helping me with his advice. I would like to extend my gratitude to Henning Andre Urke, John Birger Ulvund and Magnus Oshaug Pedersen for their support with my field experiments. A special thanks to Hans Vanhauwaert Bjelland, manager Exposed Aquaculture Operations. I gratefully acknowledge the assistance provided throughout the four years of my PhD by the people at ITK administration and workshop. Finally, the completion of my dissertation would not have

been possible without the support of my parents, wife and sisters. I have been able to achieve this feat because of you Ammi and Abbu. I hope Ammi, that you would be satisfied now that I have finished studying and have started working properly. With the completion of my doctoral studies, an important personal goal has been achieved. I would like to remind myself of something more important about achieving goals with a poetic verse from Allama Muhammad Iqbal.

تُو رہ نوردِ شوق ہے، منزل نہ کر قبول
لیلیٰ بھی ہم نشیں ہو تو محمل نہ کر قبول

To my parents, wife and sisters...

Contents

List of Tables

List of Figures

Chapter 1

Introduction

1.1 Background

Human population is growing at an unprecedented rate and is expected to reach 9 billion by the mid-21st century. To achieve zero hunger by 2030, the UN 2030 Sustainable Growth Agenda prioritises sustainable use of the ocean resources (FAO, 2020). Whereas the global capture fisheries production has levelled out at approximately 90 million tonnes per year around 1990, the global aquaculture production is increasing and is expected to grow further in the future (Fig. 1.1).

Aquaculture is defined as the controlled cultivation of living aquatic organisms. This covers both plants and animals, in fresh, brackish and marine water. Mariculture is a type of aquaculture in which organisms are cultivated in marine environment or seawater. While mariculture production only represents a small part of the overall global aquaculture production volume, its share in terms of value is larger (FAO, 2020; Asche and Bjørndal, 2011).

Salmon farming is an important high-valued segment in mariculture. With a production share of 77.9%, Atlantic salmon (*Salmo salar* L.) is the most dominant salmon species farmed at commercial level (Asche et al., 2013). Atlantic salmon constituted 4% of the global mariculture production (by volume) in 2016 (FAO, 2020). Atlantic salmon farming in Norway started in the 1960s and ever since then the industry has seen a very strong growth, making Norway the largest producer of Atlantic salmon, accounting for more than 50% of the total global salmon production (Fig. 1.2). Being a high-end food item and with a relatively small share in the overall global seafood production, Atlantic salmon farming cannot help directly in achieving the UN's zero hunger goal, nevertheless the technological solutions de-

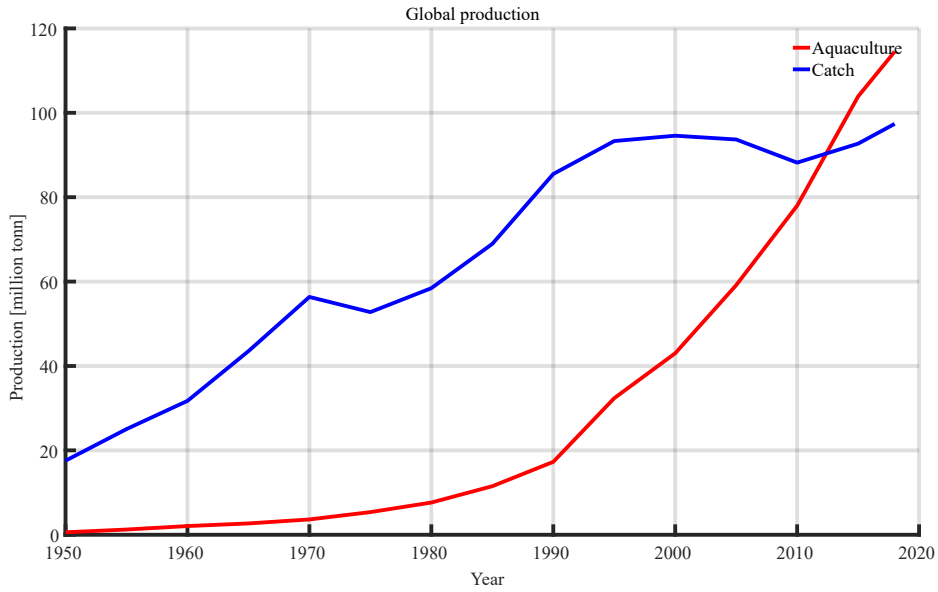

Figure 1.1: Global fisheries production from wild catch and aquaculture for all species excluding crocodiles, alligators and aquatic mammals. Data from FAOSTAT (2018).

veloped for the salmon farming industry could also be used for other aquaculture species. In addition, the industry provides a large number of jobs by employing directly and indirectly the Norwegian workforce.

1.1.1 Atlantic salmon farming

Salmon aquaculture is a form of intensive production that requires a considerable husbandry effort in terms of active control and involvement of the farmers in daily operations. For example, feeding 200,000 animals in a single sea-cage is an immense task which becomes more challenging when feed losses must also be minimised. In addition, challenges like diseases and parasites are countered through targeted vaccination programs and other measures such as lice skirts and delousing procedures. Historically, wild stocks were used for obtaining egg/fry but with the improvements and advances in hatchery technology, broodstock salmon are today raised for egg/fry production (Asche, 2008).

Atlantic salmon is an anadromous species, meaning that it migrates from seawater to freshwater for spawning. The life cycle of a wild salmon starts with eggs being laid in rivers (freshwater), which after a period develop into larvae or so-called sac fry. When the yolk sac of a fry is depleted, the fry develops into parr, a stage where they start feeding actively. Later, the parr develops into smolts after undergoing a

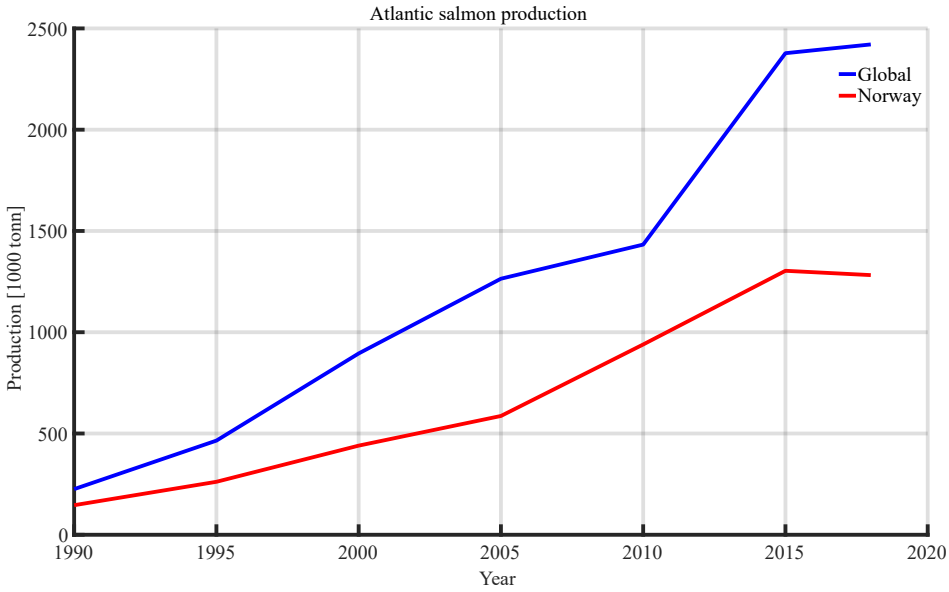

Figure 1.2: Global Atlantic salmon production. Norway is the largest producer of Atlantic salmon, producing more than 50% of the total global production. Data from FAOSTAT (2018).

process called smoltification where they adapt to seawater. After smoltification the fish migrate to sea, concluding the freshwater phase (typically 1-5 years). The fish then spend 1-3 years in seawater, before returning to their native rivers as adults for spawning (Liu et al., 2011). One of the success factors in Atlantic salmon farming has been the ability to replicate this life cycle also for farmed fish by dividing the production cycle into the following five steps (Asche and Bjørndal, 2011):

1. Collection of eggs and fertilisation
2. Development of sac fry from eggs
3. Development of sac fry into parr
4. Smoltification process
5. Grow-out phase

The first four phases of the cycle usually take place on land in freshwater inside hatcheries. Eggs are obtained from domesticated broodstock female fish and are fertilised by milt from males. Farmed salmon smoltify at a younger age than the wild fish, and the mean duration of the land-based phase is around 1 year.

Furthermore, individual farmed smolt weigh $70\,\mathrm{g}$-$140\,\mathrm{g}$ (around double that of a wild smolt). The final grow-out phase takes place in marine fish farms and lasts between 12 and 18 months. At the end of the production cycle, an adult salmon typically reaches a weight of $4\,\mathrm{kg}$-$6\,\mathrm{kg}$ before being harvested for slaughtering. The intensive farming practice thus results in that the life cycle of farmed salmon is highly optimised and much shorter than that of the wild salmon, yielding increased productivity and large-scale production of fish protein at lower production costs. However, to achieve sustained growth and optimisation, the industry highly depends on technological innovation (Asche et al., 2013).

In the beginning era of commercial salmon farming in Norway, i.e. 1960-1980, various cage structures were used for the grow-out phase. The early salmon farming started with small single cage-based farms, where the cage was attached to shore (Jensen et al., 2009). The Grøntvedt cage (Fig. 1.3a), originally octagonal in shape and made up of wood, was developed in 1970 (Tilseth et al., 1991). It was a successful cage structure, which was later refined into the circular polyethylene plastic cages prevalent in the industry today. A modern salmon farm (Fig. 1.3b) constitutes of 8-16 (each with diameter up to $50\,\mathrm{m}$, $50\,\mathrm{m}$ deep) floating plastic circular cages where each cage can contain up to 200,000 individuals (Bjelland et al., 2015).

Most modern marine farms are placed away from the shore to keep feeding and other essential infrastructure on land. There farms are largely floating structures, where sea-cages and a feeding barge are held in place by a common mooring system and are more mobile i.e. biomass is moved to new sites after one or two growth cycles (Asche and Bjørndal, 2011). Although farms are still placed relatively close to and at locations sheltered from ocean waves and the most adverse weather conditions, the recent industrial growth and competing claims from other industries and recreational activities for coastal zone area have stimulated the marine fish farming industry to start moving sites further offshore. More exposed sites may offer some advantages compared to the sheltered sites such as improved water quality, less impact on local environment and a lower parasite and disease pressure, but the harsher conditions and remoteness to shore render management and operation of the exposed farms significantly more challenging (Bjelland et al., 2015).

The Norwegian salmon farming industry initially had a "small family owned business" model that has now evolved into a considerable industrial sector that constitutes an important part of the Norwegian economy, and that creates much valued job opportunities and livelihoods in rural communities. The industry is today world leading in marine aquaculture production and the related technology and equipment supply chains, and employs either directly or indirectly a notable por-

Fig. a

Fig. b

Figure 1.3: The Grøntvedt cage (Fig. a. Source: Public domain, National Library of Norway) compared with sea-cages in a modern salmon farm (ACE, Korsneset) (Fig. b. Source: Sintef Ocean AS)

tion of the Norwegian workforce. Salmon farming in Norway is regulated by the Ministry of Fisheries, which issues licenses and regulates the industry through a strict licensing scheme in accordance with the objectives set by the Norwegian government (Liu et al., 2011). Improved environmental footprint and sustainable growth are two important strategic goals set by the government for the salmon farming industry. These two goals are difficult to achieve as larger, more intensive production farms will tend towards bigger environmental footprint in terms of interaction between farms and local marine ecosystems. Other important industrial challenges include escape of the farmed salmon and its crossbreeding with the wild salmon population (Jensen et al., 2009), diseases and ectoparasites such as sea-lice. Although moving to more exposed may contribute to countering some challenges, this may further exacerbates the challenges faced by the farmers such as Health Safety and Environment (HSE) issues, farm management and operational expenses. These challenges could be addressed through innovation and new technological solutions, as suggested by Føre et al. (2018) through the Precision Fish Farming (PFF) concept.

Although several technological solutions are already used by the aquaculture industry, Føre et al. (2018) highlight the importance of accelerating the adoption of new solutions for monitoring, controlling and documenting biological processes in marine farms. The authors point out that most of the operations in today's marine farms, both in terms of monitoring and controlling, are manually executed by the farmers. However, if a feedback control system oriented approach could be developed and applied to the marine aquaculture management operations, it could be possible to move from the existing experienced-based manual control to a knowledge centred and fully autonomous control system. The PFF concept proposes a cyclic representation of the required operations for improved farm management, where all the operations can be broken down into different phases. The fish are first observed (phase 1), their states then interpreted from the observations (phase 2) before a decision is made (phase 3) on whether or not some sort of action should be done (phase 4). Since the outcomes of the observation phase is an important foundation for the rest of the cycle, introduction of the technology to this phase is a crucial element, especially considering that observing fish underwater is more difficult than observing animals on land, where farmers have a more 'direct' contact and possibility to observe animals in the land-based farming. The underwater environment poses unique challenges for the farmers in the sense that they lack a possibility to directly monitor and observe animal behaviour which is essential for farm management (Føre et al., 2018).

1.1.2 Fish monitoring and its application in aquaculture

Knowledge of fish behaviour under production is important to understand feeding habits, growth rate, interaction with environment, welfare, health and survival of the fish, and studies have shown that such responses depend upon species being farmed, environment and location of sea-cage (Baras and Lagardère, 1995). Thus, knowledge of the spatial and temporal distribution, movement and speed of fish inside a sea-cage, behaviour parameters (e.g. swimming depth, activity, energetics, daily rhythms), environmental factors (e.g. light, temperature, water quality, oxygen level) and how the fish interact with the environment could help in taking timely (from a fish's point of view) corrective actions (Baras and Lagardère, 1995).

Fish may behave differently in a fully stocked sea-cage compared to a laboratory environment. Whereas laboratory observations are performed in a very controlled setting, often studying a single behaviour parameter, it is not possible to reproduce all the processes occurring naturally in the sea-cage inside a laboratory. Therefore, laboratory observations may deviate from the fish behaviour observed inside a full-scale production facility (Cooke et al., 2012; Baras and Lagardère, 1995). Hence, it is desirable to observe free-swimming cultured fish in their true environment. Various technological solutions exist to monitor fish behaviour in marine fish farms. Examples of such solutions are machine vision inspired fish behaviour monitoring systems (Pinkiewicz et al., 2011), and acoustic instruments such as echo sounders, sonars and split-beam sonars (Klebert et al., 2015; Soliveres et al., 2017; Arrhenius et al., 2000; Rundtop and Frank, 2016). Video techniques are non-destructive, low-cost solution that are easy to implement and provide direct observations of a group of fish. Recordings could be analysed manually or via an automated machine vision system (Williams et al., 2006). However, factors such as water turbidity, camera movements and recording under low light levels e.g. during night condition could degrade the video quality. In addition, the large absorption coefficient of light underwater limits the camera's practical range. Acoustic instruments are also inherently non-invasive solutions. However, unlike camera based solutions, they do not suffer from the issues of limited range and work well under turbid water conditions. Such instruments have been successfully used for monitoring e.g. fish speed (Arrhenius et al., 2000), body length and weight (Soliveres et al., 2017).

Although both the aforementioned solutions provide aggregated behaviour for a group of animals, they cannot provide individual histories. Such individual focused data series could give a more detailed insight about the fish behaviour (Macaulay et al., 2021). Specifically, there exists no available solution for measuring the swimming speed of an individual free-ranging fish living under farm conditions (Cooke et al., 2004), which is an important behavioural trait that could give insight

in to fish energetics, interaction with environment and response to external factors (Hvas et al., 2017; Hvas and Oppedal, 2017; Jónsdóttir et al., 2019). Telemetry represents a technology that could be used as a basis for tools for obtaining individual data histories from free swimming fish. Versatile monitoring setups could be accomplished by combining group-wise datasets acquired from the acoustic and video instruments with the individual fish observations obtained from telemetry. Telemetry solutions were focus of this study and are discussed in the next section. By using advanced signal processing techniques both in time and frequency domains e.g. Doppler shift in a signal, telemetry could also be extended for measurement of individual free-ranging fish swimming speeds.

1.1.3 Telemetry and biologging

Telemetry is derived from *tele* meaning remote and *metron* meaning measure. In a typical telemetry system, a relevant parameter is sensed and measured, then transmitted (e.g. via radio or acoustic waves) and finally picked up by a remote receiving part of the system for processing (Read, 2009). Although not strictly adhering to the above definition, devices that store data in internal mediums for later retrieval (often labelled loggers) are also sometimes included in the term telemetry. When applied to living things these technologies are often termed as biologging or biotelemetry (Rutz and Hays, 2009; Thorstad et al., 2013). Hussey et al. (2015) provides a review on different types of biologging systems commonly used to observe aquatic animals, whereas Fig. 1.4 shows various commercially available biologging systems (Read, 2009; Cooke et al., 2012). The basic building block of a biologging system is an electronic device, usually referred to as a tag. A tag is an encapsulated battery operated electrical circuit which is either implanted into or attached externally to the animal (Fig. 1.5a).

The earliest example of aquatic applications of biologging was in the 1950s for migration studies of wild salmon (Trefethen, 1956). The initial implementations of tags were extremely simple and they usually had an analogue oscillator and amplifier circuit without any on-board memory or processor. In principle, tags were non-coded continuous "pinging" devices that were primarily used for tracking the tagged animals using directional receivers. In addition to the animal tracking, triangulation by using multiple receivers dispersed in space was used for animal positioning. These tags enabled identifying and tracking wild animals in their natural habitat, giving the researchers an edge in terms of studying wild animals while moving freely and without re-catching them. The continuous operation of the tags made them power hungry and thus energy inefficient, resulting in that the early tags were operating for a period of few hours to a couple of days from the time of their attachment to an animal.

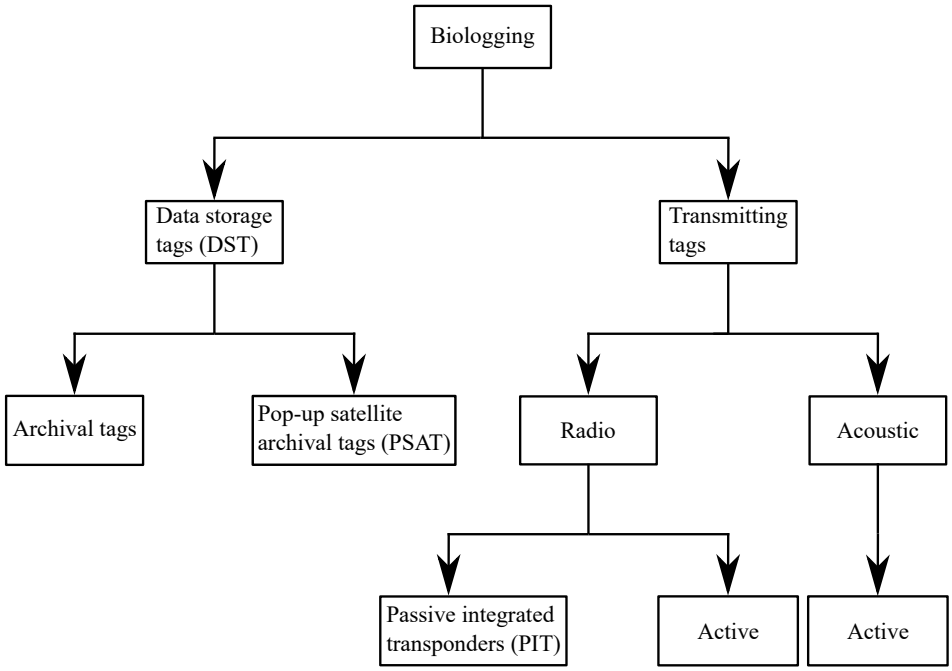

Figure 1.4: Various types of commercially available biologging systems.

With the development of Integrated Circuits (ICs), miniaturisation of the electronic circuitry and possibility of having processing power inside a small electronic chip in form of a microcontroller, the electronic tags were also improved. Miniaturised electronic components lead to smaller tags down to a few millimetres in size. Smaller size means smaller space for batteries, and to improve tag energy efficiency, pulse-based transmission schemes were introduced instead of the continuous transmissions used previously, leading to longer operational life (i.e. in the range of months and years). The inclusion of on-board microcontroller ICs enhanced the tags' data storage and processing capabilities, enabling them to process and encode data from additional on-board sensors, and transmission of these with a unique ID. Commonly used sensors include temperature (Koeck et al., 2014), depth (by measuring pressure (Skilbrei et al., 2009), accelerometer (Føre et al., 2011), ambient light (Cooke et al., 2012), tilt (activity) (Føre et al., 2011), oxygen (Cooke et al., 2012) and electromyography (EMG) (Cooke et al., 2004).

Data storage tags

Technological advancements also led to the development of small yet high capacity memory chips, providing a new dimension to the field of biologging with the development of data storage tags (DSTs) or dataloggers (Rutz and Hays, 2009).

DSTs were unique in the way that the tags only stored data inside an on-board memory and thus did not require circuitry for wireless transmission of data, saving space and energy (Thorstad et al., 2013). Once an animal is tagged with such a device, a DST measures and stores time-series of the behavioural, physiological or environmental parameters using on-board sensors and memory. To access the data, the animal or the detached tag needs to be recaptured, which is the major disadvantage of this concept, both practically and because it renders real-time data access and monitoring impossible. As DSTs do not transmit data remotely, they don't need an antenna and hence are energy efficient and could potentially be used to acquire animal data for a relatively longer duration (Read, 2009). DSTs have the advantage of very fine data collection, which essentially means that they could be used for logging large number of data samples for a given time period by operating at a very high sampling rate. However, there is a trade-off between the higher sampling rate and tag's operational life.

Traditional DSTs are also called archival tags, whereas a more recent alternative form of DSTs are the pop-up satellite archival tag (PSAT). Such tags detach from the tagged animal after a pre-programmed period and floats to the surface for transmission of the stored data via a dedicated satellite (Hoolihan et al., 2011). PSATs are usually used for longer time spans (i.e. in the range of one to several years), over large geographical areas and for very large animals (for example whales) swimming close to the water surface, providing information about spawning, migration, predator and other long-term behaviour data, rendering them different from traditional DSTs (Cooke et al., 2012). Since DSTs cannot provide real-time access, their potential use in realisation of the PFF concept and fully automated mariculture farming is limited.

Transmitting tags

Whereas archival tags store data locally, transmitting tags relay their data over a radio or an acoustic link employing the principles of modulation of acoustic or electromagnetic waves (Trefethen, 1956). Contrary to the DSTs, this approach involves at minimum a pair of devices i.e. a transmitting tag and a matched receiver. A tag attached to an animal processes the sensor data (if any) internally and transmits it, along with a unique ID, to a remote receiver that decodes the data. Instead of containing a large on-board memory like DSTs, transmitting systems require on-board antennae (radio) or acoustic transducers. Transmission of signals in a medium is energy consuming meaning that the transmitter tags usually consume more power compared to the DSTs. The receiver units are relatively flexible in terms of adding more features, power and processing capabilities compared to the tags.

Transmitting systems are more attractive for aquaculture operations than the DSTs as they enable real-time monitoring and do not require recapturing the tagged fish to obtain the data. However, the communication channel could become a bottleneck in a transmitting system. Issues such as noise, turbulence or presence of ships and other objects, fading, attenuation and absorption of energy in channel directly affect the communication range. Another important channel related issue is channel congestion in i.e. finite bandwidth of the medium when a large number of transmitters are operating simultaneously (Pincock and Johnston, 2012).

Transmitting tags could be further divided into two sub-groups based on the type of communication link used for transmission. Radio or electromagnetic waves oriented systems can be further sub-divided into passive and active tags. The most common passive tags are the Passive Integrated Transponders (PIT) which do not contain an on-board battery. PIT typically use frequencies in the Low Frequency (LF) range i.e. $125\,\mathrm{kHz}$ to $400\,\mathrm{kHz}$. The coil antenna of a PIT acts as an energy harvester and powers up the tag circuitry when energised by a proximal magnetic field. Although this gives PIT tags virtually unlimited life, most implementations of the PIT tags are simple, and they can only be used for very short ranges, maybe up to $<2\,\mathrm{m}$ but often less. Active radio tags contain a battery and are less constrained than the PIT tags in terms of range (tens of kilometres (Read, 2009)). Unlike PIT tags, such tags may have additional on-board sensors for monitoring behaviour or other parameters. They operate in the Very High Frequency (VHF) band, i.e. $30\,\mathrm{MHz}$ to $225\,\mathrm{MHz}$ (Thorstad et al., 2013).

Although, radio waves and radar are widely applied in terrestrial and to some extent freshwater communication, they are less suitable for use in seawater due to its high conductivity and attenuation of radio signals at practical frequencies. Acoustic telemetry is therefore preferred when working in the marine environment as acoustic waves tend to travel more efficiently and farther underwater than in air (Hockersmith and Beeman, 2012; Hussey et al., 2015; Hovem, 2007). This technology will be further discussed in the next section.

1.1.4 Acoustic fish telemetry

Until 1971, acoustic telemetry systems were predominately developed by individual research institutes at universities. The first commercial acoustic telemetry system was developed by Sonotronics in 1971. Today, acoustic telemetry has become established as a reliable research tool for researchers. Various commercial suppliers are making telemetry systems, using state of the art electronics which includes smart digital receivers and miniature transmitter tags having a single or a combination of on-board sensors (Hockersmith and Beeman, 2012; Pincock and Johnston, 2012). A typical acoustic telemetry setup is shown in Fig 1.5, whereas

Fig. a

Fig. b

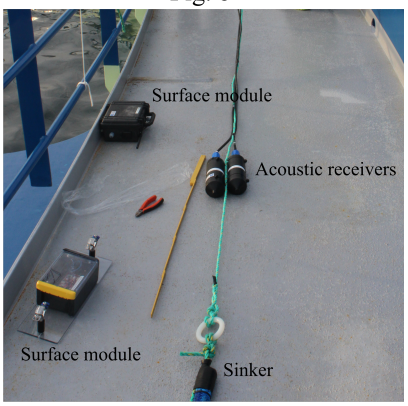

Figure 1.5: Different parts of a typical acoustic telemetry system. A tag is surgically implanted into a fish (Fig. a), which then sends acoustic data to a remote receiver. The receiver (Fig. b) stores and processes further the received data. Additionally, a surface module could provide extended functionalities to the receivers.

Fig. 1.6 shows various types of acoustic tags used in telemetry studies.

An ideal acoustic tag should be physically small such that it can be implanted inside or attached externally to a fish without affecting the fish significantly (Thorstad et al., 2013; Wright et al., 2018; Macaulay et al., 2021). Practically, tags measuring down to $5-7\,\mathrm{mm}$ in length are available and are used for small fish, whereas tags with a length of $1\,\mathrm{cm}$ and more are used for relatively larger fish. Also, tags which are implanted inside a fish are usually smaller in size than the tags that are targeted for external attachment. Similarly, the weight of a tag is an important parameter and there is a general rule of thumb that a tag should weigh (in air) less than 2-3% of the total weight of the target fish is followed, though this may vary with species, fish state and situation (Macaulay et al., 2021).

Underwater acoustic communication range is defined by the signal strength of the tag, geometric spreading loss, noise level, detection threshold and frequency dependent acoustic absorption in the medium (Hovem, 2007; Stephen Riter, 1970). The acoustic signal frequency is also a design parameter which defines physical dimensions and maximum communication range of a tag. Transducer size (diameter) is inversely related to the used frequency, meaning that higher frequency transducers are smaller in size. The underwater absorption coefficient is related to the square of the frequency, meaning that higher frequencies will be absorbed more and will have shorter range (Pincock and Johnston, 2012). Although frequencies used in underwater acoustic telemetry range from $24\,\mathrm{kHz}$ to above $400\,\mathrm{kHz}$, $69\,\mathrm{kHz}$ has become a kind of de-facto standard due to the low absorption coef-

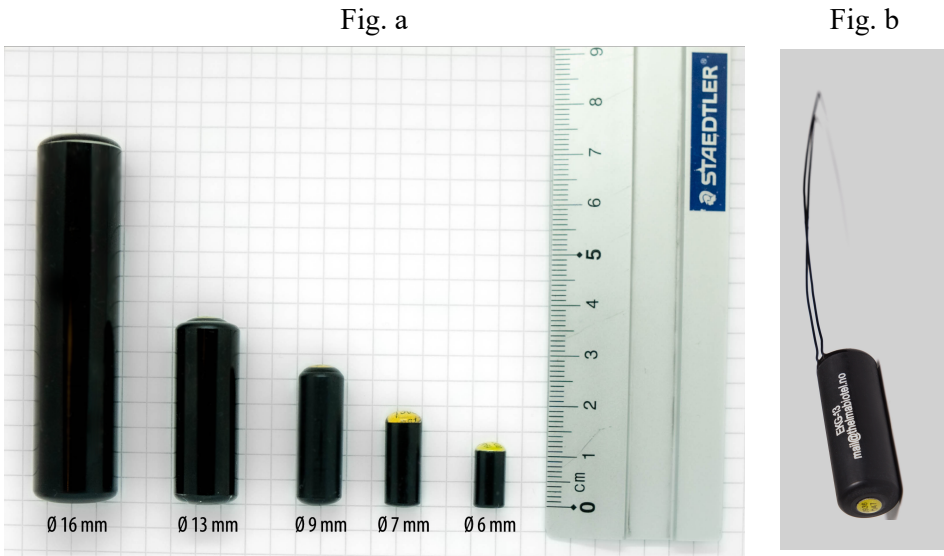

Figure 1.6: Fig. a: Various types of commercially available acoustic tags. Fig. b: Tags also have external probes requiring precise placement for measurement of parameters such as heart rate or muscle activity. (Courtesy of Thelma Biotel AS)

ficient and near absence of noise generated by the other sources in the marine environment around this frequency (Pincock and Johnston, 2012). Commercial acoustic telemetry systems have typical ranges in order of 100 s of meters, large enough to cover a single sea-cage from end-to-end.

A transmission from an acoustic tag typically encodes the tag ID and sensor data using modulation schemes such as Pulse Position Modulation (PPM) (Niezgoda et al., 2002), Frequency Modulation (FM), Frequency Shift Key (FSK) (Stephen Riter, 1970), Code Division Multiple Access (CDMA) (Niezgoda et al., 2002; Cooke et al., 2005) or Binary Phase Shift Keying (BPSK) (Weiland et al., 2011). The CDMA and BPSK modulations offer higher tag densities i.e. number of resident tags in a single study, while the FM and FSK schemes provide higher data rates. Although the PPM scheme has a limited bandwidth, it is attractive due to the fact that is robust against noise and also the simplest of all in terms of physical implementation in a tag. In a PPM scheme, information is encoded in the elapsed time between two consecutive pulses (Fig. 1.7). A pulse at start of a burst is used for synchronisation. Typical duration of a single pulse in such a PPM scheme varies from 1 ms to 10 ms, with the latter being more common (Pincock and Johnston, 2012). A single burst consists of a series of pulses (usually 7-8) and last up to a few seconds, whereas time between two consecutive bursts varies and is in order of few seconds to a few minutes.

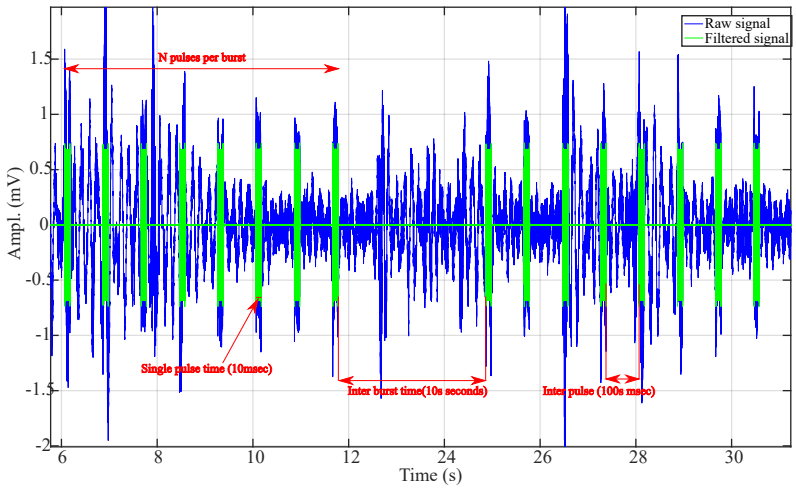

Figure 1.7: Two back-to-back messages using a PPM modulation. Information is encoded by changing inter-pulse time within a single burst of N (eight in this case) pulses.

The receiver units in acoustic telemetry systems are specialised hydrophones designed for receiving and processing information sent by the matched telemetry tags. Traditionally, acoustic receivers were used for tracking fish and thus were often cabled powered mobile devices (Pincock and Johnston, 2012; Grothues, 2009). Battery operated standalone receivers storing received telemetry data internally are also available commercially. The message reception rate at a receiver depends upon channel noise (acoustic, mechanical and electrical), tag density in an experiment, transmitted signal strength and acoustic collision at the receiver. The length of a single burst and intra-burst time along with tag density define the acoustic collision rate, which directly affects the effective message detection rate at an acoustic receiver (Pincock and Johnston, 2012). The underwater communication channel is dynamic and also affects the communication and message reception rate at the receivers via physical wave phenomena such as reverberation and refraction (Pincock and Johnston, 2012; Hovem, 2007; Stephen Riter, 1970; Føre et al., 2017).

While most historical telemetry experiments have not relied on having real-time access to the data, the desire to use telemetry as an operational tool has spawned an interest in real-time access to the data. This is today possible either through cabled (e.g. HTI and Lotek Wireless, Inc. MAP systems (Deng et al., 2011; Grothues, 2009) or wireless (e.g. Lotek Wireless, Inc. WHS and Vemco VRAP, Sonotronics CUB-1 systems (Grothues, 2009) solutions. The cabled solution is a straightforward real-time access approach, however, it is not a practical solution at a marine

fish farm as the cables are awkward to handle and may be a serious safety hazard for carrying out farm management operations. They are also limited in terms of effective coverage i.e. maximum number of receivers served and could easily become a bottleneck in a telemetry study (Grothues, 2009; Pincock and Johnston, 2012). The ideal receiver for real-time tracking of fish should be power efficient and at the same time support wireless connectivity providing real-time access to the telemetry data. It should ensure that the true advantage of the transmitting telemetry systems is not lost from the receiver to user end i.e. immediate update of the tag data as it arrives on a receiver for processing by a user.

1.2 Objectives and contributions of the thesis

The two major objectives of this study were:

1.2.1 Objective 1: Provide a practical real-time support to the existing acoustic telemetry systems.

Traditional telemetry systems use acoustic receivers as data loggers and users typically access and analyse the data retrospectively once the experiment has ended. Although, some existing solutions are using cabled, cellular or proprietary radio protocols to provide real-time access for the telemetry data (Grothues, 2009; Pincock and Johnston, 2012), such approaches often suffer from the issues of scaling, coverage area and power efficiency. A concept providing real-time support for the telemetry systems that does not suffer from the problems mentioned above would therefore be a significant innovation on the path to enabling telemetry-based monitoring in commercial sea-cages. The proposed solution should operate as a reliable communication protocol, be standalone and provide persistent access to the telemetry data.

Contributions

This objective was met by developing and successfully demonstrating a concept coined the Internet of Fish (IoF). IoF is an Internet of Things (IoT) inspired solution in terms low-power battery operated nodes, distributed over a large geographical area. As a first step, the IoF system was developed and evaluated at commercial fish farms for real-time access to the telemetry data (i.e. a real-time monitoring application). The IoF system was then extended with real-time 3D fish positioning, and an experiment to document its performance was conducted at a marine fish farm on a new type of semi-closed steel-cage named Aquatraz.

1.2.2 Objective 2: Develop a sensing principle for measurement of instantaneous fish swimming speed.

Based on its prospects for assessing the state and behaviour of fish in sea-cages, a solution enabling measurement of individual speeds of free-swimming fish could prove useful for both science and industry. However, no practical solution for measurement of instantaneous swimming speed of individual fish under farm conditions existed (Cooke et al., 2004). The second major objective for this study was to propose, develop and illustrate a practical method for measuring instantaneous swimming speed of a free-ranging fish using the principles of acoustic telemetry.

Contributions

This objective was met by developing an algorithm for instantaneous speed measurement using the Doppler effect. The proposed solution exploits the carrier signal used in an existing telemetry system and employs Doppler signal processing at the receiver end to extract speed information. The Doppler-based fish speed algorithm was developed and tested in multiple steps, first as simple 1D speed measurements in a laboratory tank, then in the sea close to shore as 2D speed measurements, and subsequently as 2D speed measurements in a fully stocked commercial sea-cage using an acoustic tag mounted on a catamaran emulating fish movements. The principle was finally verified through a field experiment in a full-scale salmon farm with live tagged fish.

1.3 Thesis outline

Chapter 1 gives the background information about marine fish farming and acoustic telemetry systems. It also points out the objectives for this study and contributions made by the thesis. Chapter 2 considers real-time monitoring of fish in marine aquaculture and presents the IoF concept, how IoF provides real-time monitoring capability to an existing telemetry system, IoF's integration with the existing telemetry system, its layered architecture, and finally experiments conducted to demonstrate and verify the performance of the IoF concept. Chapter 3 describes a Doppler swimming speed measurement method for free-ranging fish in detail and presents the results from the various experimental stages used to verify it, and concludes with the observations and experiences gathered from the live fish swimming speed experiment. Chapter 4 covers briefly the possibility of combining the IoF with the Doppler speed measurement principle to develop a real-time fish position and speed measurement telemetry system in terms of a new receiver. This chapter also concludes the thesis and presents the possible future work and objectives for further studies.

Publication	Title	Contribution to chapters
Paper J1	Hassan, Waseem; Føre, Martin; Ulvund, John Birger; Alfredsen, Jo Arve. (2019) “Internet of Fish: Integration of acoustic telemetry with LPWAN for efficient real-time monitoring of fish in marine farm”, *Computers and Electronics in Agriculture*, vol. 163.	Chap 2,4
Paper C1	Hassan, Waseem; Føre, Martin; Urke, Henning Andre; Kristensen, Torstein; Ulvund, John Birger; Alfredsen, Jo Arve. (2019) “System for Real-Time Positioning and Monitoring of Fish in Commercial Marine Farms Based on Acoustic Telemetry and Internet of Fish (IoF)”, *The 29th International Ocean and Polar Engineering Conference*, Honolulu, Hawaii, USA, 2019.	Chap 2
Paper C2	W. Hassan, M. Føre, M. O. Pedersen and J. A. Alfredsen, "A novel Doppler based speed measurement technique for individual free-ranging fish", *2019 IEEE SENSORS*, Montreal, QC, Canada, 2019, pp. 1-4.	Chap 3
Paper J2	W. Hassan, M. Føre, M. O. Pedersen and J. A. Alfredsen, "A New Method for Measuring Free-Ranging Fish Swimming Speed in Commercial Marine Farms Using Doppler Principle," in *IEEE Sensors Journal*, vol. 20, no. 17, pp. 10220-10227, 1 Sept.1, 2020.	Chap 3,4
Manuscript M1	Waseem Hassan, Martin Føre, Henning Andre Urke, John Birger Ulvund, Eskil Bendiksen and Jo Arve Alfredsen, New concept for swimming speed measurement of free-ranging fish using acoustic telemetry and Doppler analysis, *In preparation*.	Chap 3,4

Table 1.1: List of publications

Chapter 2

Real-time fish monitoring in marine aquaculture

2.1 Introduction

This chapter outlines the contributions towards solving Objective 1 i.e to provide real-time support to the existing acoustic telemetry systems. Real-time systems react to events within a predefined timing deadline and are characterised by low (i.e. in sub-second range) latency and bounded jitter values. This work has focused on soft real-time systems which are often used in monitoring applications where missing a deadline or a delayed update is acceptable and are the main focus of this chapter (Buttazzo et al., 2005). The chapter starts with brief motivation for the need of a real-time acoustic telemetry monitoring system in marine aquaculture and provides a brief survey of the currently existing solutions. Afterwards, the concept developed in this study, i.e. Internet of Fish (IoF) is explained.

2.2 Papers' introduction

Two articles J1 and C1 were published based on the work presented in this chapter. Article J1 presents the detailed implementation of the IoF concept and focuses on the communication quality (QoS) aspect of the IoF, whereas article C1 deals with real-time fish positioning aspect of the IoF and presents the results from the positioning experiment.

2.3 Motivation

Fish behaviour monitoring studies using acoustic telemetry systems are executed in two stages. The first stage consists of fish tagging and equipment deployment.

Randomly selected fish are then tagged, while the telemetry receivers and necessary support equipment (e.g. power source, buoy) are deployed in the experimental area. The duration of such studies ranges from few days, weeks up to several months or even a year (Cooke et al., 2012; Thorstad et al., 2013). During the experimental period, acoustic data is continuously sent by the tagged fish and is received, processed and finally stored locally in the receivers. Since the receivers are standalone devices, the data is often only retrieved by the user at the end of or at a few fixed intervals during the experimental period (Brownscombe et al., 2019). From a research point of view, online support might not be an important requirement of a study and post-processing of the data and analyses at the end of the study is a common practice, however for an aquaculture monitoring system, the real-time access to the telemetry data is an essential requirement. There is a need for a solution which offers real-time access to the telemetry data, while simultaneously addressing the unique requirements of the telemetry systems in terms of low power consumption, wide coverage area and scalability. Whereas modern marine farms have power supply available on the cages, battery powered standalone acoustic receivers are preferred in acoustic studies due to issues such as prevalent power outages on cages, electrical noise etc.. Long running cables are cumbersome to maintain and they limit the maximum number of receivers that could be used on a single cage. In addition, the cables in and around a sea-cage are often seen as a safety hazard for performing farm management operations. While most of the commercially available acoustic receivers do not offer real-time access as part of the solution, some commercial systems do offer real-time access for example by using cabled RS-485, Very High Frequency (VHF) and Global System for Mobile communication (GSM) receivers. However, such solutions are not designed for acoustic telemetry applications and hence suffer from the issues of energy efficiency, scaling, and physical limitations for cables (Hassan et al., 2019b).

2.4 LPWAN-based real-time monitoring telemetry system

Realising a system that fulfils the requirements of the IoF concept entails first deciding upon a suitable communication protocol, and then developing a dedicated surface communication module that facilitates communication via the chosen protocol. This section outlines this process by first addressing the choice of communication protocol, arriving at Low Power Wide Area Networks (LPWANs). LPWANs represents a novel communication paradigm which is designed for intercommunication of devices or sensing nodes distributed over a large geographical area (Raza et al., 2017; Adelantado et al., 2017). Different potential physical layers for implementation of a LPWAN are then surveyed, and the final choice for this study (LoRa) is outlined in more detail.

2.4.1 Communication protocol

Deciding upon the underlying communication protocol for a real-time telemetry system is a design choice influenced by the properties and requirements of the acoustic receivers. The acoustic receivers are low power battery-operated devices which are typically placed a few hundred meters away from the shore or feed-barge installations. In addition, the acoustic telemetry systems (PPM modulation scheme) are inherently low data bandwidth systems, typically generating 100 to 250 bytes per minute (a message rate of 15-20 messages per minute, where a single message requires ten to twelve bytes of storage inside a receiver), and hence require low data rates (in order of a few hundred bytes per second) for transmission of such data from the receiver to the user end (Hassan et al., 2019b; Pincock and Johnston, 2012). Thus, the requirements for a solution providing real-time access to telemetry data are:

- Low power consumption
- Low data rates
- Large coverage area
- Scalability in terms of adding new receivers.

Although traditional radio protocols such as cellular (Long Term Evolution (LTE), GSM), WiFi and VHF radio might cover some of the individual requirements, none of them meet all the system requirements. LPWAN is a much better fit as this is a protocol designed for small battery operated sensor nodes, distributed over large areas and perform very simple sporadic operations such as sensor value update every hour or once per day. The sensor nodes in LPWAN networks are in sleep mode for most of their operational life, but are required to operate for months or years on a single battery. LPWANs thus guarantee low power consumption at the cost of low data rates. The cell architecture of LPWANs is similar to GSM where geographically distributed mobile devices are communicating with a central node (called base station or gateway) in a star-of-star topology (Raza et al., 2017). Although both cellular networks and LPWANs offer similar coverage area, which is in order of $10\,\mathrm{km}$, LPWANs differ from the GSM in terms of data rates end nodes are using to communicate with the gateway and power consumption of the end nodes (Adelantado et al., 2017; Augustin et al., 2016).

The conformity in requirements of acoustic telemetry systems and the attributes of LPWANs suggests that the LPWANs could be ideal candidates in providing real-time support to the existing telemetry systems. Whereas the term LPWAN

covers wireless communication protocols offering low power, low data rates, wide coverage area for battery operated devices (Augustin et al., 2016), the physical implementation (PHY) of LPWANs could be realised using various competing modulation schemes such as NB-IoT (Narrow Band-IoT), LTE-M, SigFox, Weightless, Ingenu, LoRa (Long Range) (Hassan et al., 2019b). All these modulation schemes offer large coverage area and low power consumption, however they differ in terms of packet size and data rates. Since acoustic telemetry system using PPM modulation only require a packet size of 120-150 bytes, LoRa was found to be the most suitable protocol as it has sufficient packet size (up to 250 bytes) and other properties deemed beneficial, including flexibility of establishing network, Spreading Factor (SF) design parameter and relatively better power efficiency comparable to the other modulation schemes with similar packet size specifications (Hassan et al., 2019b). The SF design parameter is particularly useful in providing flexibility in terms of trade-off between the packet size and coverage area for an individual node. LoRa operates in a star-of-star network topology and nodes could be added or removed from the network dynamically (Raza et al., 2017).

2.4.2 Surface communication module

To enable interfacing of the acoustic telemetry receivers (TBR-700-RT) with a LoRa LPWAN, a dedicated embedded surface communication module was developed. This module communicates with the submerged receiver in real-time through a cabled interface and relays the received telemetry data wirelessly using the LoRa communication protocol (Fig. 2.4). The module was specifically designed for interfacing with a Thelma Biotel TBR-700-RT acoustic receiver. Two versions of the surface communication module were developed for testing and evaluation of the proposed real-time telemetry monitoring system (Fig. 2.1).

The first version, dubbed the LoRa Add-on Module (LAM), featured a LoRa radio interface chip (PHY), an RS-485 interface for the acoustic receiver (TBR-700-RT) and a Global Navigation Satellite System (GNSS) receiver for positioning and time synchronisation. An improved version in terms of better form factor, with an additional on-board display and a Universal Serial Bus (USB) interface, dubbed the Synchronisation and LoRa Interface Module (SLIM) was also developed. The LAM and SLIM modules had same basic functionality, i.e. LoRa support and RS-485 interface to the acoustic receiver. A block diagram of the SLIM/LAM surface communication module is shown in Fig. 2.2.

Both LAM and SLIM were built using a 32-bit EFM32GG842 ARM Cortex M3 microcontroller (Silicon Labs) as its core processing and control component. A Thelma Biotel TBR-700-RT acoustic receiver, forwarding all acoustic receptions on a standard RS-485 serial interface, provided telemetry data to the surface com-

Fig. a Fig. b

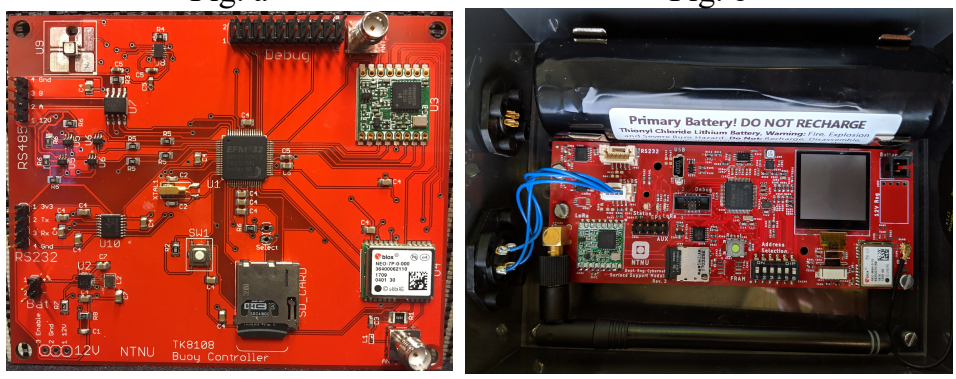

Figure 2.1: Physical implementations of the LAM (Fig. a) and SLIM (Fig. b) modules. Both modules had same basic functionalities, however SLIM had improved PCB form factor and extra debugging features.

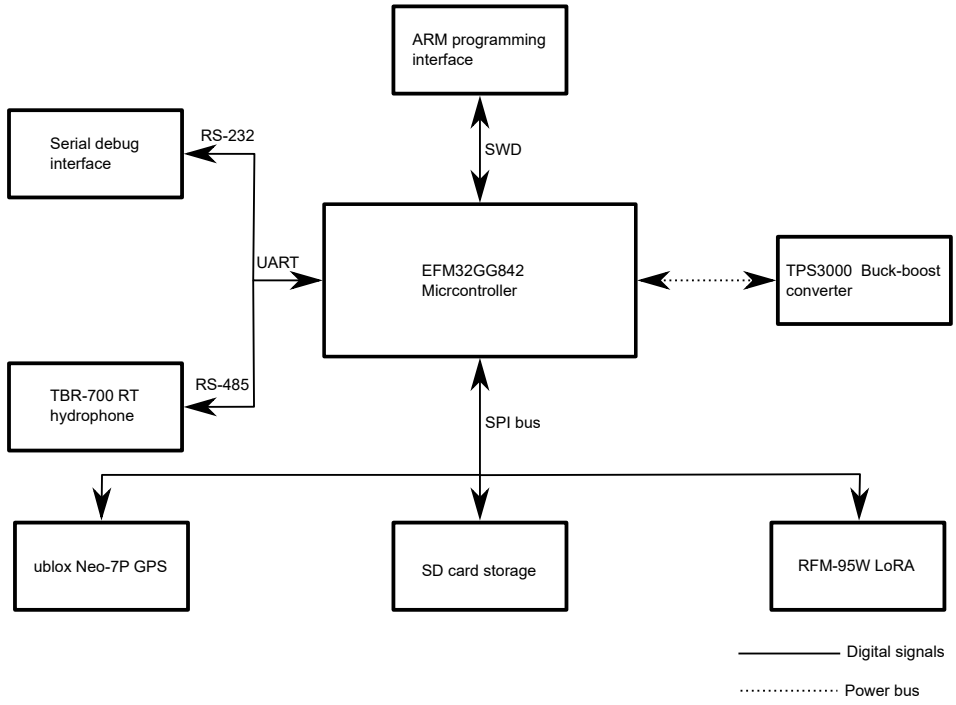

Figure 2.2: Block diagram of the LAM/SLIM module showing its various hardware peripherals.

munication module as the acoustic messages arrived. Radio communication was realised through a Serial Peripheral Interface (SPI) LoRa module (RFM95W, Hop-

eRF), that operates at 868 MHz and was set up to transmit radio packages containing the telemetry data to a gateway, which is a receiving end of the IoF concept. The surface communication module also included a Global Positioning System (GPS) receiver (u-blox, NEO-7/8P) for distributed time synchronisation of the acoustic receivers, which is important to ensure good data quality and is necessary in fish localisation and tracking (Pincock and Johnston, 2012). Current consumption of the surface communication module was around 20 mA during its normal operation and 50 mA during radio transmit mode (which is only active for very short duration). The module was designed for a 3.6 V, 35 A h Lithium primary cell giving an operational life for approximately two months.

The firmware was developed in the C programming language using Silicon Lab's Simplicity Studio Integrated Development Environment (IDE) and was based on IBM's LMiC library (IBM, 2018) which implements the LPWAN stack. The library is modular and can be ported and modified as per requirements of an application, and it also provides a timer-based scheduler. The device drivers for the GPS, the TBR-700-RT acoustic receiver and other peripherals were implemented in the Hardware Abstraction Layer (HAL) of the library. Firmware operation was interrupt driven, governed by the 1 Pulse Per Second (1PPS) signal of the GPS chip. An Interrupt Service Routine (ISR) counted instances of the PPS interrupts and executed a software task called the 'application job' on every 10^{th} second. The 10 s period was chosen to minimise the internal clock drift of the TBR-700-RT receivers. On each iteration of this job, a time synchronisation message was sent to the TBR-700-RT receiver, updating the TBR's internal clock to match the 1PPS. The application job also checked for any newly arrived telemetry messages in the last 10 s and added them to a buffer for further processing. Every 60 s the ISR set a flag triggering the application job send a data packet containing any buffered telemetry messages during the last minute over the radio link. A period of 60 s was selected since it is an acceptable update rate for a soft real-time monitoring system. Using a shorter period would have caused sending too many unnecessary radio packets effecting energy efficiency of the system, whereas a longer period would have lead to a sluggish system response for the end-user. The data was simultaneously stored locally on the SD card in the surface communication module as a backup if the radio link should be down for some reason. The operation of the firmware is explained in the flow diagram shown in Fig. 2.3.

2.4.3 Internet of Fish (IoF)

The IoF concept defines a network of IoF nodes consisting of a TBR-700-RT acoustic telemetry receiver communicating with a surface communication module (Fig. 2.4), providing real-time Internet access to the telemetry data via the LoRa LPWAN. Fig. 2.5 shows the layered architecture of the IoF concept and different

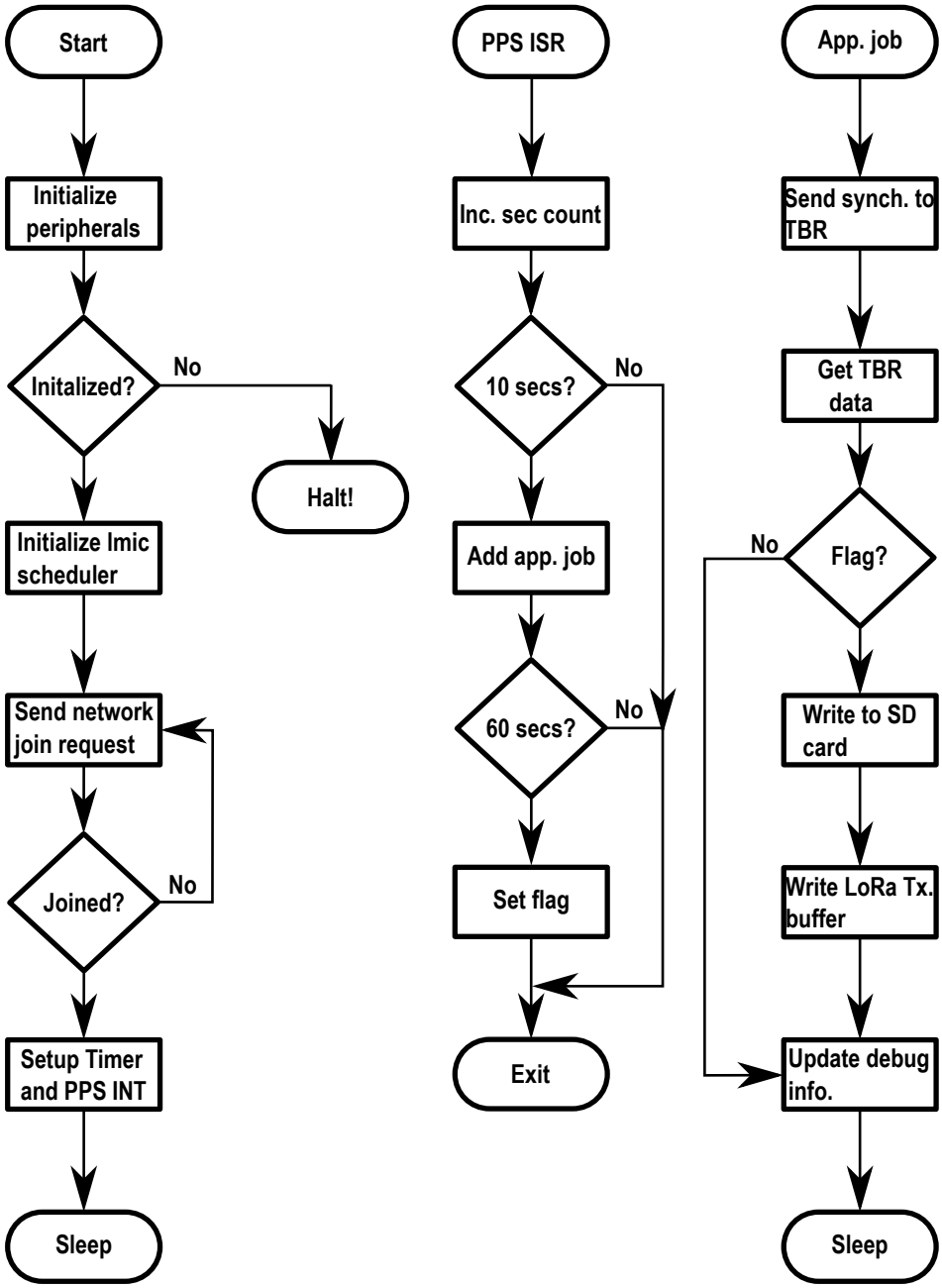

Figure 2.3: Flow diagram explaining operation of the LAM/SLIM firmware.

modules used in realisation of the concept. The first is the *perception layer*, which

consists of a submerged tag (or a tagged fish), a submerged acoustic receiver and a surface module (LAM/SLIM). The IoF concept includes the existing acoustic link, and hence the overall acoustic telemetry system. Devices in the perception layer are typically dispersed over a relatively large geographical area, e.g. multiple sea-cages in a fish farm. The nodes in the perception layer communicate via the LAM/SLIM modules with the centralised gateway representing the *network layer*. The gateway has Internet access and acts as a packet forwarder in that it receives the telemetry data over the LoRa radio link from the end nodes and forwards it to the third layer of the IoF. This layer is called the *application layer* and usually consists of a server, which has access to the Internet, and performs the tasks of receiving data from the network layer, storing the data on a reliable database and presenting the data to the end users. Communication between the gateway and server is controlled by the Message Queuing Telemetry Transport (MQTT) protocol (Light, 2017). MQTT is a subscribe/publish communication protocol, implemented in a broker/client topology. Information exchange is topic centred, instead of message contents or device IDs, making MQTT a versatile and portable protocol. In the IoF concept, the gateway runs a publishing client meaning that it produces data for the broker. The application server runs the MQTT broker which is responsible for maintaining connection between various clients and reliability of the communication. In addition, the server also runs a subscriber client which receives the data from the broker and stores it on a local database. The subscriber client is a portable application and is not limited to the server. The application could be executed on a mobile device or on any personal computer for presentation of the data.

2.4.4 Real-time fish positioning

The LAM/SLIM and hence the IoF concept was designed with a possible future extension for a real-time Time Difference of Arrival (TDoA) algorithm based fish positioning (Pincock and Johnston, 2012; Fang, 1990). In a TDoA algorithm, the arrival of the acoustic signal is timestamped by all acoustic receivers used in an experiment. Since the exact time when the tag transmits an acoustic message is unknown, arrival time cannot be directly used for position calculations. However, the difference in arrival time across receiver pairs could be used to find the relative difference in distance from the tag to the receivers. The position of a tag is then calculated using the known positions of the three receivers (Fang, 1990).

A fundamental requirement for such a positioning system is thus the use of multiple receivers in different positions. The TDoA algorithm needs three receivers in the xy-plane for 2D and four (three in xy-plane and one in yz-plane i.e. deeper than the other three receivers) for 3D positioning, respectively (Fang, 1990; Pincock and Johnston, 2012). To minimise the errors in the measured position, the

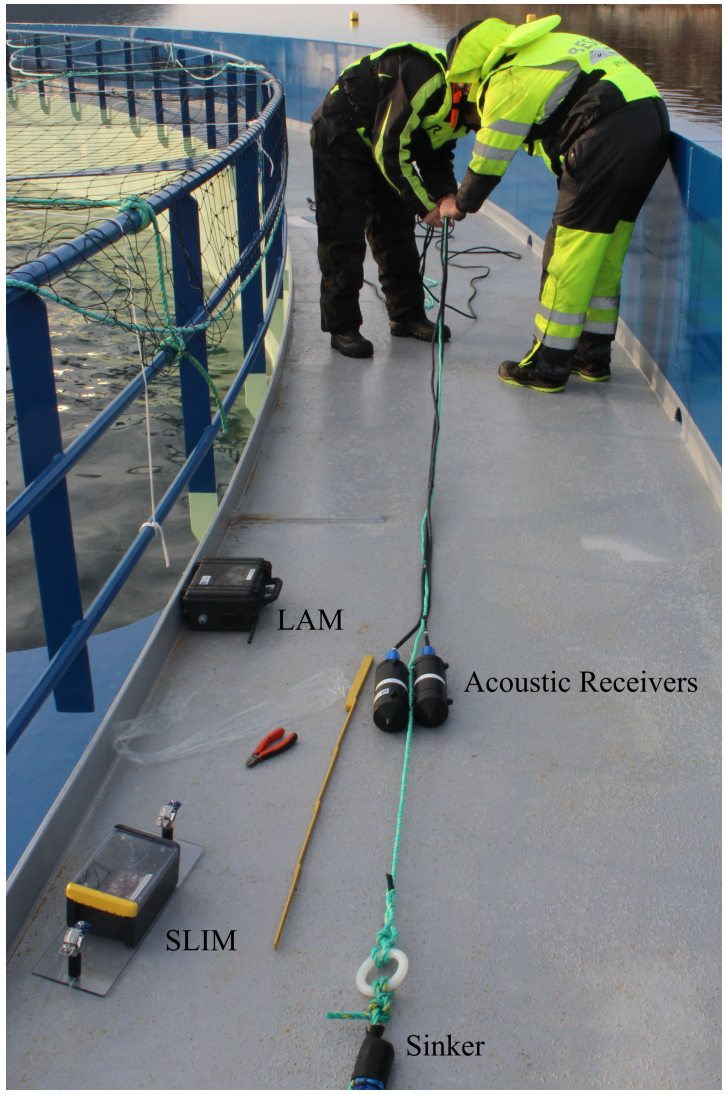

Figure 2.4: An IoF node consists of a LAM/SLIM module, communicating with a TBR-700-RT acoustic receiver via a cabled RS-485 protocol.

receivers must be dispersed in space, ideally placed in an equilateral triangle configuration . The TDoA algorithm establishes a new coordinate system with respect to the three acoustic receivers used for the position estimation (Fang, 1990). The timing accuracy of the receivers' clock signal defines the position resolution yielded by the TDoA algorithm. Although the ISR ensures that the TBRs are synchronised by the nano-level-precision 1PPS signal of the GPS chips every 10 s, the

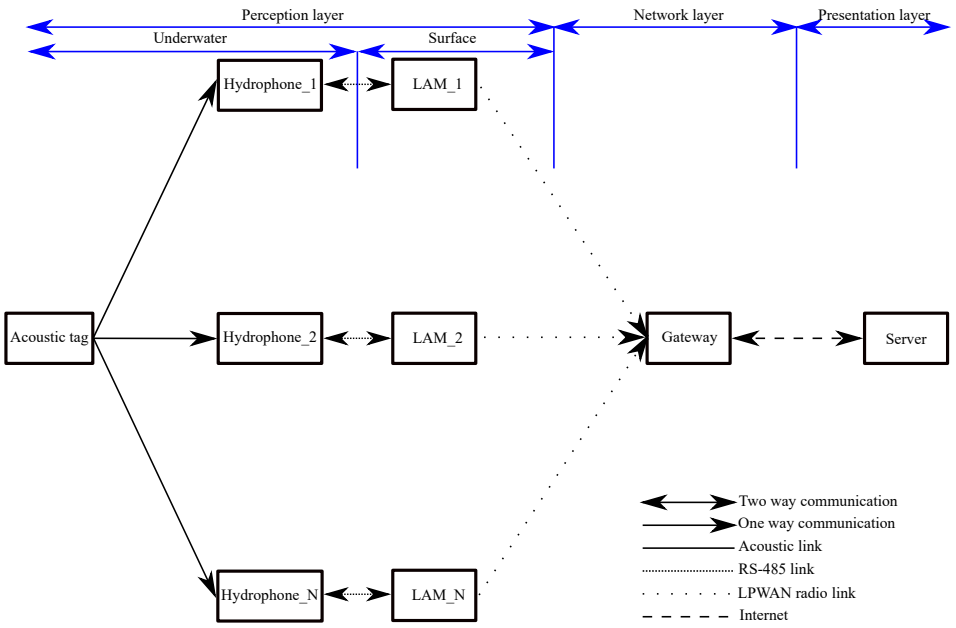

Figure 2.5: Layered view of the IoF concept. Different types of communication protocols used by the IoF are highlighted.

maximum timing resolution of the TBRs at $1\,\mathrm{ms}$ limited the maximum position resolution to $1.5\,\mathrm{m}$.

2.5 Field experiments

The IoF concept was explored and demonstrated by conducting two field experiments in commercial marine fish farms.

2.5.1 Real-time monitoring experiment

The first experiment was conducted at Kråkholmen locality of Bjørøya Fiskeoppdrett AS, and was designed to evaluate the real-time monitoring aspect of the IoF concept and to gauge the communication quality (QoS) provided by the LoRa LPWAN. Three nodes were mounted on to the perimeter of the cage structure in the farm (one cage with two units, and one cage with one unit), whereas the fourth node was fixed on a remote buoy (Fig. 2.6) placed outside the marine farm at a distance of $2.5\,\mathrm{km}$. All nodes communicated with a common gateway placed inside the feeding barge of the fish farm. The three nodes within the farm thus enabled testing the system performance across a range of distances considered as representative of large-scale salmon farms, while the buoy mounted node enabled testing at longer ranges more common to exposed farming sites and for wild fish

monitoring applications. Acoustic test tags were placed close to the receivers to generate acoustic messages for transmission through the IoF and real-time update at the server. Three different types of test tags, with update rates varying from six to ten acoustic messages per minute were used. All nodes were programmed to send one radio message per minute. The Quality of Service (QoS), defined as ratio of the number of packets successfully received at the server to the total number of packets sent by an IoF node, was evaluated as the figure of merit in the experiment.

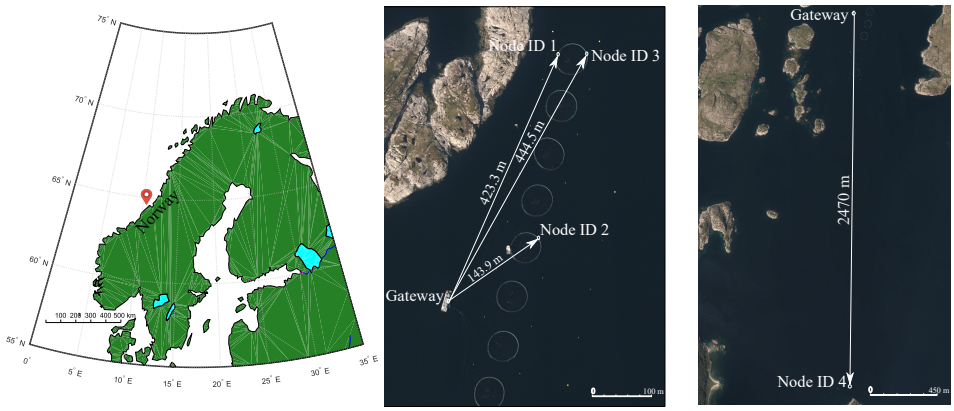

a. Nodes at fish farm b. Remote node

Figure 2.6: Geographical (map on left) deployment of IoF nodes at fish farm (Fig. a) and remote note (Fig. b).

2.5.2 Real-time fish positioning experiment

A second experiment was designed to evaluate the feasibility and positioning accuracy of the real-time underwater positioning support provided by combining the the IoF concept with the TDoA algorithm. The experiment was conducted in two fully stocked sea-cages (Eiterfjorden locality of Midt-Norsk Havbruk AS). The TDoA algorithm needs at least three IoF nodes and hence a message triplet for calculating a tag's position. To improve the chances of getting triplets through redundancy, the IoF nodes were installed in pairs (Fig. 2.7). This meant that a total of 12 IoF nodes, six on each cage were used in the experiment. A gateway was placed inside the feed barge of the farm and was located less than $400\,\mathrm{m}$ from the nodes. At the start of the experiment, a benchmark dataset for estimation of position error bounds (Circular Error Probability - CEP) was collected over a $12\,\mathrm{h}$ period using three stationary tags placed at $1\,\mathrm{m}$, $2\,\mathrm{m}$ and $3\,\mathrm{m}$ depth at the centre of one cage. The system was then used to monitor real-time position of 30 tagged salmon. The experiment lasted for three months.

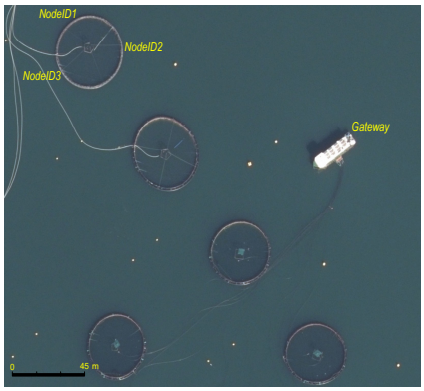

Fig. a

Fig. b

Figure 2.7: Geographical deployment of nodes and redundant installation of LAM/SLIM onto the cage structure.

2.6 Results and discussion

2.6.1 QoS

For both field experiments, a QoS of at least 90% was achieved for all nodes (Table 2.1). The QoS degraded slightly with increase in a node's distance from the gateway, but the QoS was still more than 90%, and some of the nodes placed at lesser than $400\,\mathrm{m}$ from the gateway had a QoS of around 99% for the real-time monitoring experiment. The QoS values degraded slightly for the fish positioning experiment as compared to the monitoring experiment. This could be attributed to the fact that the gateway antenna was placed inside the feed barge in the fish positioning experiment, whereas it was mounted on the roof outside the feed barge in the monitoring experiment. The monitoring experiment nodes had a clear line of sight with the gateway antenna. Nevertheless, the QoS values from the fish positioning experiment were still more than 90% for all nodes. Thus, it was concluded that the IoF could be used as a reliable real-time monitoring system in marine aquaculture farms.

2.6.2 Positioning accuracy

For the real-time fish positioning experiment feasibility of real time positioning, accuracy of the positioning algorithm and message triplet rate (i.e. messages usable by the positioning algorithm) were evaluated. It was possible for a user to select a tag ID and track the fish position in real-time (Fig. 2.8), thus proving the feasibility of real-time fish positioning using the IoF concept.

For the benchmark dataset, the message triplet rate (for the LoRa-link) was more

Table 2.1: Table comparing nodes' link length, number of transmitted (Tx) and received (Rx) packets and QoS for both the experiments. For the RT fish positioning experiment, data from the three nodes used in the benchmark dataset is presented.

Experiment	Node ID	Link length (m)	Packets Tx	Packets Rx	QoS
RT monitoring	1	444.5	10124	10021	0.989
	2	143.9	39414	38786	0.984
	3	423.2	20660	20600	0.997
	4	2470	74380	69073	0.928
RT fish positioning	1	200	1446	1381	0.955
	2	200	1386	1276	0.92
	3	200	1381	1368	0.99

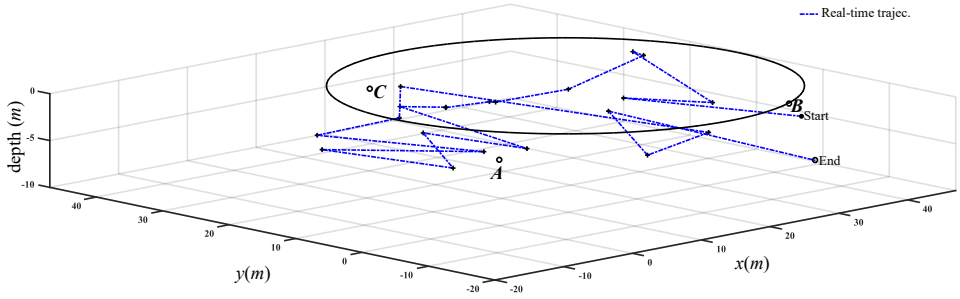

Figure 2.8: 3D position of a tagged fish tracked in real-time. Update rate of the position samples is 3 min (23 samples, ca. 1.5 h). Receivers A, B and C are located along the perimeter of the cage at a depth of 3 m.

than 90% for all the SLIM/LAM nodes, implying that most of the received acoustic messages were successfully transmitted and used for the position calculations. The CEP value reflects error in the calculated position compared to the actual known position of the test tags in the benchmark datasets. Fig. 2.9 shows the error histogram (error in x- and y-coordinate of the tags' estimated position) for the tags used in the benchmark dataset. The CEP value for the benchmark dataset was 1.37 m, 1.49 m and 1.22 m for tags at 3 m, 2 m and 1 m depth, respectively. These values are within the maximum obtainable resolution for time resolutions of 1 ms at 1.5 m. The CEP value could, in theory, be improved by using a receiver with a higher timestamp resolution.

An important limitation of the IoF concept is that it is a soft real-time system for monitoring applications without strict bounds on jitter or network delays and that

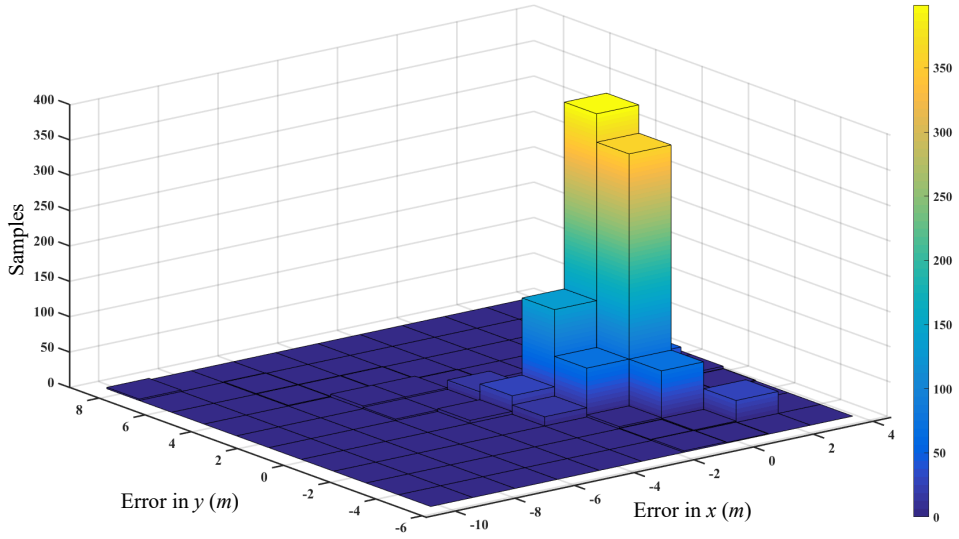

Figure 2.9: Histogram showing error in calculated position for the real-time fish positioning experiment. The dataset includes 1222 samples for the three tags used in the benchmark dataset.

it has a maximum delay of data reaching the user of 60 s. Whereas hard real-time systems should guarantee low latency and bounded jitter values, the LoRa specification neither meet nor specify such criteria (Adelantado et al., 2017). This implies that LPWANs could be used in real-time monitoring applications such as agricultural applications, but they are not suitable candidates for real-time industrial control systems (Adelantado et al., 2017). Considering that the IoF concept was designed for monitoring applications in aquaculture farms, and not as a component in a system for controlling an industrial process, a worst case delay of 60 s seems acceptable. A shorter period would have caused sending too many unnecessary radio packets effecting energy efficiency of the system, whereas a longer period would have lead to a sluggish system response for the end-user.

Acoustic telemetry systems may use acoustic tags operating at multiple frequencies and varying update rates. This could lead to a relatively high acoustic detection load and channel congestion, which could result in a situation where IoF is unable to transmit some of the acoustic messages. This problem was indeed observed in the real-time fish positioning experiment. The IoF concept was designed to accept a maximum of 11 acoustic messages per 1 min, however at times, the number of acoustic detections received during the experiment exceeded this limit, resulting in that some acoustic messages were not transmitted. In response to the congestion problem, the SLIM/LAM firmware was updated with a compres-

sion scheme where the 32-bit timestamp was sent only once at the start of a radio packet for all acoustic detections containded in the radio packet. The compression scheme saved three bytes for each acoustic detection by not repeatedly sending the full timestamp. This increased the message handling capacity of the IoF concept from 11 to 20 messages per minute.

One of the main goals of the PFF concept is to make operations at farms more autonomous in future (Føre et al., 2018). The IoF could contribute to this by representing a foundation for future system for online tracking and positioning of individual fish. This would provide data that could be useful inputs to future autonomous operations at marine fish farms.

Chapter 3

Doppler-based fish swimming speed measurement

3.1 Introduction

This chapter presents the contribution toward achieving Objective 2, which is a novel Doppler-based principle for measurement of swimming speed of individual free-ranging fish developed and verified in this thesis. First, some motivation behind development of a method for *in-situ* swimming speed measurement is briefly discussed as well as its applications in marine aquaculture. The basics of the physical Doppler effect and the proposed speed measurement principle are then presented. The speed estimation algorithm was developed from the ground up in this study and was validated through a series of experiments. The experiments ranged from very simple static speed measurements in a lab tank to speed measurements of a controlled platform with predefined motion trajectories deployed in a fully stocked sea-cage. As a final step, the measurement principle was demonstrated in an operational fish farm with tagged salmon. The various experimental stages and their results are presented at the end of the chapter.

3.2 Papers' introduction

The initial results from the sea-cage experiment were published in a conference article C2 and were also presented in a poster. This article proposes the idea of Doppler-based fish speed measurement and only discusses 2D speed computations for slow speed datasets ($<50\,\mathrm{cm\,s^{-1}}$). A more detailed implementation of the speed computation algorithm both in 3D and 2D and results from all the experimental stages are presented in article J2. J2 also shows the derivation steps for eqs. 3.18

and 3.22 in four quadrants of the coordinate system. The final manuscript M1 presents results from the live tagged fish experiment and is in preparation.

3.3 Motivation

The energy budget of a fish can be expressed by a very simple mass-balance and energy conservation equation (Cooke et al., 2016):

$$Energy\,consumed = Metabolism + Growth + Waste \tag{3.1}$$

Assuming a constant growth factor and waste, the consumed energy is directly proportional to the metabolic activity in the fish. Although there exist models to estimate the overall metabolism and growth energy consumption directly, such models are not suitable for in-situ measurement for free-ranging fish (Cooke et al., 2016). To understand the metabolism and growth in sea-cages, we therefore need tools to assess the various components in the fish' energy budget. Since locomotory activity is one of the most important components in the overall metabolic energy consumption (Cooke et al., 2004), monitoring of swimming speed would be highly relevant for energy expenditure of a fish. The fish's motion and swimming speed are also linked to its welfare in terms of stress and fatigue (Hvas and Oppedal, 2017; Johansson et al., 2014). Observing fish welfare becomes increasingly relevant in the current trend with fish farms being placed at relatively more exposed locations (Bjelland et al., 2015), where fish would potentially face stronger currents (Johansson et al., 2014).

Fish swimming is a complex process that involves a coordinated motion of various body parts. A straightforward approach for measuring fish swimming capacity is use of a swimming tunnel (Remen et al., 2016; Hvas and Oppedal, 2017). In this method, fish are forced to swim against a water current with known speed, meaning that if the fish is stationary within the tunnel, it maintains a swimming speed equal to the current induced in the tunnel. A different approach for quantifying fish swimming speed is in-situ measurement inside a sea-cage, which while being less accurate than lab trials, may provide data that is more relevant for a culture setting. Popular method to achieve this is the use of camera (Pinkiewicz et al., 2011), where a group of fish is recorded and machine vision algorithms are applied for estimation of swimming speed. Similar observations can also be made using acoustic instruments such as echosounders and split-beam sonars could also be used for fish speed measurement (Pedersen, 2001). However, both video based and acoustic instruments are limited by the field of view. Video cameras are also limited by turbidity and the propagation characteristics of light in water (Pincock and Johnston, 2012; Williams et al., 2006). In addition, such instruments cannot track individual fish swimming speed over time (Macaulay et al., 2021), as this

may allow for more accurate assessments of fish states also on an individual level.

Acoustic telemetry offers a possibility to remedy this situation in being an inherently individual centred approach that is less sensitive to the position of the fish in the cage than visual or acoustic methods. The method has been used to measure average speed of individual free-ranging fish by using the TDoA positioning algorithms and tags sending messages at a relatively high transmission rate, however, such systems are vulnerable to positioning inaccuracies (Rillahan et al., 2009; Biesinger et al., 2013; Espinoza et al., 2011). Individual fish swimming speed has also been measured using speed turbines attached externally to a fish (Gabaldon et al., 2019).Another similar external attachment technique is based on differential pressure sensor (Webber et al., 2001). However skin abrasion and minimum size of animals that could be fitted with the turbine or pressure speed sensor make this solution unfeasible for farmed salmon. It is hence desirable to develop a new acoustic telemetry solution which could provide swimming speed measurements of individual free-ranging fish without these limitations.

3.4 Proposed solution - the Doppler effect

3.4.1 Doppler effect basics

Since acoustic telemetry transmits data using acoustic signals, the Doppler shift in the carrier wave caused by the relative motion between the transmitter and receiver could, in theory, be exploited as a means to measure individual swimming speed. The Doppler effect is the change in observed frequency (from a receiver's point of view) in a signal due to relative motion between the signal's source and receiver. This is a well-established physical phenomenon first presented by Austrian physicist Christian Doppler in 1842 and later verified experimentally by the Dutch meteorologist Buys Ballot in 1845 (Halliday et al., 2013). The effect is observed both in mechanical (e.g. acoustic) and electromagnetic (e.g. visible light) waves and has wide range of applications in astronomy, radar systems, satellite communication, robotics, medicine and underwater sensors. Fig. 3.1 conceptually illustrates the Doppler effect for acoustic waves in a medium. A source S is moving along the x-axis. An observer (receiver) located on the same axis will observe that the wavelength of the transmitted signal is stretched or compressed, resulting in a decrease or increase in the observed frequency respectively, depending on the source's direction of motion.

An interesting application of the Doppler effect in nature is precise echolocation by certain species of bats (Schoeppler et al., 2018). Bats use acoustic waves and echolocation for localisation, navigation, and orientation in space and for searching for prey. A bat emits tonal acoustic signals in in the form of pulses and analyses the

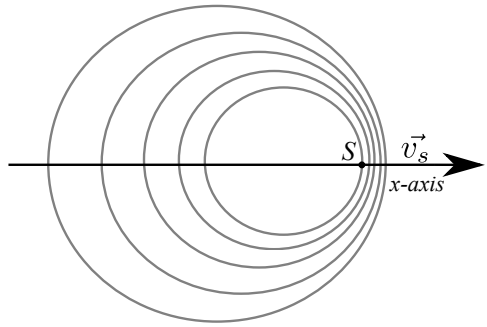

Figure 3.1: A source S moving with velocity v_s along the x-aixs. From an observer's perspective, the wavelength is compressed in the direction of the motion whereas it is stretched in the opposite direction.

returning echoes from surroundings and prey for hunting. The internal hearing system of bats is highly specialised and fine-tuned for specific acoustic frequencies. The Doppler effect states that a relative movement between a moving prey (target) and a flying bat (source) will cause a shift in frequency of the returned echo. This shifted frequency might fall outside the frequency range of a bat's internal hearing system. To ensure that the returning echoes lie within the frequencies of the hearing system, bats use a Doppler shift compensation technique, where they adjust the signal frequency by emitting a frequency chirp signal while chasing a prey such that the Doppler shifted frequency of the received echoes can be detected by the hearing system. In this way, bats use the Doppler principle for localisation and speed estimation of the prey (Schoeppler et al., 2018).

Another application of the principle is a Doppler radar which has several applications including military, civil aviation and traffic police. As an example, a traffic police radar, also known as a radar gun, transmits a pulse of electromagnetic waves with a known centre frequency. The radar gun is targeted at a vehicle of interest and the transmitted electromagnetic waves are then reflected from the vehicle and received back at the radar gun. The radar gun uses Doppler shift equations with additional signal processing techniques to calculate speed of the moving vehicle (Halliday et al., 2013).

Similarly, the Doppler effect is also exploited by acoustic devices ranging from medical ultrasonic equipment to sonars used for seabed mapping, ship speed measurement and ocean current profiling (Hovem, 2007). An acoustic instrument of particular interest in this situation are Acoustic Doppler Current Profilers (ADCPs) which are specialised multi-sonar instruments used for profiling ocean currents.

3.4.2 Proposed solution

The first step in designing a system for monitoring fish swimming speed using the Doppler effect and acoustic telemetry is to derive the equations that establish the relationship between fish movement and frequency shifts.

Fundamental equations

The relationship between the observed frequency, the source frequency and speed of the source and receiver moving in a straight line relative to each other is given by (Hovem, 2007):

$$f_d = \frac{\Delta v}{c} f_s \tag{3.2}$$

$$f_d = f_r - f_s \tag{3.3}$$

$$\Delta v = v_s - v_r \tag{3.4}$$

Where f_s is the signal's frequency at the source, f_r is the signal's frequency at the receiver, f_d is Doppler shifted frequency (DSF), Δv is difference in speed of the source (v_s) and receiver (v_r) and c is speed of the signal carrier wave in the medium.

Eq. 3.2 can be simplified for the case of a static receiver (i.e. $v_r = 0$) as:

$$f_d = \frac{v_s}{c} f_s \tag{3.5}$$

The DSF (f_d) thus depends on the component of the source velocity along the line spanned between the source and receiver. For the cases when the source movement is not directly towards or away from the receiver, a more generalised form of eq. 3.5 can be written as:

$$f_d = \frac{v_s cos\theta_s}{c} f_s \tag{3.6}$$

Where θ_s is angle between the movement vector and the straight line connecting the source and receiver. If the source's movement is directly towards or away from the receiver, i.e. $\theta_s = 0$, eq. 3.6 reduces to eq. 3.5.

Rearranging eq. 3.6 with respect to the source speed as the target variable yields:

$$v_s = \frac{f_d c}{f_s cos\theta_s} \tag{3.7}$$

In most physical systems, f_s is usually a known design parameter, while f_d can be estimated at the receiver by using standard frequency analysis methods such as the Fast Fourier Transform (FFT). If θ_s is known, a moving sources' speed (v_s) can then be determined by using eq. 3.7. It is possible to estimate θ_s by using

an array of receivers of known geometry and applying eq. 3.7 simultaneously for all receivers. An exact solution might not be achieved in such a scenario, since the procedure involves solving non-linear equations (Chan and Towers, 1992). Another possibility is to find θ_s through a geometric analysis given the source and receiver positions. This approach assumes that the source position is already known. It is then possible to get an exact solution using eq. 3.7. This approach was demonstrated by Ferguson (1993), where an array of static hydrophones (acoustic receivers) placed in water and a microphone placed on ground were employed to measure an aeroplane's speed from the Doppler shift in the acoustic tone signal generated by propeller of the plane.

Speed computation algorithm in a 2D plane

The speed computation algorithm used in the proposed method employs eq. 3.7 to measure free-ranging swimming speed of a tagged fish. In addition, it uses a geometric approach to estimate θ_s. Fig. 3.2 shows application of the algorithm in 2D (x, y) setup using two acoustic receivers A and B. A fish at position $O(x_O, y_O)$ is swimming with a velocity v_s. The velocity vector v_s makes an angle θ_s with the x-axis. The cosine components of v_s observed at the receivers A and B are $v_s cos\alpha$ and $v_s cos\beta$ respectively, where α is angle between the line OA and v_s and β is angle between the line OB and v_s. Instead of estimating the angles θ_s, α or β, the algorithm relates the difference of angles α and β to the $\angle AOB$ of the triangle $\triangle AOB$ as:

$$\angle AOB = \beta - \alpha \tag{3.8}$$

$\angle AOB$ can be calculated as long as the position of the tag $O(x_O, y_O)$ is known. Once $\angle AOB$ is known, application of trigonometric identities and simplification lead to an expression for α.

The DSFs observed at receivers A (f_{dA}) and B (f_{dB}) are given by:

$$f_{dA} = \frac{v_s cos\alpha}{c} f_s \tag{3.9}$$

$$f_{dB} = \frac{v_s cos\beta}{c} f_s \tag{3.10}$$

Dividing (3.9) by (3.10) yields:

$$\frac{cos\alpha}{cos\beta} = \frac{f_{dA}}{f_{dB}} \tag{3.11}$$

Deriving β from (3.8) and inserting it into (3.11) then yields:

$$\frac{cos\alpha}{cos(\angle AOB + \alpha)} = \frac{f_{dA}}{f_{dB}} \tag{3.12}$$

Inverting and solving (3.12) for α yields:

$$\frac{cos(\angle AOB + \alpha)}{cos\alpha} = \frac{f_{dB}}{f_{dA}} \tag{3.13}$$

$$\frac{cos(\angle AOB)cos\alpha - sin(\angle AOB)sin\alpha}{cos\alpha} = \frac{f_{dB}}{f_{dA}} \tag{3.14}$$

$$cos(\angle AOB) - \frac{sin(\angle AOB)sin\alpha}{cos\alpha} = \frac{f_{dB}}{f_{dA}} \tag{3.15}$$

$$cos(\angle AOB) - sin(\angle AOB)tan\alpha = \frac{f_{dB}}{f_{dA}} \tag{3.16}$$

$$tan\alpha = \frac{cos(\angle AOB) - \frac{f_{dB}}{f_{dA}}}{sin(\angle AOB)} \tag{3.17}$$

$$\alpha = atan(\frac{cos(\angle AOB) - \frac{f_{dB}}{f_{dA}}}{sin(\angle AOB)}) \tag{3.18}$$

Angle β can be found using eq. 3.8 and α. Finally, v_s can be calculated using:

$$v_s = \frac{f_{dA}c}{f_s cos\alpha} \tag{3.19}$$

, or in terms of β as:

$$v_s = \frac{f_{dB}c}{f_s cos\beta} \tag{3.20}$$

, and θ_s can be calculated using:

$$\theta_s = 360^\circ - \beta - \angle BOX \tag{3.21}$$

Where $\angle BOX$ is the angle calculated from the position of the tag $O(x_O, y_O)$ along the x-axis(Fig. 3.2)

Extension to 3D space

Since fish also move vertically, motion along the z-axis (depth) is also important. Speed measurement in 3D requires three acoustic receivers. Receivers A and B are then placed in the xy-plane, whereas receiver D is placed at deeper position to span a 3D space (Fig. 3.3). The above set of equations are applied twice, first for the xy-plane (A and B) and afterwards for the yz- or xz-planes formed by the third receiver (D). As a final step, equations from both the planes are combined to measure true fish speed. The fourth receiver C is present to enable TDoA localisation of the tag's position O (refer to Fig. 3.3).

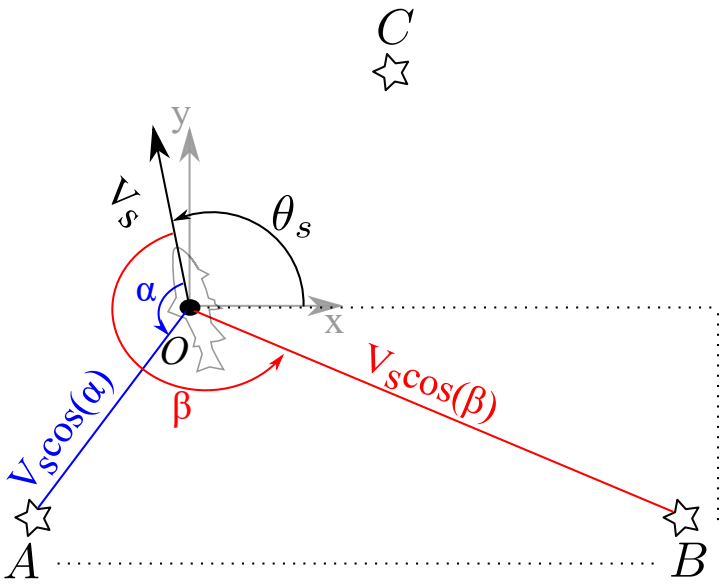

Figure 3.2: A tag located at O moving with a velocity v_s in the horizontal plane. The Doppler shift measured at receiver A and B will be proportional to the components of the transmitter speed v_s along the lines AO and BO, respectively, defined by the angles α and β. A third receiver at location C enables TDoA localisation of the tag at position O.

In case of 3D speed, eq. 3.19 is modified and v_s is given by:

$$v_s = \frac{f_{dA} c}{f_s cos\alpha sin\xi_s cos\gamma} \tag{3.22}$$

Where γ is the angle between the receivers' plane (A, B and C) and the line BO and ξ_s is the angle between v_s and z-axis (Fig. 3.3). The angle γ is measured using the 3D position of the tagged fish i.e. $O(x_O, y_O, z_O)$ and the receivers reference positions, whereas the angle ξ_s is calculated using the DSF at the receivers B and D and eq. 3.8 and 3.18. Adding a third receiver (D) thus enables the calculation of the angle ξ_s and hence the true 3D speed v_s.

3.5 Experimental verification

The proposed method was verified and validated using an incremental approach and was tested in two phases. In the first phase, the method was verified through three different experimental setups without using live fish. The first step of these was a lab experiment to evaluate the feasibility of pulse frequency extraction for a static tag and simple 1D motions, while the second experiment was conducted using a tag mounted on a catamaran moving in more complex 2D patterns in a close to shore fjord environment. In the third and final experiment, the same catamaran

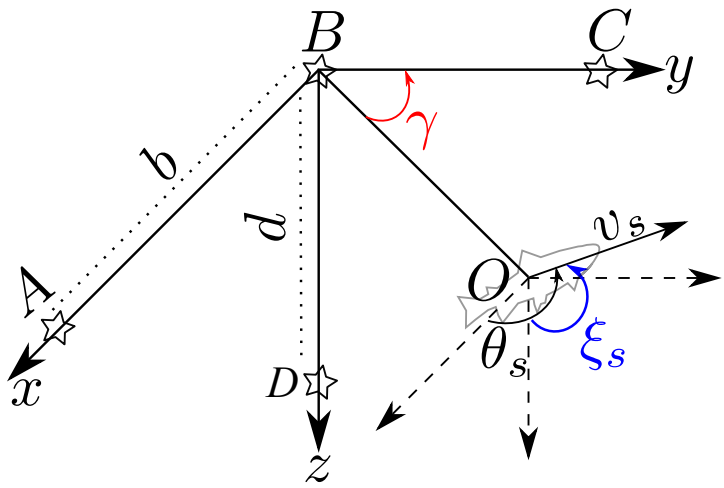

Figure 3.3: Algorithm for 3D fish velocities using three acoustic receivers. Receivers A and B are used to derive the direction of v_s in the plane spanned between them and $O(\theta_s)$, while receivers B and D are used to derive the angle in the plane $BDO(\xi_s)$. The fourth receiver C is present to enable TDoA localisation of the tag's position O. Angle γ accounts for scaling of the velocity vector v_s with the tag's depth variation.

was placed in a fully stocked commercial marine farm to evaluate the performance in a relevant environment. While the basic properties of the method was verified in the experiments in phase 1, phase 2 included an experiment using live fish carrying acoustic tags in a commercial sea-cage, with the intention of verifying the use of the method in a real farming situation.

Phase 1

The first task in phase 1 was to acquire the means to transmit a well-defined and stable centre frequency. A custom-made acoustic tag transmitting at a centre frequency of $68.968\,\mathrm{kHz}$ was therefore developed. An eight-pulse burst signal similar to the PPM, but with longer pulse duration ($128\,\mathrm{ms}$), was used as a target signal (Fig. 3.7). An embedded system that simultaneously generated the acoustic signal and logged the position and true speed of the tag was then developed. True speed and position were obtained using a rotary encoder in the lab experiment and a Real Time Kinematic (RTK) GPS in the field trials, and were used as ground truth for calculating error in the Doppler speed measurement, and input for the speed computation algorithm respectively.

For all phase 1 experiments, up to three broad spectrum digital hydrophones (Ocean Sonics Ltd., Nova Scotia, Canada) were employed as receivers. The hydrophones were set to collect and store the data in .wav file format. The duration of a single

dataset was set to $10\,\mathrm{min}$, whereas the sampling frequency was set to $256\,\mathrm{kS\,s^{-1}}$. The datasets were analysed via a signal processing script developed in Matlab (MathWorks, Inc., Natick, Massachusetts, USA) (Fig. 3.4). The FFT analysis was performed on a single pulse basis and pulses across three hydrophones were synchronised using the start time of a pulse detected via an amplitude threshold detector. The script was programmed to calculate tag speed using average (arithmetic mean) and modal values of the eight DSF peaks in a single burst, resulting in two different statistical methods for Doppler speed estimation. To explore the sensitivity of the method to imprecise position inputs, Matlab simulations where tag positions were varied with a known error were used. Typical Circular Error Probability (CEP) values for a TDoA fish positioning algorithm i.e. up to $1.5\,\mathrm{m}$ were used in the simulations.

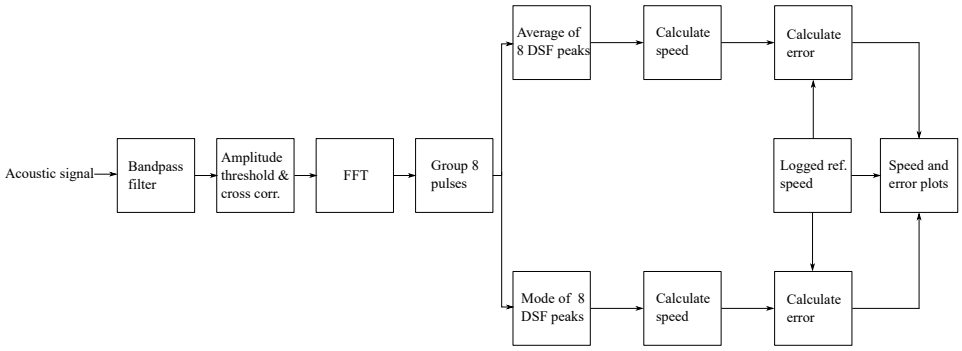

Figure 3.4: Matlab script and signal processing block diagram. After filtering the acoustic signal via a band-pass filter, amplitude threshold detection and cross-correlation operations were performed to detect the start time of a pulse. The pulse start time was then used for identifying the same pulse across all the three hydrophones and for the TDoA algorithm. For phase 1 experiments, Doppler speed was calculated using both average and modal DSF values of eight pulses in a single burst. True speed from the embedded systems' log file was used as a ground truth for error calculations and for speed time series comparison.

In all three 1 experiments in phase 1, the tag was moved along a predetermined trajectory while the embedded system simultaneously transmitted acoustic signal and logged the tag's position and speed. Afterwards, the signal received at the hydrophones was processed using the signal processing chain shown in Fig. 3.4. The target speed and trajectories varied between the three experiments. Speeds from $5\,\mathrm{cm\,s^{-1}}$ to $20\,\mathrm{cm\,s^{-1}}$ were used in the lab experiment, whereas speeds from $25\,\mathrm{cm\,s^{-1}}$ to $110\,\mathrm{cm\,s^{-1}}$ (typical swimming speed of Atlantic salmon) were used in the fjord and sea-cage trials.

Experimental setup

For the lab experiment, a DC motor cart-rail setup was developed for moving the tag (Fig. 3.5a). The tag was mounted on a rod protruding about $1\,\mathrm{m}$ into the water in a tank (dimensions $4.3\,\mathrm{m}$ x $1.3\,\mathrm{m}$ x $2\,\mathrm{m}$). A single hydrophone placed in a fixed position at approximately $1\,\mathrm{m}$ depth was used as receiver. The embedded control system was programmed to move the cart and tag along a straight line, either directly towards or away from the hydrophone, i.e. the angle between tag and hydrophone was always 0°. Since this resulted in 1D motion, the tag's true speed could be measured with an encoder mounted onto the motor shaft.

The fjord experiment was conducted closed to shore in an unrestricted sea environment, using a remote-controlled catamaran (Fig. 3.5b) to carry the embedded computer and the rod that placed the tag at $1\,\mathrm{m}$ depth. For position and reference speed measurements, an onboard RTK GPS was used. The embedded system was logging start time of the acoustic pulse-bursts, as well as the position and speed of the catamaran. The experiment was designed as an extension to the lab experiment and the proposed algorithm was evaluated for 2D trajectories. Although the catamaran (and hence the acoustic tag) had a linear trajectory in the fjord experiment, the 2D motion effect was achieved by using two hydrophones. One of the hydrophones was placed inline with the motion of the tag, whereas the second hydrophone was placed at 90°(Fig 3.6a). Due to the geometrical placement of the hydrophones, the angle between the tag trajectory and the line between the tag and the first hydrophone was constant, i.e. 0°, whereas it was changing from -45°to 60°at the second hydrophone.

The final experiment in concluding phase 1 was conducted inside an industry-scale fully stocked sea-cage (about 200,000 fish). Three hydrophones were arranged in a semi-circle configuration on the perimeter of the sea-cage as shown in Fig. 3.6b). The catamaran was moved in a circular trajectory inside the sea-cage, resulting in a scenario where the cosine angles between the tag and the three hydrophones were changing all the time (Fig. 3.6b). The experiment was designed to gauge the effect of acoustic reflections (from sea surface, biomass in the sea-cage and nearby objects) on the error bounds, to verify the speed computation algorithm by varying the cosine angles α and β (Fig. 3.2) and most importantly to demonstrate and assess the proposed method in the targeted environment.

Phase 2

Phase 2 was designed to test the feasibility of the proposed method with live tagged fish, and hence included development of a custom-made depth sensing acoustic tag that was possible to implant into live fish. The custom tag used the same

Fig. a

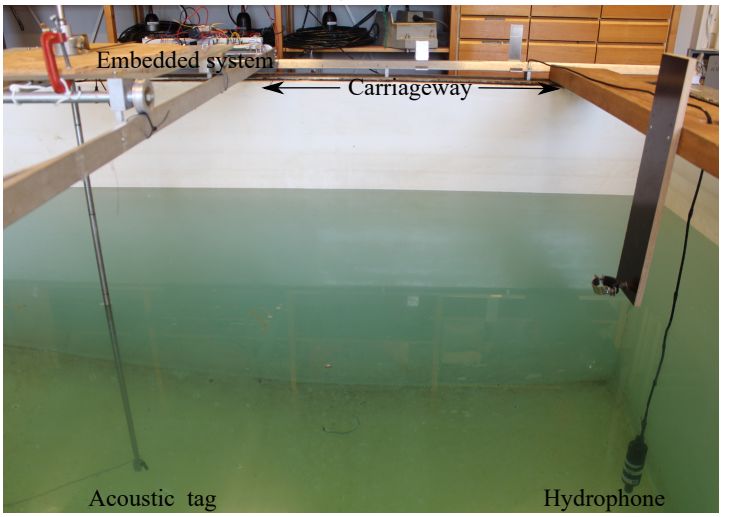

Fig. b

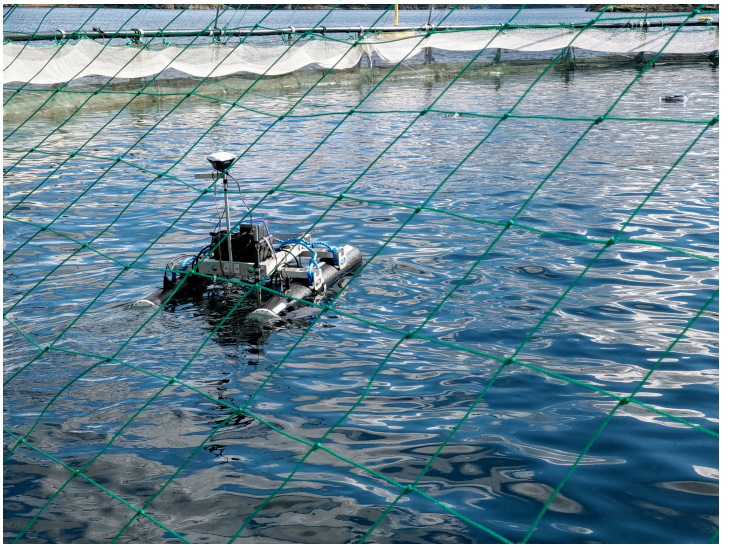

Figure 3.5: Fig. a: Mechanical setup for the lab experiment. Fig. b: Catamaran used in the sea trials.

hardware as an existing commercial off the shelf (COTS) tag (Thelma Biotel AS, Trondheim, Norway), but using a modified firmware enabling the tag to transmit both the conventional $10\,\mathrm{ms}$ PPM signals and a burst of eight $200\,\mathrm{ms}$ pulses for the Doppler computation (Fig. 3.7). The Doppler speed precision is directly related to the used pulse width and improves with longer pulses (Lhermitte and Serafin,

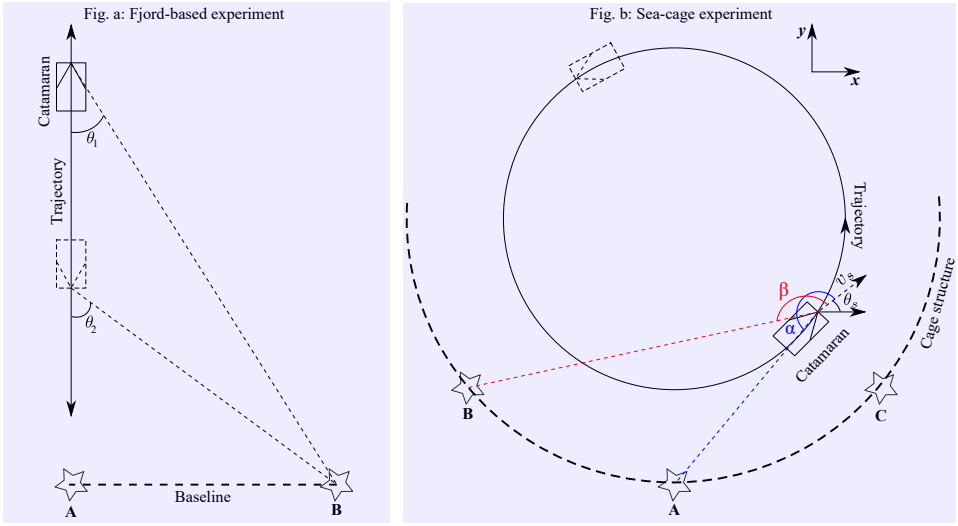

Figure 3.6: Illustration of the phase 1 fjord and sea-cage experimental setups. In the fjord experiment, (Fig. a) the catamaran and tag were moved in a straight-line trajectory and two hydrophones were placed at a distance (baseline) to capture the cosine component of the speed at one of the hydrophones. In the sea-cage experiment (Fig. b), the catamaran and tag were moved in a circular trajectory, with constantly changing cosine angles at all three hydrophones.

1984). Therefore, a relatively longer pulse widths was used, which also makes pulses robust against noise. The Doppler pulses had a fixed spacing of 300 ms. Subsequently, after a guard time of 2.5 s, the tag was programmed to transmit the conventional 10 ms PPM encoded signal containing the tag ID and the depth sensor value. The message update rate of the tag was set to 15 s, meaning that speed and depth measurement pairs were provided at this rate. Six acoustic tags were produced, each operating at unique centre frequency, ranging from 67 kHz to 72 kHz with a spacing of 1 kHz. The centre frequency and its variation due to temperature change from 6 °C to 15 °C was evaluated for all the tags prior to the experiment.

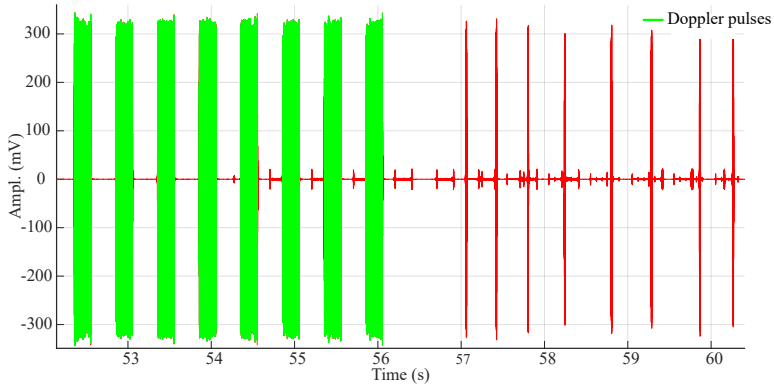

Figure 3.7: A single transmission from the custom-made Doppler acoustic tag consisted of a burst of eight pulses of extended duration (200 ms green pulses), which were used for Doppler speed calculations. In addition, the tag also transmitted the conventional PPM encoded signal (10 ms red pulses), providing tag ID and depth.

The experiment was conducted in a fully stocked sea-cage (about 200,000 fish) at the Eldviktaren farm site of the Bjørøya Fiskeoppdrett AS for a duration of eight days. Five fish (ID 110 body length 70 cm, ID 120 body length 62 cm, ID 130 body length 65 cm, ID 140 body length 64 cm and ID 150 body length 72 cm) were tagged surgically using the procedure described in Urke et al. (2013). The tagging was approved by the Norwegian Animal Research Authority (NARA, ID 23265). The sixth tag was deployed at a fixed position and depth (3.4 m) at the edge of the cage throughout the experiment. This static tag was used as a reference for calculating the minimum expected error in the measured speed for the tags implanted inside fish. In addition, the reference tag's measured speed was also used for comparison with the results from the experiments of phase 1. Four hydrophones (Ocean Sonics Ltd., Nova Scotia, Canada) were used to record data in the experiment. Three hydrophones A, B and C were placed in a circular configuration in the horizontal xy-plane along the perimeter of the sea-cage at a depth of 2 m. The fourth hydrophone (D) was placed at a depth of 18.5 m, directly below hydrophone C, making an yz-plane for 3D speed measurement. In addition, three TBR-700-RT (Thelma Biotel AS, Trondheim, Norway) acoustic receivers were co-located with the hydrophones A, B and C (Fig. 3.8) to log the fish swimming depths transmitted by the tags. Hydrophones A, B and C were used to derive the xy position of the fish using the TDoA algorithm, while the swimming depths from the TBR-700-RT receivers were used to resolve the depth. The TBR-700-RT receivers also acted as a secondary fish positioning system and logged the water temperature during the experiment every 10 min). A benchmarking dataset of approximately 20 h duration was initially collected in which all six tags were kept

stationary at known positions, before they then were surgically implanted into the fish.

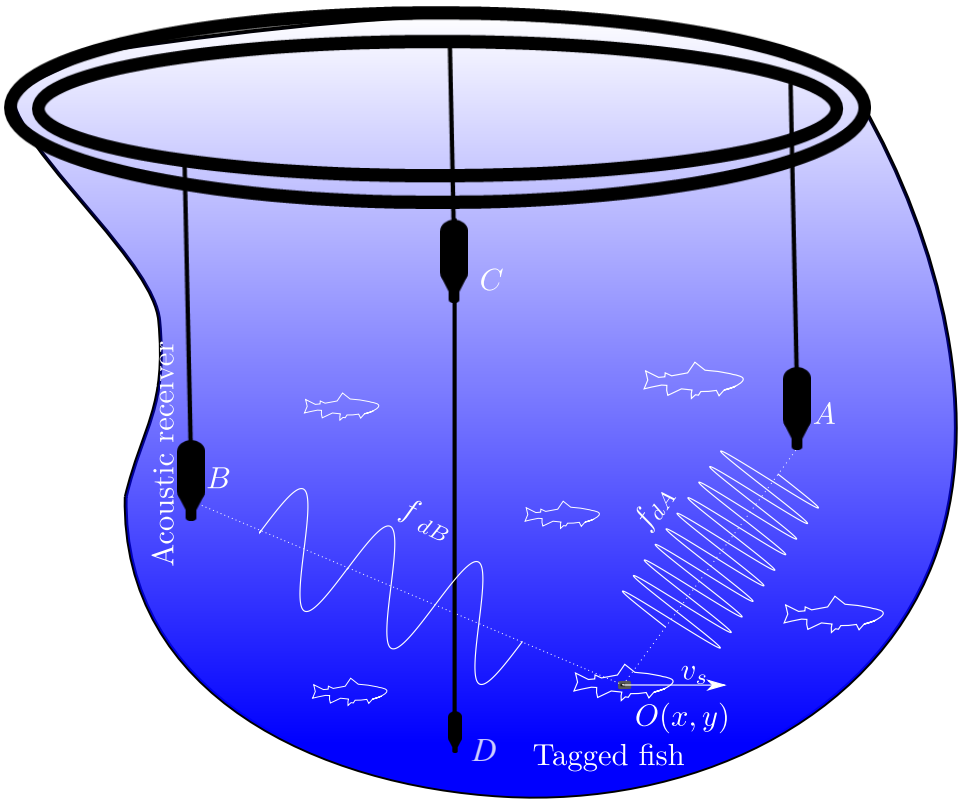

Figure 3.8: Phase 2 experimental setup. Hydrophones A, B and C were placed at same depth in the xy-plane whereas hydrophone D was placed at a depth of $18.5\,\mathrm{m}$ right below hydrophone C, making a yz-plane for speed measurement in 3D.

3.6 Results and discussion

3.6.1 Results

Phase 1

The phase 1 experiments confirmed that the deviation between the Doppler-based speed measurements and the true speed were relatively small. Moreover, the arithmetic mean was generally more accurate for Doppler speed calculation than the modal value in both lab and fjord trials (Hassan et al., 2019a), as shown in the time series of Fig. 3.9. Since the rms error was slightly higher using the modal value, the arithmetic mean was chosen as the measure of central tendency in the further

analysis of the datasets from the sea-cage experiment.

Fig. 3.9 shows how variation in the angle θ leads to differences in the measured speed obtained at the two hydrophones in the fjord experiment. The magnitude of the measured speed is constant for the inline hydrophone whereas only direction to and fro (a positive value means towards and a negative values means away) is changing, giving a rectangular waveform (Fig. 3.9a). For the receiver placed at an angle (Fig. 3.9b), not only direction but also the magnitude of the measured speed is changing due to change in the observed angle, rendering a cosine waveform. This result was corroborated by the ground truth speed obtained from the RTK GPS.

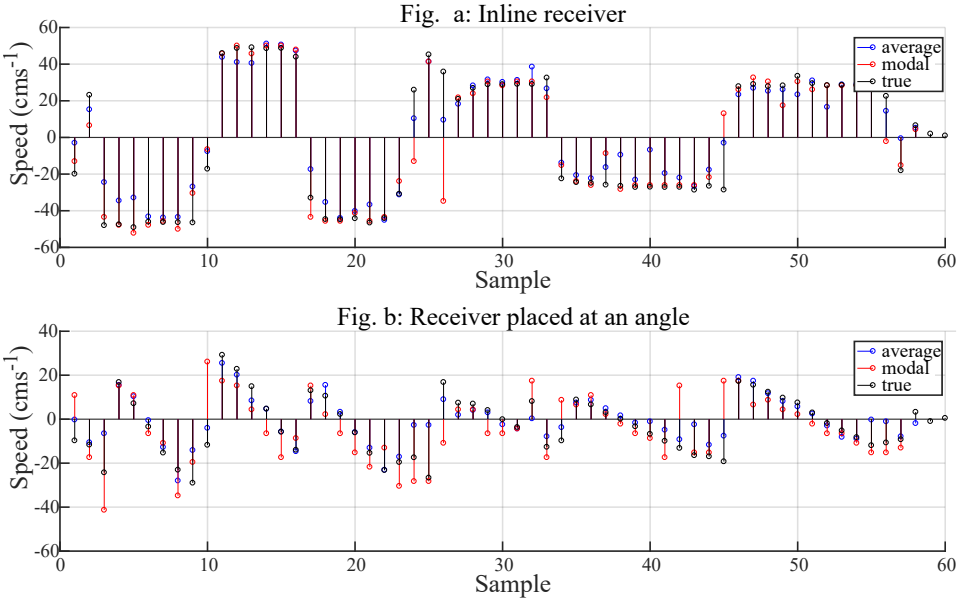

Figure 3.9: Doppler speed measurement for a hydrophone placed inline (Fig. a) and at an angle (Fig. b) with respect to a transmitting tag (see Fig. 3.6a). The rectangular-shaped waveform in Fig. a was obtained when the hydrophone was placed inline with the tag motion and relates with the straight line motion as observed by this hydrophone. The observed angle and magnitude of the measured speed were changing at the hydrophone placed at an angle with respect to the transmitter, rendering the cosine waveform in Fig. b. Both the time series represent a single 10 min dataset.

Fig. 3.10 shows the same effects of variation in angle in the sea-cage experiment. Here, the angle and hence the Doppler speed appears as a sinusoidal function at both the hydrophones, which is expected and verified by the circular motion of the catamaran.

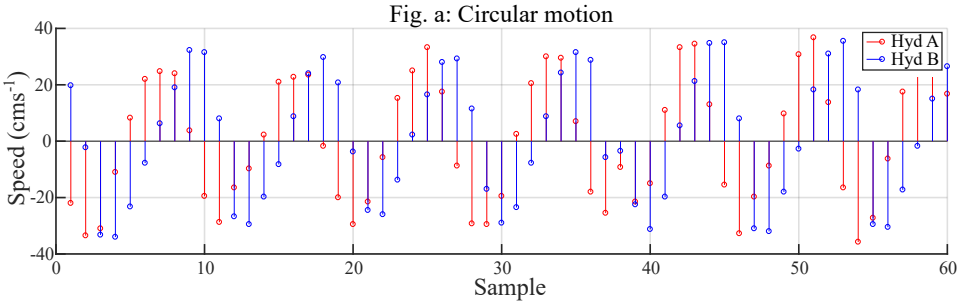

Figure 3.10: Doppler speed measurement at hydrophones A and B during the sea-cage experiment. The catamaran had a circular trajectory (see Fig. 3.6b), leading to a sinusoidal shaped speed measurement at the hydrophones. The measured speed (and hence the two sinusoids) at hydrophone A and B were at a constant offset corresponding to the distance between the hydrophones. The plot is for a single dataset of $10\,\mathrm{min}$ duration.

The cross-correlation coefficient between the measured and true speed was 0.9286 (N=357) for the entire speed range (i.e. $20\,\mathrm{cm\,s^{-1}}$ to $110\,\mathrm{cm\,s^{-1}}$). Fig. 3.11 shows a scatter plot and the cross-correlation for all datasets obtained from the sea-cage experiment.

Datasets from the sea-cage experiment were sub-divided into groups of low- and high-speed for further statistical analysis and to assess the error bounds more closely in relation with the sustained (belonging to low-speed group) and critical (belonging to high-speed group) swimming speed of Atlantic salmon. Histograms and normal distribution functions for measured and true speed and rms error (true-measured speed) were fitted to the data. The low-speed dataset had an rms error of $5.0\,\mathrm{cm\,s^{-1}}$ (mean $-1.9\,\mathrm{cm\,s^{-1}}$, std. dev. $4.7\,\mathrm{cm\,s^{-1}}$), whereas the high-speed dataset had an rms error of $10.2\,\mathrm{cm\,s^{-1}}$ (mean $-2.9\,\mathrm{cm\,s^{-1}}$, std. dev. $9.8\,\mathrm{cm\,s^{-1}}$). The relative error to speed ratio was constant at approximately 10% for both the speed groups. Fig. 3.12 and Fig. 3.13 shows speed and error histograms for the low- and high-speed datasets for the sea-cage experiment.

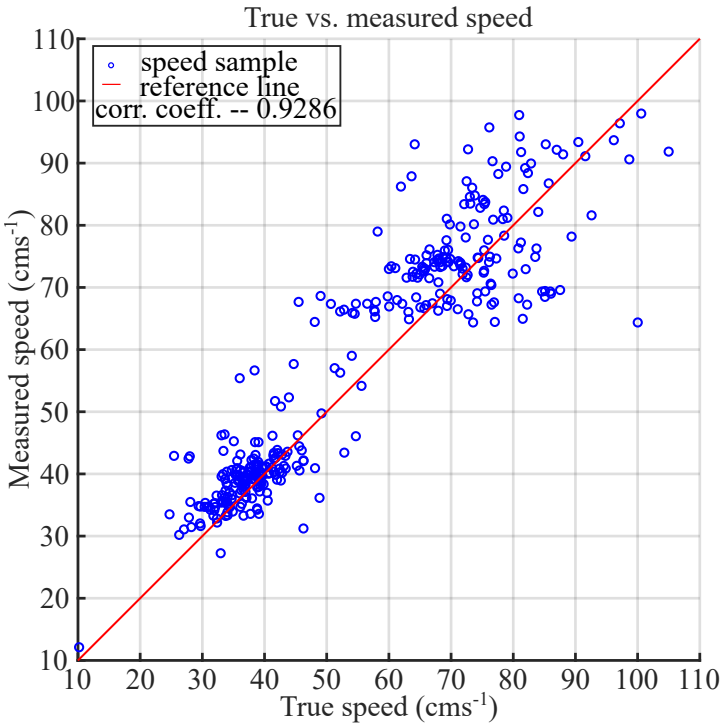

Figure 3.11: Scatter plot and reference line (1:1) for the sea-cage experiment dataset (N=357).

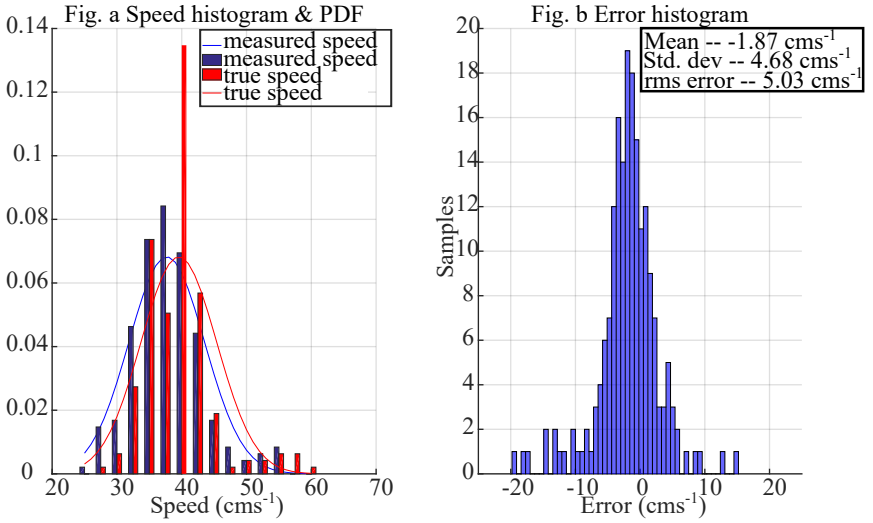

Figure 3.12: Speed and error histograms for measured and true speed. The rms error was calculated as square root of mean square values of the speed difference (measured and true). Both histograms represent the low-speed case of phase 1 of the sea-cage experiment.

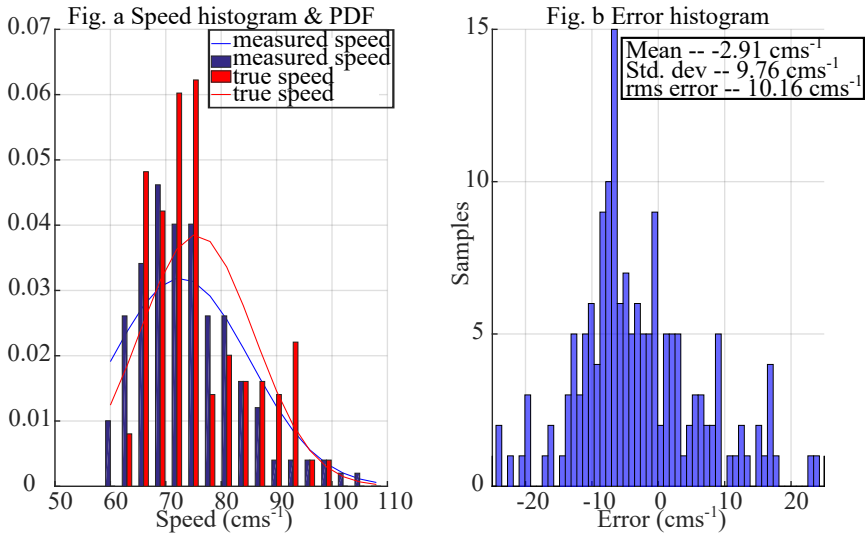

Figure 3.13: Speed and error histograms for the measured and true speed. The histograms represent the high-speed case of phase 1 of the sea-cage experiment.

The simulations showed that the cosine error in $\angle AOB$ due to a tag's position comes to its maximum when a tag lies close to one of the hydrophones. Fig. 3.14 shows variation of the error in cosine computations due to an imprecise tag position (CEP = $1.5\,\mathrm{m}$).

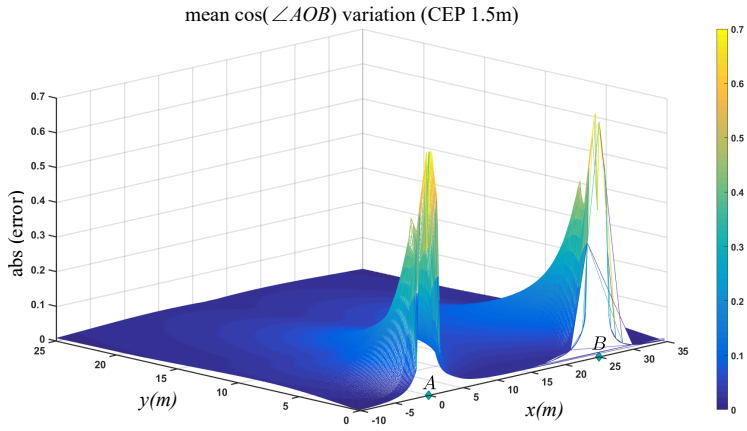

Figure 3.14: Relation between the tag's position and error in cosine of $\angle AOB$. Error was indirectly related with the tag's distance from the hydrophones, and was at minimum when located in the middle between the hydrophones, and at maximum when located close to either of the hydrophones.

Phase 2

The centre frequencies of all the tags were found during the initial benchmarking phase where the tags were held stationary in a fixed location (Table 3.1). Although the tags were found to have some temperature dependent variation in their centre frequencies (12 Hz, from 6 °C to 15 °C), temperature was almost constant throughout the water column during the field experiment (14 °C, std. dev. <0.25 °C). The centre frequencies found from this benchmarking dataset were considered constant in all further computations.

Table 3.1: Tag IDs and their calculated centre frequencies (f_s) during the benchmarking dataset.

Tag ID	Centre frequency f_s (Hz)
100	66940
110	67989
120	68970
130	69977
140	70982
150	72033

The static tag was measured to have an average speed of $10.6\,\mathrm{cm\,s^{-1}}$ (N=1080 samples), whereas tag ID 120 and 140 had an average speed of $88.1\,\mathrm{cm\,s^{-1}}$ (N=689 samples) and $108.4\,\mathrm{cm\,s^{-1}}$ (N=699 samples), respectively. Fig. 3.15 shows a histogram comparing measured Doppler speed for the three tags.

In addition to the instantaneous speed, variation in the angle (i.e. $cos\theta_s$) for the three tag IDs was also analysed (Fig. 3.16). The static tag had the majority of the $cos\theta_s$ samples close to 0°and within the first three bins (0 and ± 0.1), whereas the other two tags (implanted in fish) had relatively more dispersed $cos\theta_s$ values, implying that the velocity angle was changing from 0°to 360°due to fish' swimming behaviour.

Average swimming speed for the individual datasets (10 min averages, N=38) over time was also calculated. The average speed was varying for the tags (IDs 120 and 140) carried by fish, whereas it was constant for the static tag (ID 100) (Fig. 3.17).

3.6.2 Discussion

Phase 1

The results from the tests in phase 1 suggest that the proposed Doppler speed computation algorithm could be used for instantaneous individual fish swimming speed measurements. The rms error was less than 10% in measured speed for all

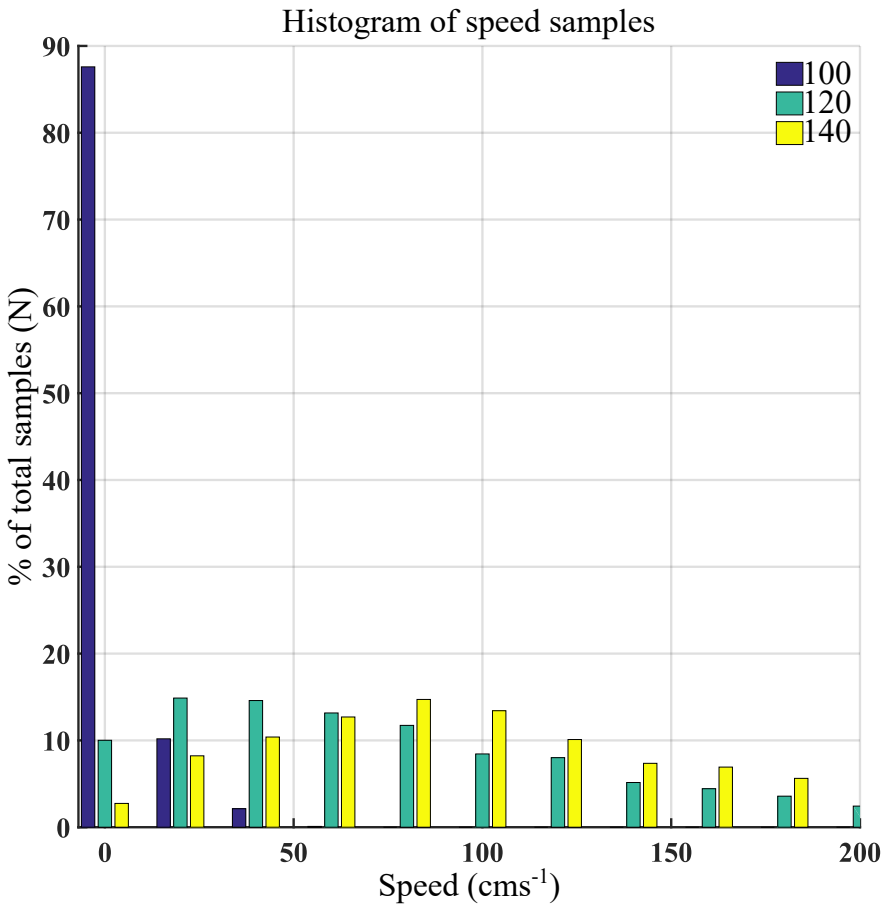

Figure 3.15: Histogram showing variation in the measured Doppler speed for the tag IDs 100, 120 and 140. More than 85% of the total speed samples are within the first speed bin ($0\,\mathrm{cm\,s^{-1}}$ to $20\,\mathrm{cm\,s^{-1}}$) for the static tag (ID 100), whereas for the tags implanted in fish (ID 120 and 140), speed samples are relatively dispersed over the entire speed range.

the experimental stages. The proposed method is elegant in the sense that the speed measurement can be piggybacked onto existing telemetry systems. In essence, this means that the new speed measurement data value could be extracted from the existing acoustic carrier wave without significantly modifying the telemetry systems. Realising the method would thus not require any added complexity on the tag side of the telemetry system, but would rather place the Doppler signal processing requirement at the receiver end. The receiver is much less resource constrained in terms of space and power consumption and could be extended relatively easy with the required hardware and signal processing capacity.

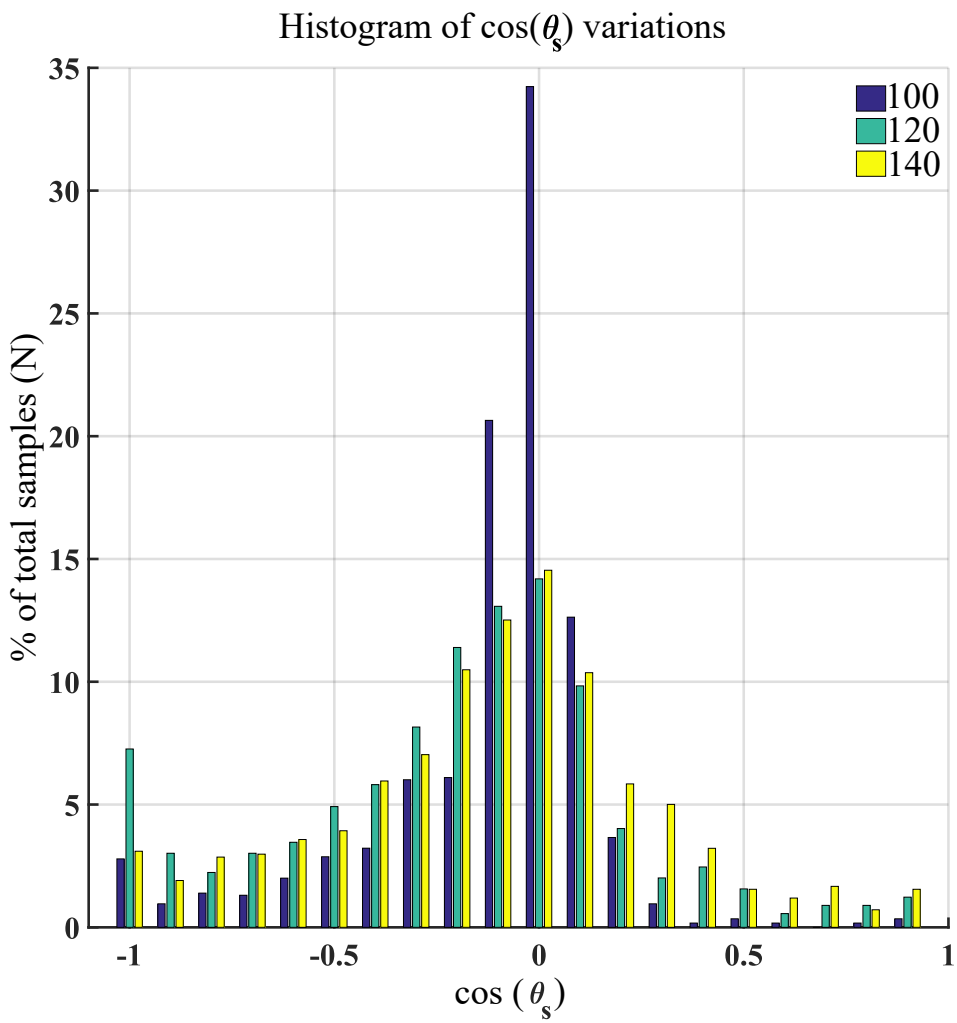

Figure 3.16: Histogram showing variation in $cos\theta_s$ for the three tag IDs. θ_s is distributed from 0°to 360°($\pm$1) for the implanted tag IDs 120 and 140, meaning that the fish were changing their velocity angle frequently, whereas the static tag (ID 100) has more than 2/3rd of the total samples inside the first three histogram bins (0 and $\pm$0.1). Histogram bin size is 0.1.

Most commercially available telemetry systems do not exploit the Doppler signal processing techniques and hence cannot perform the speed measurement. Moreover, the method requires a longer pulse duration than what is commonly used in commercially available tags (10 ms). This was observed in the initial lab trials using a ordinary acoustic tag, where it was found that with a 10 ms pulse length, the centre frequency could not be reliably estimated, leading to errors too large with respect

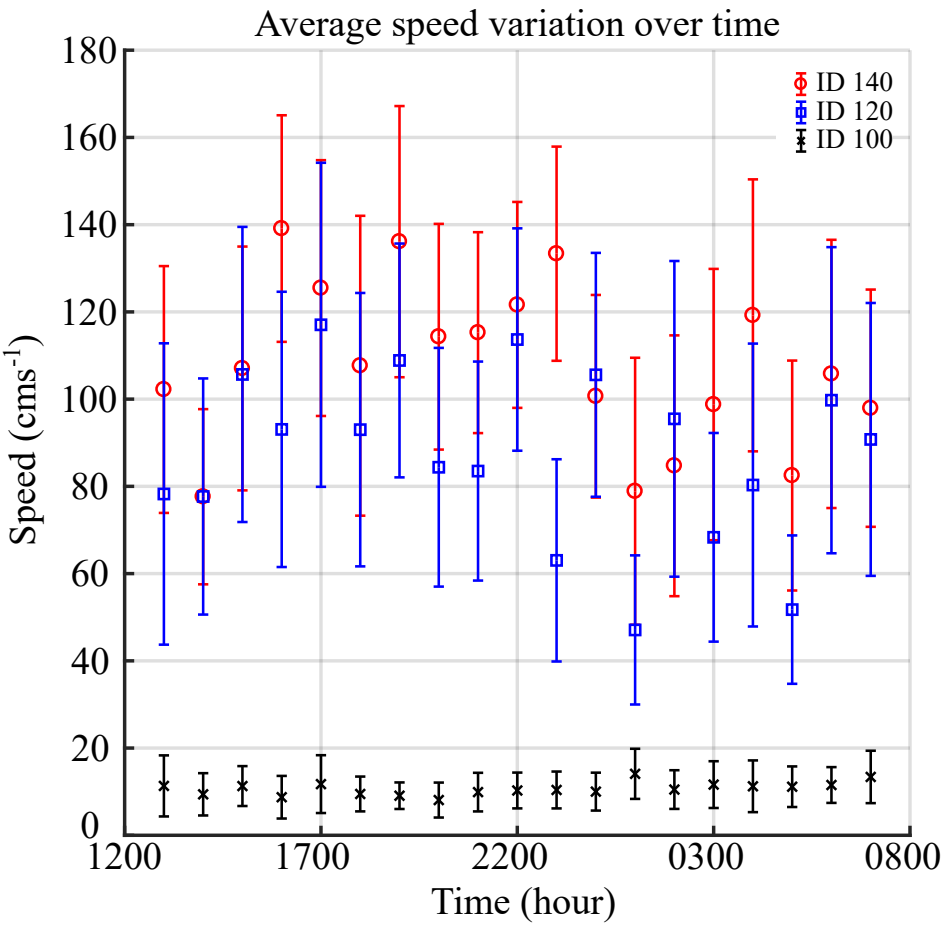

Figure 3.17: Variation in the average speed for each tag over time for day 1 and 2. The static tag (ID 100) does not show a significant variation in the average speed over time. Whereas for the tag carried by fish (ID 120 and 140), the average speed is changing. Each data point represents samples collected in one hour and includes three $10\,\mathrm{min}$ datasets with number of samples $15 < N < 82$.

to measuring the sustained swimming speed of Atlantic salmon with acceptable accuracy (Hvas and Oppedal, 2017). This can be explained by the speed resolution relation for Doppler-based instruments, which is governed by the available pulse duration (Lhermitte and Serafin, 1984). Hovem (2007) provides an equation for estimating Doppler speed resolution for a given pulse time. For a pulse duration of $10\,\mathrm{ms}$, a speed resolution of $100\,\mathrm{cm\,s^{-1}}$ is achieved, which corroborates the findings of the early lab trials. A minimum pulse time of $100\,\mathrm{ms}$ or more is required for a reasonable speed resolution for fish speed measurement using the

proposed algorithm. The custom-made acoustic tag was therefore programmed for a pulse duration of $200\,\mathrm{ms}$, yielding a speed resolution of $5.3\,\mathrm{cm\,s^{-1}}$.

The simulation results implied that when using the TDoA algorithm and a typical CEP value of $1.5\,\mathrm{m}$, the error in a tag's position and hence in cosine angle and tag's speed could be significant when a tag is located close to one of the hydrophones. However, the error decreases with increase in the tag's distance from the hydrophones used for speed computation (Fig. 3.14). Since the TDoA algorithm requires three hydrophones whereas the speed computation algorithm needs only two hydrophones (for 2D), the error due to a tag's position could be easily addressed by using that pair of hydrophones having the greatest distance from a tag for speed computation.

Phase 2

This was the first study where the feasibility of the Doppler speed approach was tested using live tagged fish in a realistic experimental setting, and the results gave several indications that the method is both practicable and sufficiently accurate to provide swimming speed measurements of free-ranging fish in various applications. First, the fact that the measurements of the stationary tag (ID 100) indeed showed a very low speed, and also had a limited error of $10.6\,\mathrm{cm\,s^{-1}}$, gives credibility regarding measurement in the low speed ranges. This fits with the results from phase 1 of the study where an error of less than 10% of the total speed range was observed. Furthermore, the tag was assumed stationary but it was held in place using a rope and sinker. Since this means that tag motion would be affected by water movements inside the cage, it is possible that the rms error of $10.6\,\mathrm{cm\,s^{-1}}$ is basically a product of current and wave induced movements inside the cage. This observation agrees well with the current measurements performed at other marine sea-cage locations (Jónsdóttir et al., 2021). Secondly, the average speed of the tagged fish when including all speed samples was approximately 1.4 and 1.6 body lengths per second (BLs^{-1}) for ID 120 and 140, respectively, which corresponds well with the sustained swimming speeds reported for Atlantic Salmon in a farm environment (Hvas and Oppedal, 2017). Finally, the swimming trajectories of the tagged fish were circular, as indicated by the measured variation in angle of the speed velocity vector, which was expected and in line with observations made in in previous studies of fish behaviour in sea cages (Oppedal et al., 2011).

However, the Doppler speed datasets proved to have some outliers with speed values of more than $200\,\mathrm{cm\,s^{-1}}$. This could be attributed to the fact that the tags used were standard acoustic tags with only firmware changes to generate the extended time pulses for the Doppler speed measurements. The hardware of the tags was not changed despite the fact that the accuracy of the method relies on the tag's ability

to maintain a very stable signal frequency. Inherent drift in the centre frequency was compensated by the firmware through re-calibration of the tag's internal clock against a local crystal oscillator with a calibration interval of $500\,\mathrm{s}$. Using the re-calibration procedure, the static tags showed a deviation of 5-7 Hz in their centre frequency. This was regarded as sufficient for the purpose of this study, but the error in measured speed could be further reduced by custom designing the hardware of the acoustic tags with an oscillator of higher precision and tight tolerance discrete components.

Although six tags were used in the experiment, data from only three of these (ID 100, 120 and 140) were used in the analysis. This experiment was designed as a proof-of-concept study for this technology, and not as a biological experiment to interpret swimming speed patterns in salmon. The reasoning behind using several tags was motivated by redundancy to counter the effect of a tag running out of power or malfunctioning rather than to extend the analysis for statistical interpretation. Since, all six tags were operational at the beginning of the experiment, it was planned that data from all of them would be used in the analyses. However, a malfunction in the cable connecting the hydrophone D to the surface synchronisation module led to that the 1PPS signal was unavailable for the hydrophone, effectually rendering it not synchronised and unable to compute TDoA. Since this meant that TDoA using all four hydrophones was not possible, finding the 3D-positions of the fish, which is necessary to use the Doppler algorithm, depended on obtaining the depth values decoded by the TBR-700-RT receivers. However, the TBRs could only monitor three frequencies simultaneously, meaning that the depth measurements from only three tags (two fish and the static tag) were available, and hence that the other three tags were not used in further analyses. Moreover, even though the experiment lasted eight days, only data from day 1 and day 2 was used in the present analyses. This was because hydrophone A experienced a hardware malfunctioned on day 3 of the experiment and did not collect acoustic data afterwards, effectually inhibiting any further Doppler assessments beyond this point in time. However, the data collected during the two days was sufficient to make our main conclusions regarding the viability of the method. The eight day period for the experiment was planned as the best case scenario for collecting maximum possible acoustic detections. In total, the experiment resulted in two 2.5 days of data that was suitable for analyses, since the number of samples ($N\approx700$ for ID 120 and 140 and $N\approx1100$ for ID 100) during this period are sufficient for concluding the feasibility of the method.

In summary, the phase 1 experiments confirmed that the Doppler approach as a feasible method for speed measurement of acoustic tags and its potential for instantaneous swimming speed measurement of fish in a large-scale sea-cage. The

rms error in the measured speed (10% of the overall speed range) in phase 1 trials was considered to be within acceptable error bounds for measuring Atlantic salmon swimming speed. The phase 2 experiment proved the feasibility of the method when applied to live fish using a commercial acoustic telemetry system. The rms error in the measured speed for the static tag matched with the rms error achieved in the phase 1 trials, and the overall swimming speed measurements of the tagged fish showed reasonable values. The method could be improved to achieve higher accuracy in the speed measurements by tailoring the acoustic tag with precise, tight tolerance discrete hardware components that ensure a more stable carrier frequency.

Chapter 4

Conclusion and Future work

4.1 Contributions and applications in marine aquaculture

The two main contributions of this thesis are the Internet of Fish (IoF) concept and a novel fish swimming speed measurement algorithm. The IoF concept is a reliable communication protocol which could relay acoustic telemetry data over long distances at very low power consumption in real-time. The speed computation algorithm provides a novel and robust approach for measuring instantaneous swimming speed for individual fish by using Doppler analysis. The IoF was tested and proven as a reliable and power efficient communication protocol through the two experiments described in chapter two of this study i.e. the real-time monitoring and real-time fish positioning experiments. LPWAN and IoT principles do not suffer form the same challenges related to scalability, coverage area, power consumption, and mismatch in data rates as the existing dedicated radio, cellular and cabled based solutions. The good match in the strengths of LPWANs with the requirements of a real-time acoustic telemetry system and the feasibility of the IoF concept were demonstrated in this study. The IoF could also play a role in enabling the observation phase defined in the PFF concept (Føre et al., 2018) by giving real-time access to fish behaviour data. Moreover, for remote and exposed farming sites (Bjelland et al., 2015), the IoF could become a key solution for monitoring fish, especially with respect to the longer distances (i.e. in range of kilometres) from shore-based infrastructure and the more extreme weather conditions making physical access to a farm site unfeasible.

Today, acoustic telemetry is a monitoring tool used only in research and conservation. This is mainly because a permit is required for surgically tagging fish, rendering routine tagging of farmed fish more difficult. Additionally, this could be

attributed partly to the presentation and accessibility of the acoustic data, which is targeted for scientific studies. During farm operations, fish farmers have many time critical tasks, and the relatively complicated and cumbersome procedures of retrieving data from a receivers may thus alone result in that such systems are discarded as operational tools. In addition, interpreting the data is a difficult process requiring specialised skills. The remote access to the acoustic data in real-time via a personal computer or a mobile phone with a user-friendly interface could potentially facilitate the acoustic telemetry to become a fish monitoring tool which is also utilised by marine farmers. The reliable communication provided by the the IoF under harsh weather conditions and over long ranges makes it a good solution that in combining with exist monitoring methods based on e.g. cameras can improve our ability to observe fish during production.

The Doppler speed computation algorithm provides a novel and robust approach for measuring instantaneous swimming speed for individual fish. Unlike most existing methods for swimming speed measurement, the Doppler principle could be applied to individual free-ranging fish in commercial marine farms. This could enable researchers and biologists to observe and understand the swimming behaviour of farmed fish in their typical habitat and relate their activity more precisely to their energy budget. In the longer run, this knowledge could be used to optimise farm management operations and fish welfare (Føre et al., 2018). The possibility of making in-cage speed measurements also gives a distinctive opportunity to document and study how fish behave in extreme currents and sea conditions, which becomes increasingly more relevant in the context of exposed farming sites (Bjelland et al., 2015). The approach is elegant in a sense that it does not require significant alterations of the existing acoustic telemetry solutions to work and can thus be applied to the already tested and validated systems used in marine farming settings. The catamaran experiments validated the method by showing that the principle works in full scale sea-cages. Finally, the experiment with live tagged fish in a fully stocked cage demonstrated that the proposed method worked as expected, yielding similar accuracy in the measurements as found in the initial validation experiments even when the acoustic tags were carried by live fish.

4.2 Future work

4.2.1 Back-end development and defining latency bounds for the IoF concept

A possible future work for the IoF concept is further development of the application layer and the back-end of the IoF to make it more user-friendly and easily accessible. A personal computer was assigned as a role of the server in this study, however the IoF back-end could be executed on any general purpose computing

device running an MQTT client. In addition, the data presentation could also be achieved via a web browser without an MQTT client. This requires developing a web server graphical interface, an MQTT broker for handling multiple incoming connections simultaneously and use of a persistent database such as a relational database management system. Another possible future improvement of the IoF concept is to define a timing deadline for a message reception at the server. The IoF concept presented in this study was designed as a soft real-time system with a worst-case delay (update rate) of $1\,\mathrm{min}$. The current LoRa standard does not provide detailed timing specifications in terms of the deadlines for signal reception (Raza et al., 2017). Thus, a possible future work could be to improve the current version of the IoF concept by measuring and specifying the worst-case delay for a message update at the server.

4.2.2 Design of a Doppler tag

The experiment involving live tagged fish proved the feasibility of fish speed measurement using the proposed Doppler principle. However, the results could further be improved by fine tuning the custom-made acoustic tag with specially selected hardware components achieving a very sharp centre frequency. The precision and tolerances of the different components used in the tag such as the internal oscillator, capacitors, inductors and resistors affect the stability of the tag's centre frequency. Therefore, hardware improvements in the custom-made acoustic tag developed in this study should be regarded as the next logical step beyond this study.

Another possible development direction could be to enhance the energy efficiency of the proposed Doppler tag. The duration of a single pulse in an acoustic burst transmitted by a tag has direct impact upon the tag's battery life. Whereas fish speed is a desired measurement, a tag's usable life is also an important design parameter. Typical usable life of acoustic tags is in range of few months to years. In this study, the focus has been on development of the Doppler speed principle and its verification under marine farm conditions. The enhancements in terms of energy efficiency were not considered and an additional sequence of relatively long ($>100\,\mathrm{ms}$) pulses to allow speed measurement was used in the custom-made tag. A potential future method could be a modulation scheme merging the currently used PPM signal modulation with the longer pulses required for the Doppler speed measurement. For example two or three pulses out of the total eight pulses in a PPM burst could be used for speed measurement ($>100\,\mathrm{ms}$ pulse length), whereas the remaining pulses in the PPM signal have normal duration and are used for encoding information, thus saving the tag's battery life. A new modified PPM modulation scheme would have implications for the receivers as they would then be required to process the new modulation scheme.

4.2.3 Receiver merging the IoF and Doppler speed measurement concept

The merger of the Doppler speed measurement approach and the IoF concept to provide real-time fish speed and position measurements is the main outcome of this thesis. A long run goal could be design of a real-time acoustic receiver which provides signals' arrival time for the TDoA positioning algorithm, DSF for the speed computation algorithm and support for real-time communication with the surface communication module. This will then give a possibility for simultaneous fish positioning and speed measurement in real-time. Although no currently available receivers are able to do this, a future receiver could be designed based on the block diagram shown in Fig. 4.1. The proposed acoustic receiver is centred around the Matlab signal processing chain presented in chapter 3 (Fig. 3.4) and performs the required Doppler signal processing steps. It includes the possibility of directly receiving an external GPS 1PPS signal for the distributed synchronisation of multiple receivers and also calculates the signal's arrival time using cross-correlation which is required for fish positioning using the TDoA algorithm. Finally, it communicates with a SLIM/LAM hardware module by using a standard serial communication protocol (RS-485).

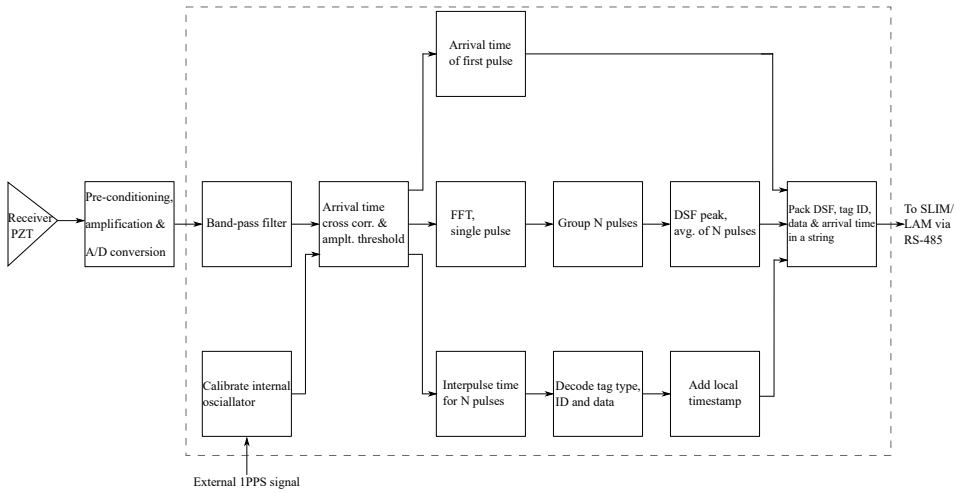

Figure 4.1: A block diagram of the proposed acoustic receiver that implements FFT at pulse level to calculate DSF peaks for swimming speed calculations. At the same time, the receiver measures pulse arrival time for fish positioning based on the TDoA algorithm. A 1PPS signal from an external source such as a GPS provides the receiver with a timing reference for accurate timestamping of received signals. The receiver then forwards the acoustic data to a SLIM/LAM module in real-time via a serial RS-485 link.

Chapter 5

Original Publications

This chapter contains four published articles and one manuscript in preparation.

- **Article J1**

  Waseem Hassan, Martin Føre, John Birger Ulvund, Jo Arve Alfredsen, Internet of Fish: Integration of acoustic telemetry with LPWAN for efficient real-time monitoring of fish in marine farms, *Computers and Electronics in Agriculture*, Volume 163, 2019, pp 104850, ISSN 0168-1699

- **Article C1**

  Hassan, Waseem; Føre, Martin; Urke, Henning Andre; Kristensen, Torstein; Ulvund, John Birger; Alfredsen, Jo Arve. (2019) “System for Real-Time Positioning and Monitoring of Fish in Commercial Marine Farms Based on Acoustic Telemetry and Internet of Fish (IoF)”, *The 29th International Ocean and Polar Engineering Conference*, Honolulu, Hawaii, USA, 2019.

- **Article C2**

  W. Hassan, M. Føre, M. O. Pedersen and J. A. Alfredsen, "A novel Doppler based speed measurement technique for individual free-ranging fish", *2019 IEEE SENSORS*, Montreal, QC, Canada, 2019, pp. 1-4.

- **Article J2**

  W. Hassan, M. Føre, M. O. Pedersen and J. A. Alfredsen, "A New Method for Measuring Free-Ranging Fish Swimming Speed in Commercial Marine Farms Using Doppler Principle," in *IEEE Sensors Journal*, vol. 20, no. 17, pp. 10220-10227, 1 Sept.1, 2020.

- **Manuscript M1**

  Waseem Hassan, Martin Føre, Henning Andre Urke, John Birger Ulvund, Eskil Bendiksen and Jo Arve Alfredsen, "New concept for swimming speed measurement of free-ranging fish using acoustic telemetry and Doppler analysis", *In preparation*

Computers and Electronics in Agriculture 163 (2019) 104850

Contents lists available at ScienceDirect

Computers and Electronics in Agriculture

journal homepage: www.elsevier.com/locate/compag

Original papers

Internet of Fish: Integration of acoustic telemetry with LPWAN for efficient real-time monitoring of fish in marine farms

Waseem Hassan[a,*], Martin Føre[a,b], John Birger Ulvund[c], Jo Arve Alfredsen[a]

[a] NTNU Department of Engineering Cybernetics, NO-7491 Trondheim, Norway
[b] SINTEF Ocean, NO-7465 Trondheim, Norway
[c] Nord University Faculty of Biosciences and Aquaculture, 8049 Bodø, Norway

ARTICLE INFO

Keywords:
Marine aquaculture
LPWAN
IoT
LoRa
Acoustic telemetry
Real-time monitoring

ABSTRACT

The aim of this study was to develop and test the feasibility of a concept called Internet of Fish (IoF). State-of-the-art acoustic telemetry systems could enable farmers to acquire behavioural data of fish in fish farms, however, the existing systems provide limited real-time access to the telemetry data. Low Power Wide Area Networks (LPWANs) are instrumental in the proliferation of the Internet of Things and enables spatially dispersed devices to communicate over long distances for months using dedicated modulations schemes. The IoF concept exploits the harmony in the performance characteristics of acoustic fish telemetry and LoRa (Long Range wireless data protocol with low power modulation) based LPWAN to provide real-time access to the telemetry data. This was achieved by developing a device designated as the LoRa Add-on Module (LAM), which provides LoRa radio support to underwater acoustic receivers. In this study, feasibility of the IoF concept was tested by conducting an experiment in a commercial marine fish farm in Norway. Four LAM and acoustic receiver pairs with a link-length to a centralized gateway of 150 m to 2.5 km were used in the field experiment. The Quality of Service (QoS) of the proposed LoRa LPWAN was determined to evaluate the effect of link-length. The QoS of more than 90% was achieved for all nodes, affirming the feasibility of real-time monitoring in marine fish farms and exposed aquaculture sites based on the IoF concept.

1. Introduction

Aquaculture is one of the fastest growing food producing industries and is believed to be instrumental in filling the future global supply-demand gap in aquatic food. Increasing demands for fish protein have stimulated expansion of both land-based and sea-based finfish aquaculture (FAO, 2016). Although the generally harsh marine environment poses substantial technological and operational challenges to sea-based fish farming, raising fish in large floating net-based sea-cages has proven as a competitive option due to its flexibility, robustness and cost effectiveness (Iversen et al., 2013). For instance, around two million tons of Atlantic salmon harvested in 2014 were produced using this farming concept (Liu et al., 2016). This production form is based on each cage containing up to 200,000 individual fish (Bjelland et al., 2015; Føre et al., 2018a), and a typical farm consisting of 8–16 cages. Such fish farms have traditionally been located in relatively protected coastal and inshore areas where they are sheltered from the harshest weather conditions and most severe sea states, and have easy access to onshore infrastructure.

However, the recent growth in the aquaculture industry has increased the demand for new fish farming sites, and simultaneously competing claims to sheltered coastal areas made by other stakeholders have reduced the access to such areas for fish farming (Bjelland et al., 2015). This has stimulated the marine fish farming industry to start moving sites further offshore where space limitations and conflicts are less pronounced. Although exposed sites may offer some appealing advantages compared to more sheltered sites such as better water quality, less impact on local environment and a lower parasite/disease pressure, the harsher conditions and remoteness to shore render management and operation of exposed fish farms significantly more challenging (Bjelland et al., 2015).

One of the obvious challenges of remoteness and more severe weather conditions relates to the limitations they inflict on the farmer's ability to get on-site and inspect the state of the fish. Observing fish behaviour is vital for farmers as the behaviour and movements of fish are inherently linked with how they perceive and interact with the cage environment. Moreover, behavioural responses may provide valuable insight into aspects of the welfare condition and performance of the

* Corresponding author.
E-mail address: waseem.hassan@ntnu.no (W. Hassan).

https://doi.org/10.1016/j.compag.2019.06.005
Received 25 September 2018; Received in revised form 2 June 2019; Accepted 4 June 2019
Available online 07 June 2019
0168-1699/

fish, such as feeding habits and responses towards potential adverse environmental factors (Føre et al., 2011). In addition, the sheer scale of contemporary commercial fish farms in terms of both volume and biomass combined with the obscurity of the underwater environment, make adequate monitoring of fish a challenge in itself (Føre et al., 2018a). Collectively, these aspects imply a need for technological solutions and tools that enable farmers to observe and monitor the behaviour of fish consistently and in real-time even in situations when physical presence on-site is not feasible.

A number of technological solutions have been proposed for monitoring the behaviour of fish (Føre et al., 2018a). Bio-telemetry is one such technique that enables monitoring of individuals and groups of fish, and that has been used to monitor wild (Davidsen et al., 2009; Hussey et al., 2015) and farmed (Føre et al., 2011, 2017) fish both in sea and fresh waters. Marine applications of fish telemetry are normally based on acoustic signals due to their good propagation characteristics in salt water compared to radio signals (Pincock and Johnston, 2012; Hussey et al., 2015). A typical acoustic telemetry system consists of acoustic transmitter tags and one or more matching acoustic receivers, and recent studies have demonstrated that such systems can be used to obtain full coverage of the volume in fully stocked commercial sea-cages (Føre et al., 2017), even during extreme operations such as crowding (Føre et al., 2018b). An acoustic transmitter tag is a miniature electronic device that maybe attached to a free-ranging fish, either by external attachment or surgical implantation. Basic ID acoustic tags only transmit a simple acoustic code that can be used for identifying and locating the fish. Advanced acoustic tags also have on-board sensors for collecting additional information related to the fish and its environment. These tags can transmit unique ID codes and additional digital data collected by on-board sensors, allowing wireless in-situ underwater monitoring of individual fish. Sensors previously used in acoustic telemetry transmitters include pressure (depth measurements e.g. Skilbrei et al., 2009; Føre et al., 2011), accelerometer (e.g. Føre et al., 2011; Kolarevic et al., 2016), electromyography (EMG) (e.g. Cooke et al., 2004) and temperature (e.g. Koeck et al., 2014). An acoustic telemetry receiver is a specialized hydrophone device which receives and decodes the acoustic signals emitted by acoustic tags (Pincock and Johnston, 2012). Acoustic receivers typically store telemetry data internally and need to be accessed manually for data retrieval, post-processing and analyses. This operation thus requires manpower and on-site presence of personnel (Grothues, 2009), which can be both impractical and expensive, and may be difficult to plan and execute due to unpredictable weather conditions, especially at exposed locations (Bjelland et al., 2015).

Although conventional acoustic receivers are normally not designed for real-time operation, real-time access to telemetry data is a desired feature that is required for specific applications such as fish tracking and real-time fish positioning algorithms (Grothues, 2009; Pincock and Johnston, 2012). Currently, real-time data access to acoustic receivers is offered by several providers of such equipment, where the most straight-forward solution is to provide cabled access to the receiver units via a standard serial communication interface (Grothues, 2009; Deng et al., 2011; Pincock and Johnston, 2012). However, cabled connection to individual acoustic receivers can only be provided close to shore or fixed sea installations and cable length will be a bottleneck because it will limit the maximum distance from the receivers to local infrastructure, thereby limiting the maximum acoustic coverage practically possible to achieve. Moreover, the presence of cables in and around the sea cages is often seen as a nuisance and liability issue by the fish farmers during farm operations. These limitations of cabled systems would be even more pronounced and inhibiting at exposed locations due to the long distance to shore-based infrastructure (Grothues, 2009).

Internet of Things (IoT) refers to a network paradigm where physical devices are integrated with embedded computers and connected to the internet, making them easier for humans and other devices to access and exchange data with. Such devices are typically powered by batteries, and most often communicate using wireless protocols. Present applications of IoT include standalone sensing nodes for home automation, automobiles, trains, and industrial and agricultural sensors and actuators (Raza et al., 2017). In addition to being small and battery powered, IoT devices are often distributed over large geographical areas, subjected to very strict energy budget requirements, and communicate at relatively low data rates. These characteristics suggest that it is not optimal to connect IoT devices to the Internet using standard non-cellular short range wireless technologies or traditional cellular networks, but rather employ low power radio protocols. LPWAN represents an emerging communication technology that complements existing standard wireless computer networks by directly addressing the unique requirements of IoT devices, and that relies on an architecture similar to the Global System for Mobile communications (GSM) cellular networks (Raza et al., 2017). LPWANs exploit the sub-gigahertz unlicensed Industrial, Scientific and Medical (ISM) bands, and provide large coverage areas and low power consumption at the end devices by utilizing efficient modulation schemes and intermittent transmit/receive cycles, with typical receiver sensitivity as low as -130 dBm to -150 dBm. The low power consumption and wide coverage areas of LPWANs are achieved at a cost of very low data rates, which are typically in the order of a few kilobytes per seconds (kbps). However, typical IoT devices, and hence end devices of LPWANs, only need to exchange small amounts of data at sporadic time intervals, usually upstream to a central IoT server through gateway nodes in a star topology, rendering high data rate less important (Raza et al., 2017).

Since acoustic fish telemetry systems share many of the properties related to battery operation, spatial distribution, low-power requirements and low data rates mentioned above, LPWANs can be regarded a highly relevant candidate for extending acoustic telemetry systems with features that enable real-time user access to telemetry data. This study was therefore focused on developing and testing a wireless and power-efficient real-time fish monitoring solution for marine aquaculture applications by integrating an acoustic fish telemetry system with LPWAN technology. The proposed solution combined a state-of-the-art submerged acoustic receiver with a surface communication module (hereafter referred to as the LoRa Add-on Module or LAM) that provided a power-efficient long range wireless communication interface for the incoming fish telemetry data. Multiple LAMs were connected in a star topology to form an LPWAN of acoustic receivers, establishing a concept called the “Internet of Fish” (IoF). The proposed system was tested in a large-scale commercial fish farm using three LAMs, each connected to an acoustic receiver and placed inside sea-cages at varying distances from a centralized gateway. A fourth LAM and acoustic receiver pair was deployed on a buoy moored at open sea at a longer distance (2.5 km) from the gateway. The aim of the experiment was to evaluate the feasibility of using LPWAN for aquaculture applications in a marine environment by considering the Quality of Service (QoS) obtained by the LPWAN in providing real-time access to acoustic telemetry data from individual fish in fish farms to users on land.

2. Materials and methods

2.1. System requirements

LPWAN link-length, bandwidth and battery operated end devices are three important dimensioning requirements for the IoF concept. The end-to-end extent of a typical fish farm for Atlantic salmon production may exceed 1 km, indicating the link-length that the LPWAN must offer. The overall acoustic message rate and the size of a single acoustic message received by the LAM from the acoustic receiver provide another important dimensioning parameter, in specifying the minimum required data transmission capacity/bandwidth of the LPWAN system. Overall acoustic message rate in a telemetry setup depends on several factors including tag density, the time interval between consecutive

messages sent by the tags, the time required to transmit one acoustic message, and messages lost due to interference from noise and message collisions at the acoustic receiver (Pincock and Johnston, 2012; Føre et al., 2017). Pincock and Johnston (2012) provides a method for estimating the average time between two consecutive acoustic messages successfully received by the receiver from a tag given different tag densities. For a tag density of 10 tags with each tag having an acoustic message update rate of 1 message per minute, this method estimates the average time between two successful detections from a tag at 2.4 min, which in average gives an overall acoustic message rate of approximately 5 messages per minute successfully detected by the receiver. In this study, acoustic test tags (Thelma Biotel AS, Trondheim, Norway) with a relatively high update rate of 1 message every 6 s were used, which corresponds to an overall acoustic update rate of roughly 10 acoustic messages per minute. A single telemetry message received from the acoustic receivers used in this study (TBR-700-RT, Thelma Biotel AS, Trondheim, Norway) consists of 11 bytes of information. Since the LPWAN system was set up to transmit one radio packet per minute, and up to 10 telemetry messages can be expected per minute, this means that a packet size of at least 110 bytes is necessary for each LPWAN message to include all telemetry messages received since last transmission. The third important system requirement is related to the energy efficiency of the end devices. End devices should be battery operated with the assumption that a power source will not be easily available at the cages and that cables should be avoided, which is especially relevant with respect to farming at exposed aquaculture sites that generally are more remote from available power sources. This requirement of battery operated end devices suggests that devices should be designed according to ultra-low power design techniques.

Most modern fish farms also have a feed barge for storage and distribution of feed, which is usually placed centrally at the site and relatively close to the sea-cages (Fig. 7a). Since the barge often has power and Internet installed, it is an ideal location to deploy the gateway of the LPWAN system.

2.2. Available physical layers for LPWAN

Various wireless technologies such as SigFox, Weightless, LoRa and Ingenu are competing as a potential physical (PHY) layer for LPWANs (Raza et al., 2017). With coverage of more than twice the length of a typical salmon farm (Table 1), all these LPWAN technologies can serve the first of the system requirements for IoF concept. However, the different technologies use different modulation schemes at the physical layer and thus differ in terms of payload size, data rates and licensing cost. SigFox and Weightless-N uses Ultra Narrowband (UNB) and Narrowband (NB) modulation schemes respectively (Raza et al., 2017), and have hard restrictions on maximum payload size, with the SigFox payload being limited to 12 bytes and the Weightless-N maximum payload size being 20 bytes (Raza et al., 2017). These restrictions make both SigFox and Weightless-N unsuitable for the present application since they cannot fulfil the minimum payload size requirement of 110 bytes. Ingenu uses Random Phase Multiple Access Modulation (RPMA), operates at the 2.4 GHz ISM band, and offers payloads of up to 10 kilobytes and data rates up to 78 kbps (Raza et al., 2017). Although Ingenu thus satisfies the packet size requirement, it has a higher power consumption compared to the other technologies due to high usage of spectrum band (Adelantado et al., 2017). The fourth LPWAN technology considered in this study is LoRa. LoRa uses Chirp Spread Spectrum (CSS) modulation, offers a payload up to 250 bytes, has data rates up to 37.5 kpbs and very low power consumption (Raza et al., 2017), thus fulfilling all three requirements for the application. A unique feature of LoRa is the Spreading Factor (SF) parameter which is closely related with the bandwidth and provides an additional degree of freedom in node/end device design. The SF can be chosen as a trade-off between coverage area, data rates and radio packet size (Augustin et al., 2016; Adelantado et al., 2017; Raza et al., 2017). This added flexibility, together with its fulfillment of all three system requirements, makes LoRa an ideal candidate as a wireless communication interface for acoustic fish telemetry. LoRa has also been identified as the best candidate for similar applications in agriculture (Adelantado et al., 2017; Talavera et al., 2017).

Table 1
Comparison of various competing technologies for LPWANs.

Parameter	Ingenu	SigFox	Weightless-N	LoRa
Modulation	RPMA	UNB	NB	CSS
Payload size	10 K bytes	12 bytes	20 bytes	250 bytes
Data rate	78 kbps	100–600 bps	30–100 kbps	37.5 kbps
Encryption	256b AES	Not supported	128b AES	128b AES
Packet limitation	n/a	16 per day	n/a	n/a
Coverage	5–6 km	10 km and 50 km	3 km	5–15 km

2.3. System description

Three layers may be identified in a typical LPWAN based monitoring system, the first layer being the perception layer which consists of sensor nodes or end devices (Talavera et al., 2017). Devices in this layer are typically distributed geographically/spatially. The second layer is the network layer and consists of a centralized device denoted as the gateway. All end devices in the perception layer communicate with this gateway in a star topology. The third layer in this representation is the application layer, which typically features a server and a database that functions as a system back-end and front-end for presentation of data to the user. The LPWAN system developed in the present study tightly conforms to this architecture and includes the same three layers, as can be seen in Fig. 1. In addition, the perception layer is split into two sub-layers distinguishing between the system components that are underwater (i.e. the acoustic telemetry system) and those at the surface (i.e. the radio communication system). The IoF concept employs an existing acoustic telemetry system (Thelma Biotel AS, Trondheim, Norway) and does not require any changes in the acoustic link (underwater part of the perception layer in Fig. 1), clearly isolating the LPWAN applications from the acoustic link. This makes the proposed LPWAN system largely independent of the acoustic telemetry system type, making it easier to adapt to different telemetry systems.

2.3.1. Perception layer: LAM

Hardware. The LoRa Add-on Module (LAM) is a microcontroller based battery operated standalone module designed in this study to act as the end device of the LoRa LPWAN and provide radio interface to the acoustic receiver. Each LAM has a unique ID and is a basic transmission device (end device) in the LPWAN system, also known as a node in the LPWAN terminology. A block diagram of the LAM is shown in Fig. 2. The LAM was designed using a 32-bit EFM32GG842 ARM Cortex M3 microcontroller (Silicon Labs) as its core processing and control component. In this study, the LAM was designed to interface with a Thelma Biotel TBR-700-RT acoustic receiver that was set up to forward all received acoustic messages on a standard RS-485 serial interface, providing telemetry data to the LAM as acoustic messages arrive. Radio communication was realized through a Serial Peripheral Interface (SPI) based LoRa module (RFM95W, HopeRF), that operates at 868 MHz and transmits the radio packages containing the telemetry data to a gateway. The LAM also includes a Global Positioning System (GPS) receiver (u-blox, NEO-7P) that allows for distributed time synchronization of the attached acoustic receivers, which is important to ensure good data quality and is necessary in fish localization and tracking (Grothues, 2009; Pincock and Johnston, 2012). Fig. 3 shows the Printed Circuit Board (PCB) and physical realization of the LAM.

Power consumption. To fulfil the requirement of battery operated end devices, the LAM was designed using ultra-low power design techniques, which implies careful design choices with respect to selection of

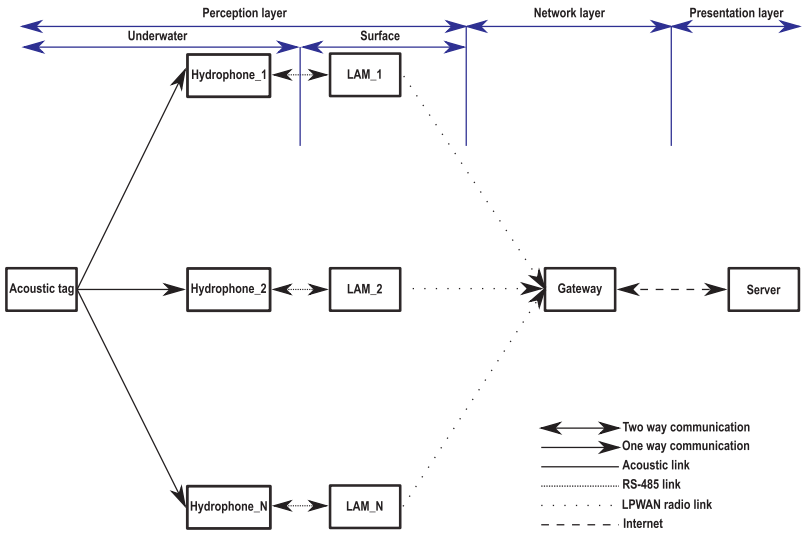

Fig. 1. Overview of different modules in three layers of the IoF concept and their inter-communication.

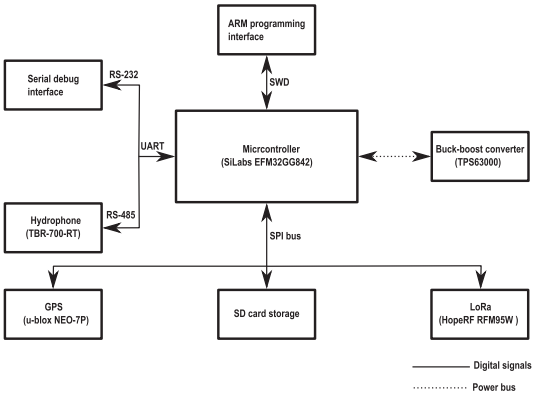

Fig. 2. LAM block diagram highlighting different modules and their interfaces with EFM32GG842.

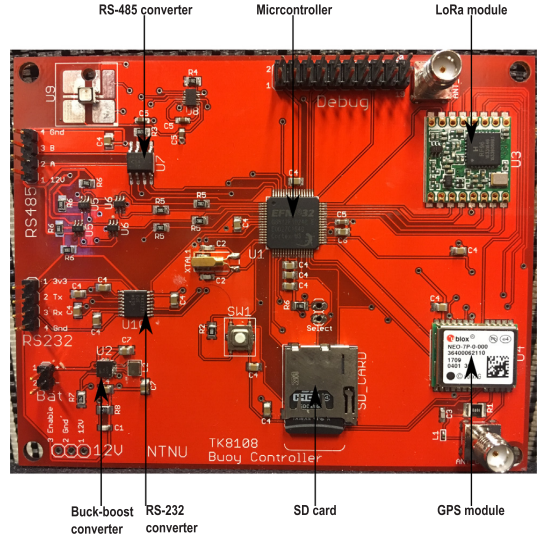

Fig. 3. PCB of the LAM showing different modules.

microcontroller and peripheral circuits. The EFM32GG microcontroller supports a range of low energy modes for battery powered applications and includes peripherals such as timers, real-time clocks and communication interfaces that operate in low energy modes. At the circuit level, hardware modules were power gated by transistor switches to optimize power consumption. Current consumption of the LAM is 20 mA during its normal operation and 50 mA during radio transmit mode (which is only active for very short duration). The LAM is designed for a 3.6 V, 35 A h Lithium primary cell and will operate for approximately 2 months.

LoRa Spreading Factor (SF). Effective communication range, maximum payload size and time-on-air are determined in LoRa by the parameters spreading factor (SF), bandwidth and transmit power (Augustin et al., 2016). For a fixed bandwidth and transmit power, SF thus defines the maximum size of a radio message in bytes, time-on-air (data rate) and receiver sensitivity. Typical values of SF vary from SF7 to SF12. Messages sent with a SF7 spend least time-on-air, require sensitive receivers and can have a payload size of up to 250 bytes, whereas messages sent with SF12 spend most time-on-air, require less sensitive receivers and have a maximum payload size of up to 60 bytes (Augustin et al., 2016; Adelantado et al., 2017; Raza et al., 2017).

Duty cycle and time-on-air. For LPWAN modulations operating in the free sub-gigahertz ISM band, time-on-air and frequency sub-bands are regulated in different regions of the world by the responsible telecommunication regulatory bodies (Adelantado et al., 2017; Raza et al., 2017). In the European region (EU), LPWAN/LoRa modulation uses the 868 MHz ISM band with an allowed duty cycle of 1%, which gives a maximum time-on-air of 36 s per hour (Adelantado et al., 2017). The time-on-air for each transmission in LoRa modulation depends on the payload size, bandwidth, header size and SF (Augustin et al., 2016), and can be calculated by using software tools supplied by the LoRa modulation chip manufacturer. The LAM was programmed to use SF7, coding rate of 4/5, with a bandwidth of 125 kHz and a transmit power of 14 dBm. For a payload of 111 bytes, time-on-air for a single radio packet transmitted by the LAM using SF7, is 187.65 ms, or 11.259 s for

60 transmissions over a period of one hour. The time-on-air increases with higher SF values, for example time-on-air for a single radio packet transmitted with SF9 and a payload size of 111 bytes is 586.75 ms or 35.205 s for 60 transmissions per hour. The LAM complies with the duty cycle regulations of the EU region for both SF7 and SF9 configurations.

Firmware. The firmware of the LAM was developed in the C programming language using Silicon Lab's Simplicity Studio Integrated Development Environment (IDE), and was based on IBM's LMiC library which implements the LPWAN stack. The library is modular and can be ported and modified based on the requirements of the application, and it also provides a timer-based scheduler. The device drivers for GPS, the TBR-700-RT acoustic receiver and other peripherals were implemented in the Hardware Abstraction Layer (HAL) of the library. Firmware operation is based on timer interrupts with an Interrupt Service Routine (ISR) being executed every 10 s, executing a job called 'application job'. On each iteration of this job, a time synchronization message is sent to the TBR-700-RT receiver, updating the TBR's internal clock to match the GPS clock of the LAM. This mechanism allows accurate distributed time synchronization of multiple TBRs and is instrumental for the localization of acoustic tags. The application job also checks for any newly arrived telemetry messages in the last 10 s and adds them to a buffer for further processing. A flag is set by the timer ISR every 60 s, and is used by the application job to trigger sending a data packet containing buffered telemetry messages over the radio link. The flag is also used to store the data locally on the SD card in the LAM as a backup. Operation of the firmware is explained in the flow diagram shown in Fig. 4.

2.3.2. Network layer: gateway

The gateway in the IoF concept works as a centralized node for all end devices (LAMs) and is responsible for forwarding all incoming messages from nodes with authorized IDs to a server. A MultiConnect Conduit (MTCDT-H5-210L, Multi-Tech Systems, Inc.) was used as the gateway in this study which is a Commercially Off The Shelf (COTS) module. The gateway was equipped with a suitable RF antenna to receive data from nodes via the LoRa radio link and an Ethernet connection for transmitting received data to the server.

Message Queuing Telemetry Transport (MQTT). The gateway supports the Eclipse Mosquitto MQTT protocol (Light, 2017) for sending data over the Internet. The MQTT is a subscribe/publish-based protocol used in Machine to Machine (M2M) and IoT applications that works on top of the TCP/IP protocol and has two elements: a client and a broker (Hunkeler et al., 2008). Any device supporting a MQTT protocol is a MQTT client, and a client can either be a subscriber (that is receiving data) or a publisher (that is producing data) of data. A client connects with a MQTT broker, which is the central application in the protocol. The broker is responsible for connecting and maintaining connections with all clients, and for receiving data from the clients. Messages exchanged in MQTT are provided with an additional field denoted as the *topic*. This field makes MQTT scalable and more versatile by allowing the broker to do message filtering and forwarding based on this value. This is possible because MQTT subscribers subscribe to a *topic* instead of data from a specific publisher, meaning that the broker is responsible for ensuring that data tagged with a specific *topic* is forwarded to all subscribers of that topic (Hunkeler et al., 2008). A JavaScript MQTT-publisher application (packet forwarder) that effectively forwards all received data from the LAMs to the server over the Internet, was developed and implemented on the Linux-based gateway.

2.3.3. Application layer: server

A personal computer with Internet access was assigned the role as the server in the application layer. The server was responsible for receiving and storing data locally on its hard drive, and presenting telemetry data to end users. For this, three applications were developed: an MQTT broker, an MQTT subscriber client and a MATLAB Graphical User Interface (GUI). The open source HBMQTT was used to implement the MQTT broker and client applications on the server, where the broker was set up to accept connections and receive data from all publishing clients including the publisher client running on the gateway, while the subscriber client was set up to subscribe to and store all received messages in text files on the local hard drive. In this case, the text files functioned as a database with a unique file containing the data received from each LAM. Fig. 5 shows how the MQTT protocol was used in the overall LPWAN system, whereas Fig. 6 shows a flow diagram explaining the operation of the subscriber client application. The third application running on the server was a Graphical User Interface (GUI) developed using the MATLAB GUIDE environment (The MathWorks, Inc., USA). The GUI is the presentation layer application visible to users, and enables a user to select a specific LAM based on its ID and plot and inspect the telemetry data recorded by the associated acoustic receiver in real-time.

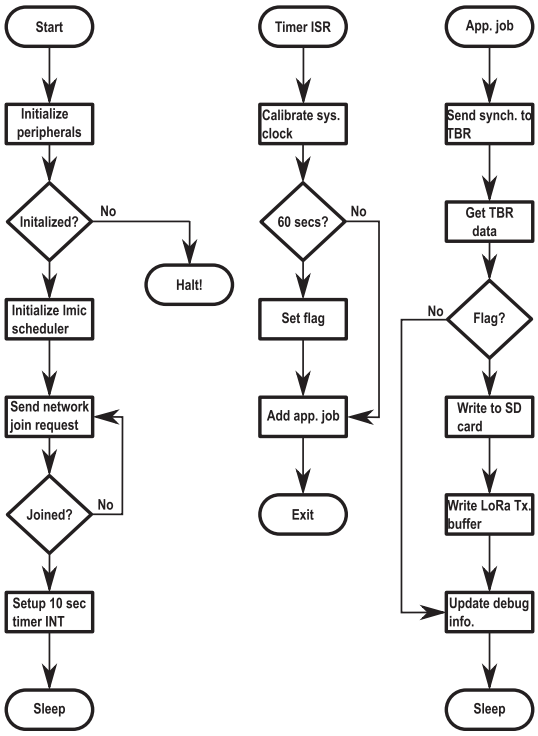

Fig. 4. Flowchart explaining operation of the LAM firmware.

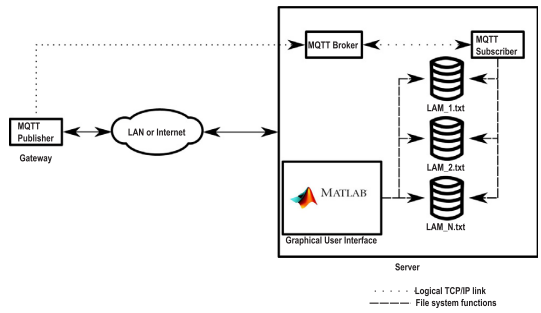

Fig. 5. Overview of the server applications and MQTT based communication.

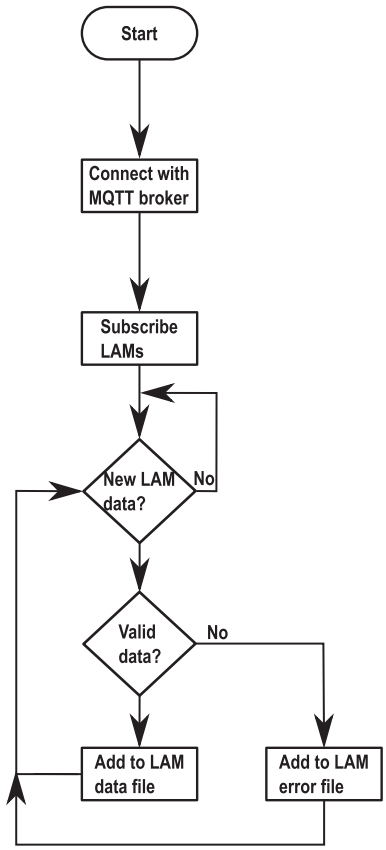

Fig. 6. Flowchart of the MQTT-subscriber client application (server).

2.4. Field experiment and validation

The IoF concept functionality was first dry-tested and verified in a series of laboratory experiments. Subsequently, an extensive field test was conducted at a commercial marine fish farm in Norway, with the goal of studying the feasibility of using LoRa-based LPWAN for real-time fish monitoring in marine aquaculture sites. Four LAMs and a gateway were used during the field test, where each node consisted of a surface LAM connected to a submerged TBR-700-RT acoustic receiver. Three of the nodes were installed in two fish cages, each having different distances from the gateway (Fig. 7a) and with the antennas 0.8 m above sea level. In order to increase the span of transmission ranges tested, the fourth node was deployed on a remote buoy located considerably farther away from the gateway than the other nodes (Fig. 7b). In this case the antenna was raised to 2 m above sea level, to reduce the chance that wave induced buoy movement could prevent line of sight between the LAM and the gateway. All nodes were set to transmit one radio message over the LPWAN every minute where the size of the radio messages varied depending on the number of acoustic messages received since last transmission. Acoustic transmitter test tags were deployed in the water at fixed locations in the vicinity of the nodes to emulate tagged fish and generate test messages that could be picked up by the acoustic receivers and subsequently relayed through the LPWAN. Three different types of test tags that were programmed to transmit on average 6 to 10 acoustic messages per minute, were used in the experiment. The gateway was placed inside the feed barge with an RF antenna mounted on the roof of the barge at a height of approximately

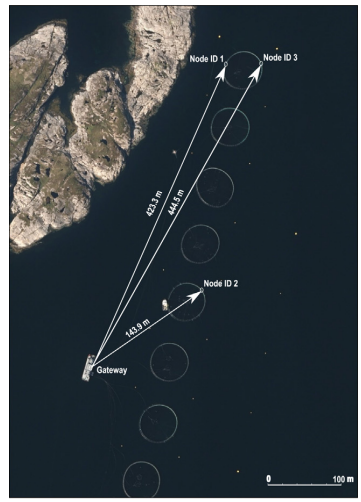

(a) Gateway and nodes placement in the fish farm.

(b) Remote node and its distance from the gateway.

Fig. 7. Geographical nodes placement.

10 m above sea level to ensure line of sight communication with the nodes. The gateway was connected to the Internet via an Ethernet port on a standard network router that was installed on the barge. The relative locations of the nodes and the gateway are shown in the map given in Fig. 7. The server was placed in an office environment approximately 150 km away from the test site.

Following deployment of the nodes and initialization of the network, the experiment ran for fourteen days without any intervention. During the course of the experiment, it was possible for an operator to select a desired LAM ID and display real-time and recorded telemetry data through the GUI running on the server.

An important aspect of the experiment was to evaluate the Quality of Service (QoS) of the proposed LPWAN implementation. The

International Telecommunication Union - Telecommunication Standardization Sector (ITU-T) defines QoS as a satisfaction indicator perceived or experienced by a user of a service (ITU-T, 2008), and also proposes end-to-end QoS and layer-based QoS of a communication system. According to Raza et al. (2017), existing LPWAN technologies provide no or limited QoS. Duan et al. (2011) also points out the lack of a generic definition of QoS in IoT and LPWANs, and proposes layer-based QoS for each layer of the three layers in LPWAN based systems. Parameters that may be used to evaluate the network QoS of an LPWAN include packet loss, delay and bandwidth (Duan et al., 2011). Petrić et al. (2016) also proposes packet loss or Packet Error Rate (PER) as one of the target parameters to evaluate QoS in LoRa based LPWAN. End-to-end PER is therefore used in this study to define the systematic QoS, and is computed based on the equations:

$$PER = (1 - QoS_{E2E}) \times 100 \quad (1)$$

$$QoS_{E2E} = \frac{number\ of\ uncorrupted\ messages\ received\ at\ server}{total\ number\ of\ messages\ transmitted\ by\ a\ LAM\ node} \quad (2)$$

The number of packets transmitted by a node and the corresponding total number of uncorrupted packets received at the server are hence the only parameters required in order to evaluate the QoS_{E2E} of a node. QoS_{E2E} of all LAMs were calculated based on the log files acquired during the experiment to evaluate the general performance of the LPWAN/IoF concept in the marine fish farming environment, and subsequently compared to assess the effect of distance/link-length between the nodes and the gateway.

3. Results

The overall performance of the nodes during the experiment satisfied the system requirements defined for the IoF concept. The first system requirement (i.e. a minimum link-length of 1 km) was fulfilled by that most acoustic data received at node 4 (2.5 km from the gateway) got successfully transmitted over the LPWAN and updated onto the server during the experiment. Further, the nodes that were equipped with acoustic test tags and had an overall reception rate of 10 acoustic messages per minute (node 2 and 4) were transmitting all received telemetry messages over the radio link, fulfilling the system requirement related to data rate. The last system requirement concerning energy efficiency of the LAM was also satisfied, in that all LAMs operated throughout the 14 day experiment without battery replacement. In addition, the average current consumption of the LAM was measured to around 20 mA, which indicates a theoretical life expectancy of more than two months when running on the 35 A h Lithium primary cell. In terms of reliability, operation of the LAMs proved to be stable throughout the experiment in open sea and none of the modules had to be restarted or otherwise serviced during the experiment.

Table 2 shows the total number of messages transmitted (Packets Tx) and uncorrupted messages received at the server (Packets Rx), PER values and QoS_{E2E} throughout the 14 days experiment for each of the nodes. The difference in the number of transmitted messages for the different nodes is due to that different types of acoustic tags were used for different nodes, with some tag types transmitting acoustic messages at a higher rate than other tag types. As can be seen from Table 2, all nodes achieved a QoS_{E2E} of more than 90%. The remote node (node 4) had the lowest QoS_{E2E} of 92.8%, while the other three nodes lying less than 500 m from the gateway had in average QoS_{E2E} of 99%. The QoS_{E2E} of the LPWAN was more than 90% (Table 2) for all nodes during the 14 day trial period, and observed PER values were close to 1% for all nodes closer than 500 m to the gateway (node 1, 2 and 3; Fig. 7a). Table 3 shows the total number of packets transmitted by the nodes and number of packets lost from the network to the application layer along with the QoS_{N2A} (QoS from the network to the application layer) for the entire experimental period, including when power loss and hacking affected the system. The QoS_{N2A} was lower than the previously calculated QoS_{E2E} which is to be expected since QoS_{N2A} also accounts for non-LPWAN-related packet loss, but despite this, QoS_{N2A} was still higher than 81.5% for the closest nodes and 78.8% for the most remote node.

Table 2
QoS_{E2E} and PER values for individual nodes, with actual number of packets transmitted and received.

LAM node ID	Link-length (m)	Packets Tx	Packets Rx	PER	QoS_{E2E}
1	444.5	10124	10021	1.01%	0.989
2	143.9	39414	38786	1.59%	0.984
3	423.3	20660	20600	0.29%	0.997
4	2470	74380	69073	7.13%	0.928

Table 3
Packet lost from the network layer to the application layer and QoS_{N2A}.

LAM node ID	Packets Tx	Packets lost	QoS_{N2A}
1	12294	2170	0.815
2	45282	5868	0.856
3	22879	2219	0.900
4	87683	13303	0.787

4. Discussion

4.1. QoS and system performance

The QoS_{E2E} for nodes 1, 2 and 3 (Table 2) implies that almost all messages arrived successfully and uncorrupted at their destination, meaning that the total QoS of the system can be rated as good. Previous studies have found similar results for LoRa-based LPWANs when placing nodes within a distance of 420 m from the gateway (Petäjäjärvi et al., 2016; Raza et al., 2017). Petäjäjärvi et al. (2016) found a PER of 5.3% when testing in an urban environment. This is slightly higher than the PER found in the present study, probably because the urban setup did not achieve line of sight communication due to features in the environment such as buildings and other obstacles. Due to the lack of such obstacles in the marine environment, line of sight communication is highly feasible in marine applications, exemplified by the lower PER achieved in this study compared with earlier terrestrial studies. The node furthest away from the gateway (2.5 km) had a QoS_{E2E} of more than 92%. This is in accordance with the maximum operational distance of up to 15 km for line of sight communication claimed by the LoRa specification (Raza et al., 2017). Jovalekic et al. (2018) achieved a communication link-length of more than 22 km in a sea based environment using LoRa.

During the experiment there was a power outage on the feed barge and the Internet connection with the gateway was lost for 6 h. Similarly, the MQTT broker was hacked and stopped multiple times during the experiment, although password authorization was used at the broker. These issues caused loss of the data transmission from the network to the application layer. Since data loss due to such issues is not being directly related with the LPWAN performance, the periods where these problems occurred were omitted from the QoS_{E2E} analyses. However, such effects do affect the overall system performance, and should therefore be considered. Using the notion of layered QoS, this packet loss is reflected in QoS_{N2A}. It was not possible to segregate the QoS_{N2A} from the QoS_{P2N} (QoS from the perception to the network layer) in the current version of the LPWAN system since the number of successfully received packets was not stored at the gateway. The QoS values due to such issues (Table 3) are still regarded as acceptable considering that the system was based on a prototype installation. These outcomes also imply that the QoS of the system could be significantly improved by relatively simple measures such as using uninterruptible power supply

Table 4
Comparison of the existing real-time telemetry systems and proposed IoF concept.

Characteristics	Wired hydrophones	GSM hydrophones	VHF hydrophones	Proposed IoF
Range	cables	10–50 km	few 100 m	5–15 km
Scaling	poor	high	low	high
Energy efficiency	n/a	poor	low	high
Licensing cost	n/a	high	free ISM band	free ISM band, duty cycled

for the gateway, and enforcing strong password control and join request control for the MQTT broker.

4.2. Comparison with existing real time telemetry systems

To further evaluate the utility of the IoF concept, it is useful to compare its properties with those of alternative solutions for real-time access to acoustic telemetry data (Table 4). Although different acoustic telemetry vendors (e.g. Thelma Biotel AS, HTI Sonar Inc., Lotek Wireless Inc.) offer commercial cabled solutions, cabling to individual acoustic receivers will mostly be limited to nearshore applications. Together with the increased challenges related to cage management when introducing more cables to sea-cages, this renders the cabled solution unsuitable for industrial application. However, there exist commercially available alternatives to cabled solutions, such as the Vemco VRAP system, the Lotek Wireless MAP600, and HTI Model 290/291 (Grothues et al., 2005; Grothues, 2009). These systems typically utilize Very High Frequency (VHF) or Ultra High Frequency (UHF) bands for radio communication. A drawback of using these frequency bands without LoRa or similar long range based modulation schemes is that the communication suffers from scaling issues (meaning that the number of receivers/nodes served by such a system will be limited), short range, vulnerability to narrowband noise and relatively higher power consumption (Grothues et al., 2005). Other alternatives using cellular or GSM communication (e.g. Sonotronics, Lotek Wireless Inc MAP) are also commercially available (Grothues, 2009). However, these systems require a Subscribers Identity Module (SIM) to transmit telemetry data in form of text messages, and thus suffer from licensing costs in addition to challenges with respect to energy consumption (Grothues, 2009).

The IoF concept based on LPWANs and IoT principles presented in this study does not suffer from the same challenges as the cabled and existing wireless alternatives. Moreover, the LAM units were designed to be energy efficient which is an important requirement in this particular use-case. Finally, since data rates generated by a typical acoustic fish telemetry solution are low (Pincock and Johnston, 2012), the generally lower data rates obtained with LPWANs than when using solutions based on VHF/UHF or GSM will not impair the system's ability to relay the data stream to the user. Based on these observations, the IoF concept proposed in this study emerges as a highly relevant candidate for realizing real-time monitoring of acoustic telemetry data in sea-cages.

4.3. Limitations

An important limitation of the LoRa based LPWAN system is that it is a real-time system for monitoring applications without strict bounds on jitter or network delays. Adelantado et al. (2017) points out that whereas real-time systems should guarantee low latency and bounded jitter values, the LoRa specifications does not specify or meet such criteria. This implies that LPWANs can be used in real-time monitoring applications such as agricultural IoT systems, but are not suitable as wireless communication networks in real-time industrial control systems (Adelantado et al., 2017). In this study, the server got updates from the nodes every 60 s and a telemetry message will therefore face a worst case delay of 60 s. Considering that the system was designed for monitoring applications in aquaculture farms and remote buoys, and not as a component in a system for controlling an industrial process, a worst case delay of one minute seems acceptable. The requirement of a minimum payload size of 110 bytes restricts the LAM to use spreading factors values up to SF9, which allows a maximum payload size of 135 bytes. For the LPWAN system in the experiment, all LAMs were programmed to SF7 except the remote node which was programmed to use SF9 due to the long distance from the gateway. The inability to use SF values higher than SF9 may mean that the effective spatial coverage provided by the LAMs may be lower than specified in the LoRa specifications (15 km).

5. Conclusion

The results of the experiment affirm the feasibility of the proposed IoF-concept and its potential use in marine aquaculture monitoring applications. Specifically, a PER of less than 2% was achieved for all nodes placed inside fish cages in the marine farm, proving that LoRa based LPWAN is a promising candidate for real-time monitoring of fish in marine aquaculture applications. The PER of node 4 (placed 2.5 km away from the gateway) was also less than 8%, also suggesting that LoRa-based LPWAN is a suitable candidate for situations where real-time long range wireless access to an acoustic telemetry system is required (for example in wild fish monitoring and exposed aquaculture applications where nodes will often be placed further from a gateway than in conventional fish farms). The system based on LPWANs and IoT principles presented in this study does not suffer from the challenges faced by existing real-time telemetry systems based on cabled receivers or communication through UHF/VHF or GSM. Moreover, requirements related to coverage area and data rate of the acoustic telemetry system closely match with those provided by LoRa based LPWANs. This harmony in performance characteristics represents a good foundation for integrating LPWANs with acoustic telemetry and realizing the IoF concept. In conclusion, this makes the IoF concept a reasonable choice as a radio technology for real-time fish telemetry applications in being both energy efficient and scalable.

As an extension to the study, a real-time fish positioning system based on LPWAN is planned. The position of a fish will then be calculated based on the reception timestamps of a single acoustic message on three separate acoustic receivers using Time Difference of Arrival localization (TDoA). TDoA positioning requires that the clocks of the three acoustic receivers are synchronized (Grothues, 2009; Pincock and Johnston, 2012). Fish positioning seems a natural extension of the LPWAN system as the LAM already provides synchronization of the clocks of all receivers connected with LAMs using the Pulse Per Second (PPS) signal of the included GPS receivers.

Acknowledgements

The authors would like to thank Bjørøya Fiskeoppdrett AS for providing an opportunity to conduct experiment at their fish farm, and the NTNU-ITK mechanical workshop for their help on the mechanical setup of the experiment. This work was funded in parts by Bjørøya Fiskeoppdrett AS through the "CycLus" R&D project, and the Norwegian Research Council through the Centre for Research-based innovation in Aquaculture Technology, the EXPOSED (Grant No.

237790).

References

Adelantado, F., Vilajosana, X., Tuset-Peiro, P., Martinez, B., Melia-Segui, J., Watteyne, T., 2017. Understanding the limits of LoRaWAN. IEEE Commun. Mag. 55, 34–40. https://doi.org/10.1109/MCOM.2017.1600613.

Augustin, A., Yi, J., Clausen, T., Townsley, W.M., 2016. A study of LoRa: long range & low power networks for the Internet of Things. Sensors 16. https://doi.org/10.3390/s16091466.

Bjelland, H.V., Føre, M., Lader, P., Kristiansen, D., Holmen, I.M., Fredheim, A., Grøtli, E.I., Fathi, D.E., Oppedal, F., Utne, I.B., Schjølberg, I., 2015. Exposed Aquaculture in Norway. In: OCEANS 2015 – MTS/IEEE Washington, pp. 1–10. https://doi.org/10.23919/OCEANS.2015.7404486.

Cooke, S.J., Thorstad, E.B., Hinch, S.G., 2004. Activity and energetics of free-swimming fish: insights from electromyogram telemetry. Fish Fish. 5, 21–52. https://doi.org/10.1111/j.1467-2960.2004.00136.x.

Davidsen, J.G., Rikardsen, A.H., Halttunen, E., Thorstad, E.B., Økland, F., Letcher, B.H., Skarðhamar, J., Næsje, T.F., 2009. Migratory behaviour and survival rates of wild northern Atlantic salmon Salmo salar post-smolts: effects of environmental factors. J. Fish Biol. 75, 1700–1718. https://doi.org/10.1111/j.1095-8649.2009.02423.x.

Deng, Z.D., Weiland, M.A., Fu, T., Seim, T.A., LaMarche, B.L., Choi, E.Y., Carlson, T.J., Eppard, M.B., 2011. A cabled acoustic telemetry system for detecting and tracking juvenile salmon: part 2. Three-Dimensional Tracking and Passage Outcomes. Sensors 11, 5661–5676. https://doi.org/10.3390/s110605661.

Duan, R., Chen, X., Xing, T., 2011. A QoS architecture for IOT. In: 2011 International Conference on Internet of Things and 4th International Conference on Cyber, Physical and Social Computing, pp. 717–720. https://doi.org/10.1109/iThings/CPSCom.2011.125.

FAO (2016). The State of World Fisheries and Aquaculture 2016. Rome.

Føre, M., Alfredsen, J.A., Gronningsater, A., 2011. Development of two telemetry-based systems for monitoring the feeding behaviour of Atlantic salmon (*Salmo salar* L.) in aquaculture sea-cages. Comput. Electron. Agric. 76, 240–251. https://doi.org/10.1016/j.compag.2011.02.003.

Føre, M., Frank, K., Dempster, T., Alfredsen, J., Høy, E., 2017. Biomonitoring using tagged sentinel fish and acoustic telemetry in commercial salmon aquaculture: a feasibility study. Aquacult. Eng. 78, 163–172. https://doi.org/10.1016/j.aquaeng.2017.07.004.

Føre, M., Frank, K., Norton, T., Svendsen, E., Alfredsen, J.A., Dempster, T., Eguiraun, H., Watson, W., Stahl, A., Sunde, L.M., Schellewald, C., Skøien, K.R., Alver, M.O., Berckmans, D., 2018a. Precision fish farming: a new framework to improve production in aquaculture. Biosyst. Eng. 173, 176–193. https://doi.org/10.1016/j.biosystemseng.2017.10.014.

Føre, M., Svendsen, E., Alfredsen, J., Uglem, I., Bloecher, N., Sveier, H., Sunde, L., Frank, K., 2018b. Using acoustic telemetry to monitor the effects of crowding and delousing procedures on farmed Atlantic salmon (Salmo salar). Aquaculture 495, 757–765. https://doi.org/10.1016/j.aquaculture.2018.06.060.

Grothues, T.M., 2009. A review of acoustic telemetry technology and a perspective on its diversification relative to coastal tracking arrays. In: Nielsen, J.L., Arrizabalaga, H., Fragoso, N., Hobday, A., Lutcavage, M., Sibert, J. (Eds.), Tagging and Tracking of Marine Animals with Electronic Devices. Springer, Netherlands, Dordrecht, pp. 77–90. https://doi.org/10.1007/978-1-4020-9640-2_5.

Grothues, T.M., Able, K.W., McDonnell, J., Sisak, M.M., 2005. An estuarine observatory for real-time telemetry of migrant macrofauna: design, performance, and constraints. Limnol. Oceanogr.: Methods 3, 275–289. https://doi.org/10.4319/lom.2005.3.275.

Hunkeler, U., Truong, H.L., Stanford-Clark, A., 2008. MQTT-S x2014; A publish/subscribe protocol for Wireless Sensor Networks. In: Communication Systems Software and Middleware and Workshops, 2008. COMSWARE 2008. 3rd International Conference on, pp. 791–798. https://doi.org/10.1109/COMSWA.2008.4554519.

Hussey, N.E., Kessel, S.T., Aarestrup, K., Cooke, S.J., Cowley, P.D., Fisk, A.T., Harcourt, R.G., Holland, K.N., Iverson, S.J., Kocik, J.F., Mills Flemming, J.E., Whoriskey, F.G., 2015. Aquatic animal telemetry: a panoramic window into the underwater world. Science 348. https://doi.org/10.1126/science.1255642.

ITU-T, 2008. Definitions of terms related to quality of service. Recommendation E.800 International Telecommunication Union Geneva.

Iversen, A., Andreassen, O., Øystein Hermansen, Larsen, T.A., Terjesen, B.F., 2013. Oppdrettsteknologi og konkurranseposisjon. Rapport 32/2013 Nofima.

Jovalekic, N., Drndarevic, V., Pietrosemoli, E., Darby, I., Zennaro, M., 2018. Experimental study of LoRa transmission over seawater. Sensors 18. https://doi.org/10.3390/s18092853.

Koeck, B., Pastor, J., Saragoni, G., Dalias, N., Payrot, J., Lenfant, P., 2014. Diel and seasonal movement pattern of the dusky grouper *Epinephelus marginatus* inside a marine reserve. Mar. Environ. Res. 94, 38–47. https://doi.org/10.1016/j.marenvres.2013.12.002.

Kolarevic, J., Aas-Hansen, Ø., Espmark, Å., Baeverfjord, G., Terjesen, B.F., Damsgård, B., 2016. The use of acoustic acceleration transmitter tags for monitoring of Atlantic salmon swimming activity in recirculating aquaculture systems (RAS). Aquacult. Eng. 72–73, 30–39. https://doi.org/10.1016/j.aquaeng.2016.03.002.

Light, R.A., 2017. Mosquitto: server and client implementation of the MQTT protocol. J. Open Sour. Softw. 2. https://doi.org/10.21105/joss.00265.

Liu, Y., Rosten, T.W., Henriksen, K., Hognes, E.S., Summerfelt, S., Vinci, B., 2016. Comparative economic performance and carbon footprint of two farming models for producing Atlantic salmon (Salmo salar): land-based closed containment system in freshwater and open net pen in seawater. Aquacult. Eng. 71, 1–12. https://doi.org/10.1016/j.aquaeng.2016.01.001.

Petäjäjärvi, J., Mikhaylov, K., Hämäläinen, M., Iinatti, J., 2016. Evaluation of LoRa LPWAN technology for remote health and wellbeing monitoring. In: 2016 10th International Symposium on Medical Information and Communication Technology (ISMICT), pp. 1–5. https://doi.org/10.1109/ISMICT.2016.7498898.

Petrić, T., Goessens, M., Nuaymi, L., Toutain, L., Pelov, A., 2016. Measurements, performance and analysis of LoRa FABIAN, a real-world implementation of LPWAN. In: 2016 IEEE 27th Annual International Symposium on Personal, Indoor, and Mobile Radio Communications (PIMRC), pp. 1–7. https://doi.org/10.1109/PIMRC.2016.7794569.

Pincock, D.G., Johnston, S.V., 2012. Acoustic telemetry overview. In: Adams, N.S., Beeman, J.W., Eiler, J.H. (Eds.), Telemetry Techniques: A User Guide for Fisheries Research. American Fisheries Society, Bethseda, Maryland, pp. 305–338.

Raza, U., Kulkarni, P., Sooriyabandara, M., 2017. Low power wide area networks: an overview. IEEE Commun. Surv. Tutorials 19, 855–873. https://doi.org/10.1109/COMST.2017.2652320.

Skilbrei, O.T., Holst, J.C., Asplin, L., Holm, M., 2009. Vertical movements of “escaped” farmed Atlantic salmon (*Salmo salar* L.)–a simulation study in a western Norwegian fjord. ICES J. Mar. Sci. 66, 278–288. https://doi.org/10.1093/icesjms/fsn213.

Talavera, J.M., Tobón, L.E., Gómez, J.A., Culman, M.A., Aranda, J.M., Parra, D.T., Quiroz, L.A., Hoyos, A., Garreta, L.E., 2017. Review of IoT applications in agro-industrial and environmental fields. Comput. Electron. Agric. 142, 283–297. https://doi.org/10.1016/j.compag.2017.09.015.

System for Real-time Positioning and Monitoring of Fish in Commercial Marine Farms Based on Acoustic Telemetry and Internet of Fish (IoF)

Waseem Hassan, Martin Føre
Department of Engineering Cybernetics, NTNU, Trondheim, Norway

Henning Andre Urke
INAQ AS, Trondheim, Norway

Torstein Kristensen, John Birger Ulvund
Faculty for Biosciences and Aquaculture, Nord University, Bodø, Norway

Jo Arve Alfredsen
Department of Engineering Cybernetics, NTNU, Trondheim, Norway

ABSTRACT

In this study the performance of the Internet of Fish (IoF) concept, a real-time acoustic positioning and fish monitoring system, was assessed in a commercial marine fish farm in Norway. Central to the IoF concept is the Synchronisation and LoRa Interface Module (SLIM), which is a battery operated surface unit that provides distributed time synchronisation and LPWAN support to a submerged digital acoustic receiver. Six SLIM/acoustic receiver pairs were placed inside a fish cage with acoustically tagged fish at a link-length of 200 m from a centralised gateway. All nodes achieved a Packet Error Rate of less than 8% and a position accuracy of 1.5 m.

KEY WORDS: Internet of Fish; LPWAN; acoustic telemetry; TDoA algorithm; marine aquaculture.

INTRODUCTION

Aquaculture is one of the fastest growing food producing industries in the world and is believed to be instrumental in filling the future global supply-demand gap in aquatic food (FAO., 2016). Raising fish in large floating net-based sea-cages have proven as a competitive option due to its flexibility, robustness and cost effectiveness (Føre et al., 2017), despite the generally harsh marine environment and technological and operational challenges it poses to the aquaculture industry. For instance, more than two million tons of Atlantic salmon are produced annually using this farming concept (Liu et al., 2016). The ability to monitor fish behaviour is important, as it is a key element in determining the stress and welfare conditions experienced by the fish in a farm situation (Oppedal, Dempster, and Stien, 2011). In addition, quantifying the movement patterns of fish is critical to understand feeding behaviours, resource utilisation and animal-environment interactions in cages (Espinoza et al., 2011; Biesinger et al., 2013). Acoustic telemetry is fish monitoring concept where individual animals are equipped with miniature electronic devices called transmitter tags that contain sensors and an acoustic modem for wireless underwater data transmission (see Føre, Alfredsen, and Gronningsater (2011) for a more thorough description of the contents of acoustic transmitter tags). This method has been used to observe detailed movement patterns of individual fish by employing source localisation algorithms (Pincock and Johnston, 2012). Previous applications of this approach include tracking of both wild (Espinoza et al., 2011; Biesinger et al., 2013) and farmed fish (Rillahan et al., 2009). Since farmed fish are generally restricted by the confines of the cages, their movement patterns are restricted to be within a much smaller volume than free swimming wild fish. This suggests that it is possible to realise automated positioning systems for aquaculture applications that are more precise than those developed for wild fish monitoring. Considering the large biomass, cage volumes and expected future growth trends in the marine finfish aquaculture industry, a remote monitoring system that can provide input to the day-to-day farm decisions is an essential requirement for realising the benefits and advances of the Precision Fish Farming (PFF) concept (Føre et al., 2017).

In this study, we developed and tested a real-time acoustic positioning and monitoring system for individual fish based on the Internet of Fish (IoF) concept. IoF is a concept similar to the Internet of Things (IoT) that provides real-time access to fish telemetry data by integrating a LoRa based Low Power Wide Area Network (LPWAN) with acoustic telemetry. The proposed solution combines a state-of-the-art submerged acous-

tic receiver with a surface communication module, hereafter referred to as the Synchronisation and LoRa Interface Module (SLIM), that provides a power-efficient long range wireless radio communication interface for relaying the fish telemetry data collected by the acoustic receiver. Multiple SLIMs were connected in a star topology to form an LPWAN of acoustic receivers, establishing the IoF concept. While the concept in itself provides access to telemetry data in real-time, IoF was extended with a Time Difference of Arrival (TDoA) algorithm to enable localisation in 3D. The system was tested in a commercial fish farm using six SLIM-acoustic receiver pairs placed inside a commercial-scale cage with fish carrying acoustic transmitter tags. The gateway, placed 200 m from the cage, was forwarding the received data to the user via the Internet. Communication quality provided by the IoF concept and position accuracy of the TDoA algorithm were analysed to evaluate the feasibility of an IoF based real-time fish positioning system.

MATERIALS AND METHODS

System Requirements

Link-length, bandwidth and battery operated end devices are three dimensioning requirements of the IoF concept. The end-to-end extent of a typical Atlantic salmon marine farm may be larger than 1 km, indicating that the minimum link-length supported by the IoF concept should exceed this distance. The minimum data transmission capacity/bandwidth is another important dimensioning parameter for the IoF concept, and is determined by the overall acoustic message rate and the size of a single acoustic message received by the SLIM from the acoustic receiver. In this study, 33 acoustic tags (Thelma Biotel AS, Trondheim, Norway) with a time interval between consecutive transmissions varying from 30 s to 90 s were used, roughly corresponding to an overall acoustic update rate of 10 acoustic messages per minute for the system as whole. After being interpreted by the acoustic receivers used in this study (TBR-700-RT, Thelma Biotel AS, Trondheim, Norway), a single telemetry message consisted of 11 bytes of information. The SLIMs were set up to transmit one radio packet per minute meaning that a packet size of at least 110 bytes was required to be able to include all telemetry messages received since last transmission. A final requirement for the IoF concept is that the end devices should be battery operated as electrical power may not be easily available and because cables are preferably avoided out of safety and practical reasons in floating sea-cages.

The aim to determine the fish position using a TDoA algorithm introduces additional system requirements due to the fact that acoustic messages from a single tag then need to be received by three or four acoustic receivers to achieve positioning in 2D or 3D, respectively. The TDoA algorithm also requires that the internal clocks of all acoustic receivers are synchronised (Juell and Westerberg, 1993; Grothues, 2009; Pincock and Johnston, 2012).

Internet of Fish (IoF) and LPWAN

The IoF concept (Hassan et al., n.d.) is based on LPWAN which is an emerging communication technology that addresses the unique requirements of IoT devices and that exploits the sub-gigahertz unlicensed Industrial, Scientific and Medical (ISM) radio bands. LPWAN provides large area coverage combined with low power consumption at the end-devices by utilising efficient modulation and duty-cycled transmission/reception schemes (Raza, Kulkarni, and Sooriyabandara, 2017). However this comes at a cost of very low data rates, which are in order of a few kilobytes per second (kbps) for a typical LPWAN (Centenaro et al., 2016; Raza, Kulkarni, and Sooriyabandara, 2017). Low data rates combined with duty-cycled operation yields low data throughput (in order of few bytes per second). Acoustic fish telemetry systems share many of these properties as end devices tend to rely on battery operation and have low power requirements and intrinsically low data throughput. This makes the combination of LPWANs and acoustic telemetry systems a reasonable approach for providing real-time user access to telemetry data. This is realised in the SLIM by providing LoRa based LPWAN support to extend an acoustic receiver with a radio interface for real-time access to the data.

The IoF concept used in the present study (Fig. 1) is made up of three layers and conforms to the architecture presented in Talavera et al., 2017. The first layer is the perception layer that contains end-devices that are typically distributed geographically/spatially. The second layer is the network layer and consists of a centralised network gateway which communicates with all end-devices in the perception layer. The third layer in this representation is the application layer which features a server and a database that together function as a system back-end and front-end for presentation of data to the user. The TDoA algorithm in the current study is implemented in the application layer and executes on the server.

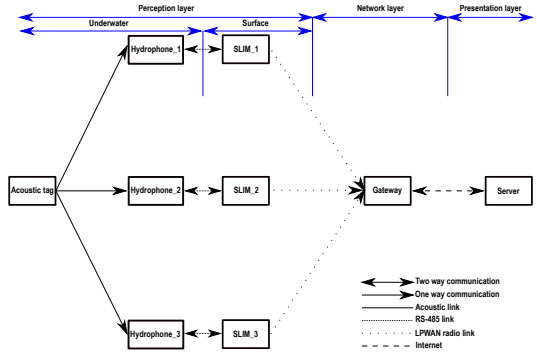

Fig. 1 Layered view of the IoF concept and modules used in different layers

Perception Layer: Synchronisation and LoRa Interface Module (SLIM)

The SLIM is a microcontroller (SiLabs EFM32GG842 32-bit ARM Cortex M3) based battery operated standalone module designed to provide LoRa radio interface to an acoustic receiver. In the LPWAN system, each SLIM has a unique ID and is a basic transmission device. A block diagram of the physical components in the SLIM is shown in Fig. 2. The SLIM was designed to interface with a Thelma Biotel TBR-700-RT acoustic receiver that was set up to forward all acoustic data received onto an RS-485 link, sending the decoded acoustic telemetry messages to the SLIM continually as they arrive. Radio communication was realised through a Serial Peripheral Interface (SPI) based LoRa module (RFM95W, HopeRF), and a Global Positioning System (GPS) module (u-blox, NEO-7P) was included to provide the receivers connected to the SLIM units with a system for distributed time synchronisation. The SLIM was designed using low power design techniques, and had a current consumption of 20 mA during normal operation (i.e. registering and storing messages received from the acoustic receiver), and 50 mA dur-

ing radio transmit mode (lasting for very short duration). Power was provided through a 3.6 V, 35 A h Lithium primary cell which allows the SLIM to operate for approximately 2 months.

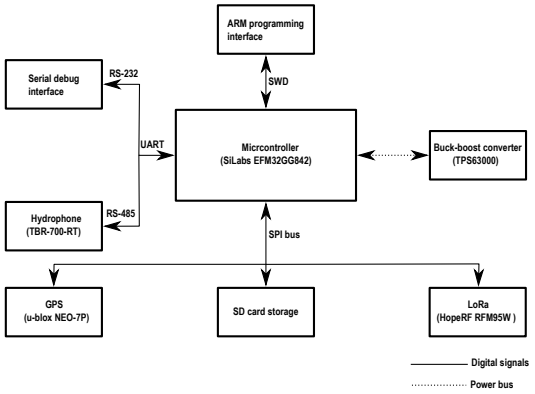

Fig. 2 Block diagram of the SLIM showing its peripherals

LoRa has previously been identified as the best candidate for IoT applications in agriculture (Adelantado et al., 2017; Talavera et al., 2017), and was used here as a physical (PHY) layer to realise the LPWAN in the IoF concept due to its relatively large coverage area and energy efficiency features. LoRa offers a coverage area of 5-15 km, thus satisfying the link-length requirement of the IoF concept. It also offers a payload up to 250 bytes, data rates up to 37.5 kpbs and a very low power consumption at the end-devices, thereby satisfying the system requirements associated with bandwidth and battery operated end devices (Goursaud and Gorce, 2015; Augustin et al., 2016; Adelantado et al., 2017; Raza, Kulkarni, and Sooriyabandara, 2017). The internal clocks of the acoustic receivers were synchronised using the Pulse Per Second (PPS) signal of the GPS chip of the SLIM, satisfying the TDoA-specific requirement of synchronisation of the acoustic receivers. In the European region (EU), LPWAN/LoRa modulation uses the 868 MHz ISM band with a maximum allowed duty cycle of 1%, which gives each end device a maximum time-on-air of 36 s per hour (Adelantado et al., 2017). The SLIM were programmed to comply with these duty cycle regulations, and use a spreading factor SF7, a coding rate of 4/5, a bandwidth of 125 kHz and a transmit power of 14 dBm. For a payload of 111 bytes, time-on-air for a single radio packet transmitted by the SLIM was 187.65 ms, or 11.259 s for 60 transmissions over a period of one hour. The firmware of the SLIM was developed in the C programming language using Silicon Lab's Simplicity Studio Integrated Development Environment (IDE), and was based on IBM's LMiC library which implements the LPWAN stack. Firmware operation was based on timer and PPS signal interrupts with an Interrupt Service Routine (ISR) being executed every 10 s, performing synchronisation and other radio transmission related tasks. Operation of the firmware is explained in the flow diagram shown in Fig. 3.

Network and application layers

The network layer includes the gateway, which works as a centralised node for all end devices (SLIMs) and is responsible for forwarding all incoming messages from nodes with authorised IDs to a server. A MultiConnect Conduit (MTCDT-H5-210L, Multi-Tech Systems, Inc.) which is a Commercially Off The Shelf (COTS) module, was used as the gateway in this study. The gateway was equipped with a Radio Frequency (RF) antenna to receive data from nodes via the LoRa radio link, and an Ethernet connection for transmitting all received data to the server. The gateway was communicating with the application layer using the Message Queuing Telemetry Transport (MQTT) protocol. MQTT is a subscribe/publish-based protocol often used in IoT applications, and that follows software client/broker architecture (Light, 2017).

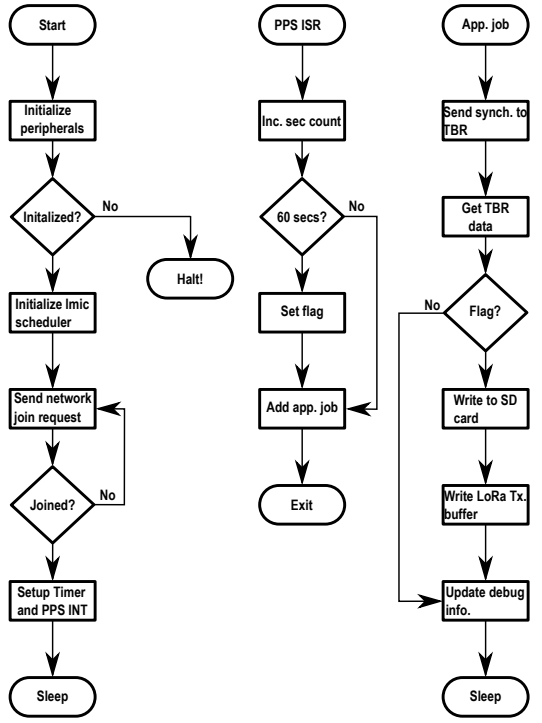

Fig. 3 Flowchart explaining firmware operation of the SLIM

A computer with Internet access was assigned the role as the server in the application layer. The server was responsible for receiving data from the gateway, storing the data locally on its hard drive, executing the TDoA algorithm for tag positioning and presenting the resulting data to end users. HBMQTT, which is an open source implementation of the MQTT protocol was used to implement the broker and client applications on the server, with the broker being set up to accept connections and receive data from the publisher-client running on the gateway, while the client was set up to subscribe to and store all received messages on the local hard drive in text files, acting as a database. A MATLAB script was continually executed on the server to run the TDoA algorithm to derive positioning data. This application enabled the user to select an array of SLIM nodes based on their IDs and plot associated fish position data in real-time.

Positioning Algorithm

The TDoA positioning method provided by Fang (1990) was used in this study. 2D position i.e. in the xy-plane, was achieved by using three acoustic receivers. Combined with the depth information provided by the on-board pressure sensor in the acoustic tags (Skilbrei et al., 2009; Føre, Alfredsen, and Gronningsater, 2011) the fishes' position in 3D could be determined. This method establishes an xyz-coordinate system (Euclidean space) which is defined with respect to the known 3D placement of the acoustic receivers. In this coordinate system, the position of the first acoustic receiver (A) was used as the origin $(0, 0, 0)$, the second receiver (B) was placed along the x-axis $(b, 0, 0)$, while the third receiver (C) was placed inside the xy-plane $(c_x, c_y, 0)$ having non-zero x- and y-coordinates. The placement of receivers and their coordinates are shown in Fig. 6. While Fang (1990) provided detailed equations for source localisation based on TDoA algorithm, equations are reproduced here for the purpose of clarity.

If the arrival times of an acoustic signal transmitted from a position (x, y, z) at acoustic receivers A, B and C are denoted by T_a, T_b and T_c respectively, T_{ab} denotes difference of arrival time between receivers A and B and T_{ac} denotes difference of arrival time between receivers A and C, giving the equations:

$$T_{ab} = T_a - T_b$$

$$T_{ac} = T_a - T_c \tag{1}$$

If the sound speed in water is denoted as c, and the distance of the acoustic tag from acoustic receivers A, B and C are denoted by R_a, R_b and R_c respectively, the difference of time equations can be written in terms of range difference equations using the distances between receivers A and B (R_{ab}) and receivers A and C (R_{ac}):

$$R_{ab} = T_{ab} * c$$

$$R_{ac} = T_{ac} * c \tag{2}$$

Using the geometry of the acoustic receiver setup, the distance of a tag placed at coordinates (x, y, z) from the three acoustic receivers is given by:

$$R_a = \sqrt{x^2 + y^2 + z^2}$$

$$R_b = \sqrt{(x - b)^2 + y^2 + z^2}$$

$$R_c = \sqrt{(x - c_x)^2 + (y - c_y)^2 + z^2} \tag{3}$$

These distances can be written in terms of difference of range with respect to acoustic receiver A using:

$$R_{ab} = \sqrt{x^2 + y^2 + z^2} - \sqrt{(x - b)^2 + y^2 + z^2}$$

$$R_{ac} = \sqrt{x^2 + y^2 + z^2} - \sqrt{(x - c_x)^2 + (y - c_y)^2 + z^2} \tag{4}$$

Squaring and simplifying Eq. (4) yields:

$$R_{ab}^2 - b^2 + 2 * b * x = 2 * R_{ab} * \sqrt{x^2 + y^2 + z^2}$$

$$R_{ac}^2 - (c_x^2 + c_y^2) + 2 * c_x * x + 2 * c_y * y = 2 * R_{ac} * \sqrt{x^2 + y^2 + z^2} \tag{5}$$

When R_{ab} and R_{ac} are non-zero, Eq. (5) can be written in parametric form in terms of x- and z-coordinates by eliminating y as:

$$z^2 = d * x^2 + e * x + f \tag{6}$$

where parameters are d, e, f, g and h are given by:

$$d = -1 * \left\{1 - (b/R_{ab})^2 + g^2\right\}$$

$$e = b * \left\{1 - (b/R_{ab})^2 - 2 * g * h\right\}$$

$$f = (R_{ab}^2/4) * \left\{1 - (b/R_{ab})^2 - h^2\right\}$$

$$g = \left\{R_{ac} * (b/R_{ab}) - c_x\right\} / c_y$$

$$h = \left\{c_x^2 + c_y^2 - R_{ac}^2 + R_{ab} * R_{ac} * (1 - (b/R_{ab})^2)\right\} / 2 * c_y$$

Similarly, tag's y-coordinates can be written in terms of x-coordinates using:

$$y = g * x + h \tag{7}$$

Depth (z) information is provided by tag's on-board depth sensor, whereas R_{ab} and R_{ac} can be calculated by the arrival time of the acoustic signals (Eq. (2)). Once R_{ab} and R_{ac} are known, parameters d, e, f, g and h can be calculated. Afterwards, x- and y- coordinates can be found by using equations Eq. (6) and Eq. (7), respectively. Cases when R_{ab}, R_{ac} or both are zero are solved trivially. For example when $R_{ab} = 0$, the x-coordinate of the tag is given by $b/2$. Similarly, when both $R_{ab} = 0$ and $R_{ac} = 0$, x- and y-coordinates of the tag are at an equal distance from all three acoustic receivers (Fang, 1990).

Experimental Setup

A series of dry tests in the lab were first conducted to test the general functionality of the IoF concept and the TDoA positioning algorithm separately, before testing a single integrated system that combined both functions. A field trial at a commercial marine fish farm in Norway was then conducted to test the use of the LoRa-based LPWAN for real-time acoustic tag positioning in the real setting. Six nodes and one gateway were used in the field test. Each node consisted of a surface mounted SLIM connected to a submerged TBR-700-RT acoustic receiver. The nodes were set up in a redundant configuration (Fig. 4), but only three nodes were used by the positioning system. The nodes were installed in an equilateral triangle configuration in a fish cage, with the antennas 0.8 m above sea level and with a link-length of 200 m from the gateway (Fig. 5). Acoustic receivers were placed 3 m below the sea-surface, firmly fixed to the cage structure to maintain the receiver geometry during the experiment. All nodes were set to transmit one radio message over the LPWAN every minute where the size of the radio messages varied depending on the number of acoustic messages received during the past minute. Three acoustic test transmitter tags (R-MP9L Thelma Biotel AS, Trondheim Norway) were deployed in the water at fixed known locations with varying depths inside the fish cage for 12 h to benchmark the communication quality of the LPWAN and determine position accuracy of the positioning system. After collecting the benchmarking dataset, the system was used to monitor 30 fish carrying acoustic tags with acceleration/activity and depth sensors (AD-MP9L, R-MP9L and D-LP7 Thelma Biotel AS, Trondheim Norway). The tags were divided into three groups transmitting at different acoustic frequencies to reduce acoustic interference (69 kHz, 71 kHz and 73 kHz) inside the cage. Although only the depth data values were used for fish positioning, the data from the activity sensor was also sent over the radio link. The gateway was placed inside the fish farm's feed barge with an RF antenna mounted inside the barge approximately 8 m above sea level to ensure line of sight communication with the nodes. The gateway was connected to the Internet via an Ethernet port on a standard network router installed on the barge. The relative locations of the nodes and the gateway are shown in Fig. 5. The server was placed in an office environment.

The surgical protocol for implanting acoustic tags in the fish followed the general recommendations given by Mulcahy (2003) and Cooke, Thorstad, and Hinch (2004). Approval was granted by the Norwegian

Animal Research Authority (ID 15491). All surgical equipment was sterilised before use, and care was taken to maintain conditions as aseptic as possible. A well-documented protocol for anaesthesia, analgesia and surgery described by Urke et al. (2013) was used. The total length L_T of the fish was recorded. Total handling time was around 2 min, per fish. Immediately after surgery, the fish were transferred to a recovery tank and closely monitored. Fish regained balance ability and showed active swimming behaviour within 0.5 min-2 min of recovery. After a recovery period of 10 min, the fish were released into the cage.

Fig. 4 SLIM nodes installed in redundant configuration on cage structure

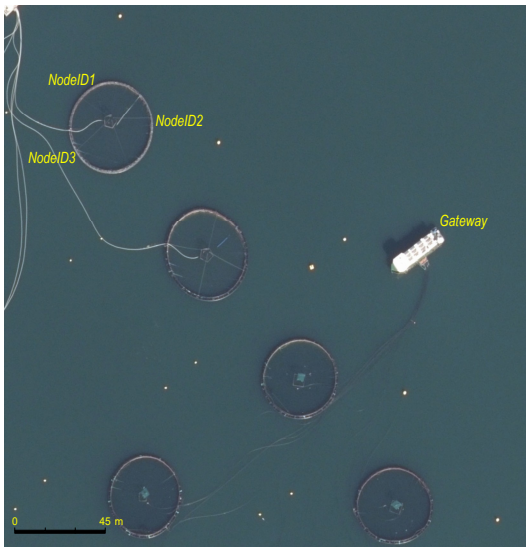

Fig. 5 Map showing position of nodes and gateway in the fish farm

RESULTS

The overall performance of the nodes during the experiment satisfied all system requirements specified for the system. The benchmark dataset was used to evaluate system performance in terms of the communication quality provided by the IoF concept and the accuracy bounds of the positioning algorithm.

Packet Error Rate (PER) of the IoF Concept

PER is defined as ratio of packets lost in transmission from nodes to server and was used to evaluate the performance of the IoF concept and quality of communication provided by the radio interface (LPWAN). PER includes two types of losses due to the radio interface and an additional loss of packets from gateway to the server i.e. loss over the Internet. The first type of radio loss includes those acoustic messages that were successfully received and processed by a SLIM node but did not arrive at the gateway, whereas the second type of radio loss includes radio packets that were received at the gateway and successfully transmitted to the server but which were based on corrupted acoustic data. Mathematically, PER is defined as:

$$PER = 1 - \frac{uncorrupted\ messages\ received\ at\ server}{total\ messages\ transmitted\ by\ a\ node} \quad (1)$$

Table 1 shows the total number of messages transmitted (Packets Tx), uncorrupted messages received at the server (Packets Rx) and PER values of the nodes for the benchmark dataset. All nodes achieved a PER of less than 8%.

While the PER values of the nodes describes the overall quality of the communication system, the positioning system requires the successful reception of a single acoustic message on all three receivers and that this message is transferred from at least three SLIM nodes to the server over the radio link. Table 2 shows the number of messages received for each tag ID (Tag ID) in the benchmark dataset that were detected by all three SLIM modules and thus were usable for the positioning algorithm (Message triplets), the average number of messages for each tag ID received by the individual SLIM units (Average messages received) and the percentage of the average number of messages that were part of a message triplet (Percent usable). More than 90% of the received messages were used by the position algorithm for each tag ID.

Accuracy of the Positioning Algorithm

The accuracy of the positioning algorithm is affected by geometry, variations in position and uncertainties/bias in the clocks and timestamping accuracy of the acoustic receiver array (Juell and Westerberg, 1993). Errors related to array geometry and acoustic receiver positions were minimised in the field experiment by mounting the nodes at known position on the cage structure. The PPS signal of the GPS chip was used to synchronise the acoustic receivers, thus minimising the impact of clock difference as an error source. Acoustic receivers (TBR-700-RT) timestamped the incoming acoustic signals with a resolution of 1 ms, setting an upper bound of 1.5 m on to the position resolution of the algorithm. Fig. 6 shows the calculated positions of reference tags, whereas Fig. 7 shows a histogram of radial error ($\sqrt{x_{error}^2 + y_{error}^2}$) for the benchmark dataset. A Circular Error Probability (CEP) of 1.37 m, 1.49 m and 1.22 m were achieved for tag ID 90 (depth 3 m), tag ID 91 (depth 2 m) and tag ID 92 (depth 1 m), respectively.

Table 1 PER values of individual nodes, with number of packets transmitted by nodes and received at server.

Node ID	Packets Tx by node	Packets Rx at server	PER
1	1446	1381	4.5%
2	1386	1276	7.94%
3	1381	1368	1%

Table 2 Benchmark data set tag IDs, number (average) of messages received at server and number of messages usable for positioning algorithm.

Tag ID	Average messages received	Message triplets	Percent usable
90	462	419	90.69%
91	423	392	92.67%
92	446	411	92.15%

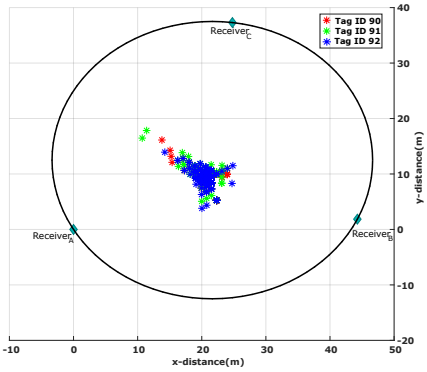

Fig. 6 Horizontal placement of acoustic receivers inside the cage (all receivers at 3 m depth). TDoA calculated positions for the benchmark data set are shown in the middle of cage.

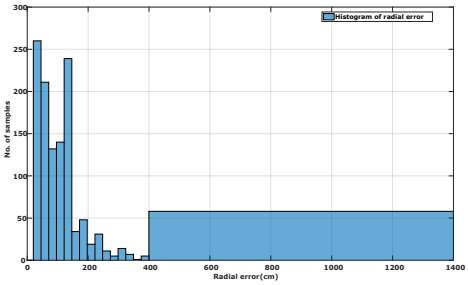

Fig. 7 Radial error distribution ($\sqrt{x_{error}^2 + y_{error}^2}$) of the TDoA calculated tag positions based on the benchmark dataset. The dataset includes a total number of 1222 message triplets.

DISCUSSION

In this study, the server got updates from the nodes every 60 s and the positions of fish carrying tags would therefore face a worst case delay of

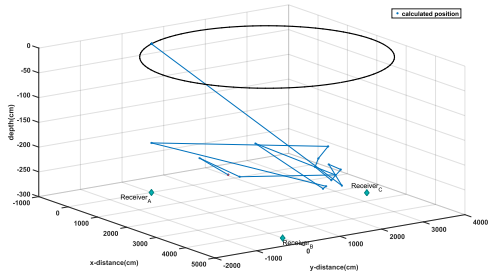

Fig. 8 A trajectory of a tagged fish (tag ID 102) tracked in real-time with an average sampling time of 3 minutes. Acoustic receivers are placed at a depth of 3 m inside cage.

60 s. Since the system was designed to be a real-time system for monitoring applications, as opposed to a critical industrial control system, a worst case delay of one minute seems acceptable. The CEP values for the tags used in the benchmark data set suggests that the positioning error stayed within the bounds of the expected resolution of about 1.5 m (i.e. the distance sound travels in sea water in 1 ms). This confirms that the accuracy of the positioning system is limited by the minimum resolution of the timestamp provided by the acoustic receiver, which for a TBR-700-RT is 1 ms. When a tag is placed close to an acoustic receiver, the error in calculated position may increase thus leading to lower position accuracy. It is also possible that the algorithm cannot find a valid position solution in such a scenario. The position resolution of the IoF based real-time positioning system can be increased by using acoustic receivers with finer timestamp resolutions, or by using the Signal to Noise Ratio (SNR) value when a tag detection is close to one of the acoustic receivers. The TBR-700-RT already provides the SNR value for each received acoustic signal, making the latter of these algorithm improvements relatively easy to achieve. There exist several acoustic positioning systems using TDoA algorithms to calculate positions, including both wired (e.g. Vemco VPS, HTI Inc) and wireless (e.g. Vemco VRAP, Lotek inc Wireless WHS 3060 MAP) systems (Espinoza et al., 2011; Biesinger et al., 2013). In wired system, cables are used to provide real-time access and may also be used to synchronise the acoustic receivers making them generally more precise in terms of positioning than wireless systems (Andrews et al., 2011). However, wired systems suffer from coverage areas issues, are labour intensive with respect to retrieving telemetry data and can only be used in

near-shore applications (Espinoza et al., 2011). Moreover cables in and around fish farms and cages are also seen as a liability issue by the farmers, rendering wired systems impractical for applications in the marine environment. Wireless positioning systems typically use radio interfaces to provide real-time access to the telemetry data. However, commercially available wireless systems are typically not designed to use modulation schemes such as LoRa and LPWAN protocols, and may therefore suffer from issues such as limited range, inferior scaling (i.e. number of acoustic receivers served) and too low energy efficiency of the end devices (Espinoza et al., 2011). These systems tend to be more expensive than wired position systems (Andrews et al., 2011). The LoRa/LPWAN based IoF concept does not suffer from these shortcomings in having long range and low power end devices. This is achieved at the cost of low data transmission rates for the end-devices. Since data rates in acoustic telemetry and similar applications are inherently low, the benefits in range and power consumption of using LPWAN-based solutions for the wireless components in such systems outweigh the disadvantage of reduced data rates.

The field experiment for real-time tagged fish position monitoring was planned for 4 months. The LPWAN system proved the feasibility of real-time fish monitoring in a commercial aquaculture farm. Fig. 8 shows a sample trajectory track of a tagged fish (tag ID 102) over a 45 min duration, illustrating a typical output and the capability of the IoF based positioning system. However, the fish behaviour data of the experiment is not studied in this paper.

CONCLUSIONS

In this study, the IoF concept was extended with a TDoA positioning algorithm for real-time estimation of acoustic tags positions in marine aquaculture farms. The results of the experiment affirm that the IoF and TDoA positioning can be used to provide real-time positions of acoustic tags in marine aquaculture monitoring applications. An average PER of 4.48% was achieved for all nodes used in the experiment, which proves that the system was able to upload field telemetry data in real-time to a server in a reliable manner. Furthermore, the TDoA algorithm was able to achieve a resolution/CEP of 1.5 m, which can be further improved by using acoustic receivers with finer timestamp resolution. The SLIM units developed in this study can potentially operate for months on a single battery with sufficiently long link-lengths to cover any configuration of a commercial marine aquaculture fish farm. In summary, this demonstrates that the IoF positioning system developed in this study was able to provide users with real-time access to position data for acoustic tags in sea-cages without suffering from the challenges faced by existing commercially available cabled or wireless real-time positioning systems.

ACKNOWLEDGMENTS

The authors would like to thank Midt-Norsk Havbruk AS for providing an opportunity to conduct experiment at their fish farm, and the NTNU-ITK mechanical workshop for their help on the mechanical setup of the experiment. This work was funded by the Norwegian Research Council through the Centre for Research-based innovation in Exposed Aquaculture Technology (grant number 237790) and by Bjørøya Fiskeoppdrett AS through the "CycLus" R&D project.

REFERENCES

Adelantado, F., X. Vilajosana, P. Tuset-Peiro, B. Martinez, J. Melia-Segui, and T. Watteyne. 2017. "Understanding the Limits of LoRaWAN." *IEEE Communications Magazine* 55 (9): 34–40. ISSN: 0163-6804.

Andrews, Kelly S., Nick Tolimieri, Greg D. Williams, Jameal F. Samhouri, Chris J. Harvey, and Phillip S. Levin. 2011. "Comparison of fine-scale acoustic monitoring systems using home range size of a demersal fish." *Marine Biology* 158, no. 10 (May): 2377. ISSN: 1432-1793.

Augustin, Aloÿs, Jiazi Yi, Thomas Clausen, and William Mark Townsley. 2016. "A Study of LoRa: Long Range & Low Power Networks for the Internet of Things." *Sensors* 16 (9). ISSN: 1424-8220.

Biesinger, Zy, Benjamin M. Bolker, Douglas Marcinek, Thomas M. Grothues, Joseph A. Dobarro, and William J. Lindberg. 2013. "Testing an autonomous acoustic telemetry positioning system for fine-scale space use in marine animals." *Journal of Experimental Marine Biology and Ecology* 448:46–56. ISSN: 0022-0981.

Centenaro, M., L. Vangelista, A. Zanella, and M. Zorzi. 2016. "Long-range communications in unlicensed bands: the rising stars in the IoT and smart city scenarios." *IEEE Wireless Communications* 23, no. 5 (October): 60–67. ISSN: 1536-1284.

Cooke, Steven J, Eva B Thorstad, and Scott G Hinch. 2004. "Activity and energetics of free-swimming fish: insights from electromyogram telemetry." *Fish and Fisheries* 5 (1): 21–52.

Espinoza, Mario, Thomas J. Farrugia, Dale M. Webber, Frank Smith, and Christopher G. Lowe. 2011. "Testing a new acoustic telemetry technique to quantify long-term, fine-scale movements of aquatic animals." *Fisheries Research* 108 (2): 364–371. ISSN: 0165-7836.

Fang, B. T. 1990. "Simple solutions for hyperbolic and related position fixes." *IEEE Transactions on Aerospace and Electronic Systems* 26, no. 5 (September): 748–753. ISSN: 0018-9251.

FAO. 2016. *The State of World Fisheries and Aquaculture*. Food and Agricultural Organization of the United Nations. ISBN: 978-92-5-109185-2.

Føre, Martin, Jo Arve Alfredsen, and Aage Gronningsater. 2011. "Development of two telemetry-based systems for monitoring the feeding behaviour of Atlantic salmon (Salmo salar L.) in aquaculture sea-cages." *Computers and Electronics in Agriculture* 76 (2): 240–251. ISSN: 0168-1699.

Føre, Martin, Kevin Frank, Tomas Norton, Eirik Svendsen, Jo Arve Alfredsen, Tim Dempster, Harkaitz Eguiraun, et al. 2017. "Precision fish farming: A new framework to improve production in aquaculture." *Biosystems Engineering.* ISSN: 1537-5110.

Goursaud, Claire, and Jean-Marie Gorce. 2015. "Dedicated networks for IoT : PHY / MAC state of the art and challenges." *EAI endorsed transactions on Internet of Things* (October).

Grothues, Thomas M. 2009. "A Review of Acoustic Telemetry Technology and a Perspective on its Diversification Relative to Coastal Tracking Arrays." In *Tagging and Tracking of Marine Animals with Electronic Devices,* edited by Jennifer L. Nielsen, Haritz Arrizabalaga, Nuno Fragoso, Alistair Hobday, Molly Lutcavage, and John Sibert, 77–90. Dordrecht: Springer Netherlands. ISBN: 978-1-4020-9640-2.

Hassan, Waseem, Martin Føre, John Birger Ulvund, and Jo Arve Alfredsen. n.d. "Internet of Fish: Integration of acoustic telemetry with LPWAN for efficient real-time monitoring of fish in marine farms." *(Submitted, under review).*

Juell, Jon-Erik, and Håkan Westerberg. 1993. "An ultrasonic telemetric system for automatic positioning of individual fish used to track Atlantic salmon (Salmo salar L.) in a sea cage." *Aquacultural Engineering* 12 (1): 1–18. ISSN: 0144-8609.

Light, Roger A. 2017. "Mosquitto: server and client implementation of the MQTT protocol." *Journal of Open Source Software* 2, no. 13 (May).

Liu, Yajie, Trond W. Rosten, Kristian Henriksen, Erik Skontorp Hognes, Steve Summerfelt, and Brian Vinci. 2016. "Comparative economic performance and carbon footprint of two farming models for producing Atlantic salmon (Salmo salar): Land-based closed containment system in freshwater and open net pen in seawater." *Aquacultural Engineering* 71:1–12. ISSN: 0144-8609.

Mulcahy, Daniel M. 2003. "Surgical Implantation of Transmitters into Fish." *ILAR Journal* 44 (4): 295–306.

Oppedal, Frode, Tim Dempster, and Lars H. Stien. 2011. "Environmental drivers of Atlantic salmon behaviour in sea-cages: A review." *Aquaculture* 311 (1): 1–18. ISSN: 0044-8486.

Pincock, Douglas G., and Samuel V. Johnston. 2012. "Acoustic Telemetry Overview." In *Telemetry Techniques: A User Guide for Fisheries Research,* edited by Noah S. Adams, John W. Beeman, and John H. Eiler, 305–338. Bethseda, Maryland: American Fisheries Society. ISBN: 978-1-934874-26-4.

Raza, U., P. Kulkarni, and M. Sooriyabandara. 2017. "Low Power Wide Area Networks: An Overview." *IEEE Communications Surveys Tutorials* 19 (2): 855–873.

Rillahan, Chris, Michael Chambers, W. Huntting Howell, and Winsor H. Watson. 2009. "A self-contained system for observing and quantifying the behavior of Atlantic cod, Gadus morhua, in an offshore aquaculture cage." *Aquaculture* 293 (1): 49–56. ISSN: 0044-8486.

Skilbrei, Ove T., Jens Christian Holst, Lars Asplin, and Marianne Holm. 2009. "Vertical movements of "escaped" farmed Atlantic salmon (Salmo salar L.)—a simulation study in a western Norwegian fjord." *ICES Journal of Marine Science* 66 (2): 278–288.

Talavera, Jesús Martín, Luis Eduardo Tobón, Jairo Alejandro Gómez, María Alejandra Culman, Juan Manuel Aranda, Diana Teresa Parra, Luis Alfredo Quiroz, Adolfo Hoyos, and Luis Ernesto Garreta. 2017. "Review of IoT applications in agro-industrial and environmental fields." *Computers and Electronics in Agriculture* 142:283–297. ISSN: 0168-1699.

Urke, H. A., T. Kristensen, J. V. Arnekleiv, T. O. Haugen, G. Kjærstad, S. O. Stefansson, L. O. E. Ebbesson, and T. O. Nilsen. 2013. "Seawater tolerance and post-smolt migration of wild Atlantic salmon Salmo salar × brown trout S. trutta hybrid smolts." *Journal of Fish Biology* 82 (1): 206–227.

A novel Doppler based speed measurement technique for individual free-ranging fish

Waseem Hassan, Martin Føre
Department of Engineering Cybernetics, NTNU
Trondheim, Norway
waseem.hassan,martin.fore@ntnu.no

Magnus Oshaug Pedersen
SINTEF Ocean AS
Trondheim, Norway
magnus.pedersen@sintef.no

Jo Arve Alfredsen
Department of Engineering Cybernetics, NTNU
Trondheim, Norway
jo.arve.alfredsen@ntnu.no

***Abstract*—A novel Doppler based speed measurement technique for free-ranging acoustically tagged fish was developed and validated through a field experiment in a marine aquaculture farm. For emulated swimming speeds in the range $25\,\mathrm{cm\,s^{-1}}$-$60\,\mathrm{cm\,s^{-1}}$, an rms error of $5\,\mathrm{cm\,s^{-1}}$ with a standard deviation of $4.7\,\mathrm{cm\,s^{-1}}$ was achieved, and with a relative error typically less than 10% of measured speed. The technique is designed to integrate easily with existing acoustic fish telemetry systems and requires only three hydrophones to determine swimming speeds. Measurement of fish swimming speed has a wide range of applications within fisheries sciences and may become a valuable tool for assessing fish behavior and performance in marine farms.**

***Keywords*—** Acoustic telemetry; Doppler measurement; marine aquaculture; signal processing; sensor phenomena

I. Introduction

Fish swimming arises from coordinated motion of various body systems and is a key parameter in understanding fish behavior, and more intrinsic properties such as energy expenditure, stress and hunger levels. Knowing the swimming speed of the fish can therefore be essential for improving farm management operations and animal welfare conditions in the marine aquaculture industry [2, 6, 12]. Fish swimming performance is possible to assess accurately in controlled laboratory trials [16], but such data may not reflect the true swimming speeds seen in free-ranging fish [13]. Achieving adequate speed measurements on fish in large marine fish farms is also considerably more challenging than in a confined laboratory setup.

Underwater speeds are often measured using acoustic instruments such as Acoustic Doppler Current Profilers (ADCPs) [10] and Acoustic Doppler Velocimeters (ADVs) [18], but these methods are unsuitable for measuring individual fish speeds. Other technologies such as split beam sonars [13] and camera solutions coupled with machine vision techniques [15] can estimate individual swimming speeds, but only for the group of fish that are within their field of view at any given time. None of these solutions are therefore able to track the speeds of specific individuals over time, which is essential to obtain individual data histories. Such data would facilitate more precise evaluations of e.g. the ultimate welfare impacts of being exposed to strong and sustained currents [8], as these are important to consider on the individual level [9]. This highlights the need for new technological tools to objectively assess individual swimming speeds in fish farms.

Acoustic telemetry is a monitoring method where individual animals are equipped with miniature electronic tags that contain an acoustic transmitter for wireless underwater data transmission and sensor circuitry for sensing relevant parameters in or near the fish [4, 17]. A typical acoustic telemetry system consists of acoustic transmitter tags and one or more matching acoustic receivers (i.e. specialized hydrophone devices that receive and decode acoustic signals emitted by the tags). Although this method has been used to measure behavior in aquaculture settings (e.g. depth [5], activity [2, 11]), no existing systems measure instantaneous fish swimming speed. Many acoustic telemetry systems employ modulation schemes where information is encoded in the time domain as the time interval between uniform acoustic pulses of fixed frequency and duration [14]. Transmitter movement will inevitably cause Doppler shifts in the carrier frequency of these pulses, potentially representing a novel approach to acquiring the swimming speeds of individual fish through frequency analysis of the received signals.

In this study, we propose a system for measuring individual fish speed using the Doppler shift in the carrier wave of acoustic transmitter tags. By using the already existing carrier wave, the method does not add complexity on the transmitter side or consume extra acoustic bandwidth. This keeps the most resource constrained end of the system (i.e. the tag) intact, while all signal processing to obtain the Doppler Shifted Frequency (DSF) is conducted by the less resource constrained acoustic receivers. A field experiment to validate the speed measurement principle was executed in a marine fish farm stocked with Atlantic salmon at commercial density.

II. Materials and Methods

A. Theory and Speed Computation Algorithm

Relative motion between an acoustic source and a receiver will shift the acoustic frequency of the received signal through what is known as the Doppler effect. This effect is widely employed to calculate the speed and position of a moving source based on the DSF received by a stationary receiver. The method can be used as a reliable speed measurement tool if the position of the acoustic transmitter and the transmitted signal frequency are known since a closed form solution for

speed based on DSF is then possible [1]. A DSF (f_d) relates to the transmitted source frequency (f_s) and the frequency (f_r) received at a receiver by:

$$f_d = f_s - f_r \tag{1}$$

A DSF can have both positive and negative values, with positive values meaning that the transmitter is moving towards the receiver while a negative DSF implies movement away from a receiver. Since a DSF is proportional to the velocity component parallel to the direct line between receiver and transmitter, the angle between the velocity vector and this line (θ_s) needs to be considered. The relationship between transmitter speed relative to a stationary receiver (v_s) and the resulting DSF (f_d) is given by:

$$v_s = \frac{f_d c}{f_s cos\theta_s} \tag{2}$$

Where c is speed of acoustic signal inside propagation medium and f_s is the source frequency. Equation 2 can thus be used to calculate v_s for a moving source if θ_s and f_d are known. To illustrate how this method works, a case of 2D ($xy-$plane) speed extraction is shown in Fig. 1. An acoustic transmitter tag at position O is moving with velocity v_s at an angle θ_s with respect to the local $x-$axis.The first step in calculating v_s is to find the angles θ_A and θ_B between the velocity vector and the lines between the receivers at positions A and B and the tag. Based on the known positions O, A and B it is possible to find the angle $\angle AOB$, which relates to θ_A and θ_B as:

$$\angle AOB = \theta_B - \theta_A \tag{3}$$

Once $\angle AOB$ is known, θ_A and θ_B can be obtained by applying (2) and the measured DSFs f_{dA} and f_{dB} to each of the acoustic receivers separately along with (3). θ_A is then found as:

$$\theta_A = atan(\frac{cos(\angle AOB) - \frac{f_{dB}}{f_{dA}}}{sin(\angle AOB)}) \tag{4}$$

, while θ_B is found by inserting (4) into (3). Assuming that the acoustic telemetry systems use a fixed known transmission frequency (f_s), v_s can be calculated from (2), by inserting θ_A and f_{dA} or θ_B and f_{dB} to obtain the components along lines AO and BO, respectively. The angle θ_s can then be found as:

$$\theta_s = 360° - \theta_B - \angle BOX \tag{5}$$

In the case shown in Fig. 1, the velocity vector is in the 2^{nd} quadrant, however $\angle AOB$ can be found using the same angle difference equation (3) in the other three quadrants as long as angles are similarly defined in a counter-clockwise manner. The position of the acoustic tag must be known for this method to work, which may pose a challenge when the tag is carried by a fish. However, if a third receiver, as indicated by C in Fig. 1, is used, a hyperbolic Time Difference of Arrival (TDoA) approach can be used to obtain tag position if all three receivers have known positions A, B and C and are time synchronized [7, 14].

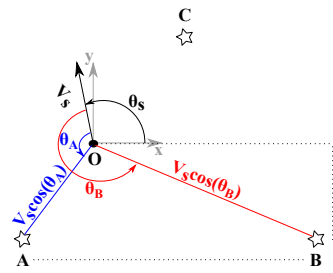

Fig. 1. A transmitter tag located at O moving with a velocity $\vec{v_s}$ in the horizontal plane. The Doppler shift measured at receiver locations A and B will be proportional to the components of the transmitter speed v_s along the lines AO and BO, respectively, defined by the angles θ_A and θ_B. A third receiver at location C enables TDoA-based transmitter localization.

B. Experimental Setup

A field experiment was conducted inside a large-scale fish cage containing Atlantic salmon to validate the proposed speed measurement technique in a relevant environment. A custom-made acoustic tag generating an acoustic burst signal at $68.968\,\mathrm{kHz}$, representative of frequencies typically employed in acoustic fish telemetry systems, was used in the experiment. The tag was mounted to a rod attached to a small remotely controlled catamaran, placing it at a constant depth of $1\,\mathrm{m}$. The catamaran was moved with speeds in the range of $25\,\mathrm{cm\,s^{-1}}$-$60\,\mathrm{cm\,s^{-1}}$, which is similar to sustained swimming speeds commonly observed in Atlantic salmon [8], thus emulating fish movement. Movement trajectories were kept circular to generate a data-set where the tag position varied sufficiently to cover a wide range of geometries, and where the velocity vector covered all possible directions relative to the hydrophones. A Real Time Kinematics (RTK) GPS with position accuracy of $< \pm 5cm$ was employed to determine the exact position and speed of the tag and was used as ground truth for the Doppler speed calculations. In this case, the GPS position was also used as a substitute of TDoA based localization of the tag to calculate $\angle AOB$, θ_A and θ_B. An embedded computer installed in the catamaran synchronized the transmission of the acoustic pulses with the RTK GPS positions and stored continuous records of reference data. Three icListen HF recording hydrophones (Ocean Sonics Ltd., Nova Scotia, Canada) were placed at $1\,\mathrm{m}$ depth in a configuration similar to that of A, B and C in Fig. 1, and were set to record the acoustic signal at a sampling rate of $256\,\mathrm{kS\,s^{-1}}$. The data from the hydrophones were processed in Matlab (The MathWorks, Inc., Natick, Massachusetts, USA) using Fast Fourier Transform (FFT), and the average value of DSF peaks for each pulse in a single burst was applied in the speed calculations.

III. Results

A mean error of $-1.9\,\mathrm{cm\,s^{-1}}$ with a standard deviation of $4.7\,\mathrm{cm\,s^{-1}}$ and an rms error of $5\,\mathrm{cm\,s^{-1}}$ was achieved for all data-sets (190 samples), giving a relative error of 10% or

less in the speed measurements. Fig. 2a shows normalized histograms of all true and measured speeds together with their respective probability distribution functions fitted to the normal distribution. The corresponding error distribution is shown in Fig. 2b.

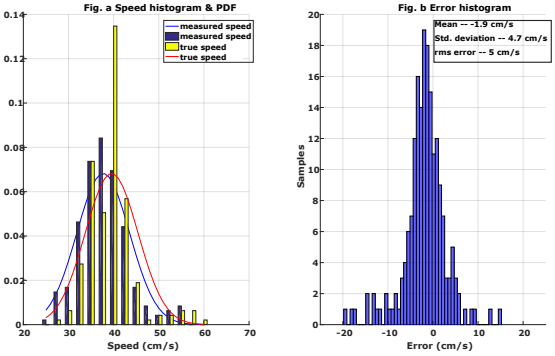

Fig. 2. (a) Speed distributions and histograms (b) error in measured and reference speed histogram.

IV. Discussion

The speed measured using the proposed Doppler based technique matched closely with the reference speed measurements from the RTK GPS. This study has therefore validated the feasibility of the proposed Doppler based technique as a method for measuring the horizontal swimming speed of acoustically tagged fish, either free-ranging or within the confines of a fish farm. Although the method needs an accurate characterization of the carrier frequency and its variability due to e.g. temperature fluctuations and drift, it requires no major modifications to the transmitter tags commonly used in commercial telemetry systems [5, 17]. This implies that the technique can extend the capabilities of existing solutions solely by adding the required signal processing capacity at the receiver end, either embedded as part of the real-time receiver function or as a post processing feature. The speed range selected for the experiment was motivated by wanting to cover swimming speeds typically observed in farmed Atlantic salmon during production, as this represents a prospective application area for the method [6, 8]. A relative measurement error of less than 10% throughout this range suggests that the technique may be applied reliably to characterize individual swimming speeds in salmon farms. The frequency resolution of the FFT analyses was set to $1\,\mathrm{Hz}$, yielding a speed resolution of $2.17\,\mathrm{cm\,s^{-1}}$. An rms error of $5\,\mathrm{cm\,s^{-1}}$ thus indicates that speed was measured with an accuracy close to the resolution of the system. To benefit from future improvements in accuracy, a higher resolution FFT would be required. However, increasing measurement accuracy in this way would represent a trade-off against availability of computing resources and energy efficiency on the receiver side. TDoA positioning systems will typically be necessary to obtain the position of a tag when it is carried by a fish. Such systems have a resolution/Circular Error Probability (CEP) in range of a few meters down to $1\,\mathrm{m}$ [7, 14]. Since $\angle AOB$ is estimated by using arc tangent of the ratio of distances OA and OB, this resolution may also impact the accuracy of the Doppler method. Errors in $\angle AOB$ due to imprecise position will be highest when the distances OA and OB (Fig. 1) are short, as even small errors ($1\,\mathrm{m}$ or less) then will strongly affect the angle estimate. However, assuming that the resolution/CEP value is kept constant, increasing distances OA and OB will gradually reduce the impact of this effect on the estimated $\angle AOB$, as the ratio between OA and OB and the potential error would then decrease. Since the Doppler based speed measurement principle requires only two acoustic receivers for speed measurement, whereas TDoA employs three or four receivers, the error due to variation in tag's position can be avoided in speed measurement by selecting the receivers having longest OA and OB distances. Moreover, although the proposed speed measurement technique has been outlined and demonstrated for the horizontal case, it could readily be extended to accommodate 3D speeds by including a third hydrophone. This could be done without requiring any principal changes to the derivation of the algorithm in itself, underlining the suitability of combining this method with TDoA. An underlying assumption for the measurement technique presented here is that the acoustic wave travels in a direct path between transmitter and receiver. However, in a real-world applications, acoustic waves are subject to multipath propagation and various fading effects that may arise at the receiver end [3]. Doppler spread caused by strong and moving reflectors could potentially have detrimental effects on the accuracy of the speed measurements. Although some such effects can be avoided, reflections from the sea surface will often occur in acoustic telemetry applications since the fish often reside near the surface. Surface reflections did not appear to contribute significantly to the measurement error in the present study, however error contribution due to reflections may be more substantial during rough or less calm sea conditions that what was the case during the experiment.

V. Conclusion and Future work

This study demonstrates the feasibility of using Doppler shift measurements on acoustic tag signals to determine the movement speeds of individual fish. An rms error of $5\,\mathrm{cm\,s^{-1}}$ with a relative error of less than 10% was achieved for a speed range relevant for farmed Atlantic salmon. This suggests that the technique can be used to study individual swimming behavior of fish in large-scale fish farms, observations that otherwise would be hard to obtain. Finally, the proposed method requires minimal modifications of existing tag designs as the speed measurements are extracted solely based on the acoustic carrier wave, allowing easy integration with existing telemetry systems. Future work will include testing of the system close to Atlantic salmon critical swimming speeds [8] and a test involving live fish in a large-scale fish farm

to investigate the properties and long-term robustness of the method as scientific tool for studying swimming behaviour in fish.

Acknowledgment

The authors would like to thank the NTNU-ITK mechanical workshop for their help on the mechanical setup of the experiment. This work was funded by the Norwegian Research Council through the Centre for research-based innovation in Exposed Aquaculture Technology (grant number 237790).

References

[1] Y. T. Chan and J. J. Towers. Passive localization from doppler-shifted frequency measurements. *IEEE Transactions on Signal Processing*, 40(10):2594–2598, Oct 1992.

[2] S. J. Cooke, E. B. Thorstad, and S. G. Hinch. Activity and energetics of free-swimming fish: insights from electromyogram telemetry. *Fish and Fisheries*, 5(1):21–52, 2004.

[3] B. G. Ferguson. Doppler effect for sound emitted by a moving airborne source and received by acoustic sensors located above and below the sea surface. *The Journal of the Acoustical Society of America*, 94(6):3244–3247, 1993.

[4] M. Føre, J. A. Alfredsen, and A. Gronningsater. "Development of two telemetry-based systems for monitoring the feeding behaviour of Atlantic salmon (Salmo salar L.) in aquaculture sea-cages". *Computers and Electronics in Agriculture*, 76(2):240 – 251, 2011.

[5] M. Føre, K. Frank, T. Dempster, J. Alfredsen, and E. Høy. Biomonitoring using tagged sentinel fish and acoustic telemetry in commercial salmon aquaculture: A feasibility study. *Aquacultural Engineering*, 78:163 – 172, 2017.

[6] M. Føre, K. Frank, T. Norton, E. Svendsen, J. A. Alfredsen, T. Dempster, H. Eguiraun, W. Watson, A. Stahl, L. M. Sunde, C. Schellewald, K. R. Skøien, M. O. Alver, and D. Berckmans. Precision fish farming: A new framework to improve production in aquaculture. *Biosystems Engineering*, 173:176 – 193, 2018. Advances in the Engineering of Sensor-based Monitoring and Management Systems for Precision Livestock Farming.

[7] W. Hassan, M. Føre, H. A. Urke, T. Kristensen, J. B. Ulvund, and J. A. Alfredsen. System for Real-time Positioning and Monitoring of Fish in Commercial Marine Farms Based on Acoustic Telemetry and Internet of Fish (IoF). *(Accepted, 29th International Society of Offshore and Polar Engineers (ISOPE) conference)*, June 2019.

[8] M. Hvas and F. Oppedal. Sustained swimming capacity of atlantic salmon. *Aquaculture Environment Interactions*, 9:361–369, 2017.

[9] K. E. Jónsdóttir, M. Hvas, J. A. Alfredsen, M. Føre, M. O. Alver, H. V. Bjelland, and F. Oppedal. Fish welfare based classification method of ocean current speeds at aquaculture sites. *Aquaculture Environment Interactions*, 11:249–261, 2019.

[10] P. Klebert, Øystein Patursson, P. C. Endresen, P. Rundtop, J. Birkevold, and H. W. Rasmussen. Three-dimensional deformation of a large circular flexible sea cage in high currents: Field experiment and modeling. *Ocean Engineering*, 104:511 – 520, 2015.

[11] J. Kolarevic, Ø. Aas-Hansen, Å. Espmark, G. Baeverfjord, B. F. Terjesen, and B. Damsgård. The use of acoustic acceleration transmitter tags for monitoring of Atlantic salmon swimming activity in recirculating aquaculture systems (RAS). *Aquacultural Engineering*, 72-73:30 – 39, 2016.

[12] F. Oppedal, T. Dempster, and L. H. Stien. Environmental drivers of atlantic salmon behaviour in sea-cages: A review. *Aquaculture*, 311(1):1 – 18, 2011.

[13] J. Pedersen. Hydroacoustic measurement of swimming speed of north sea saithe in the field. *Journal of Fish Biology*, 58(4):1073–1085, 2001.

[14] D. G. Pincock and S. V. Johnston. Acoustic telemetry overview. In N. S. Adams, J. W. Beeman, and J. H. Eiler, editors, *Telemetry Techniques: A User Guide for Fisheries Research*, pages 305–308. American Fisheries Society, Bethseda, Maryland, 2012.

[15] T. Pinkiewicz, G. Purser, and R. Williams. A computer vision system to analyse the swimming behaviour of farmed fish in commercial aquaculture facilities: A case study using cage-held atlantic salmon. *Aquacultural Engineering*, 45(1):20 – 27, 2011.

[16] M. Remen, F. Solstorm, S. Bui, K. Pascal, T. Vågseth, D. Solstorm, M. Hvas, and F. Oppedal. Critical swimming speed in groups of atlantic salmon salmo salarã?â? *Aquaculture Environment Interactions*, 8:659–664, 2016.

[17] C. Rillahan, M. Chambers, W. H. Howell, and W. H. Watson. A self-contained system for observing and quantifying the behavior of atlantic cod, gadus morhua, in an offshore aquaculture cage. *Aquaculture*, 293(1):49 – 56, 2009.

[18] P. Rundtop and K. Frank. Experimental evaluation of hydroacoustic instruments for rov navigation along aquaculture net pens. *Aquacultural Engineering*, 74:143 – 156, 2016.

A New Method for Measuring Free-Ranging Fish Swimming Speed in Commercial Marine Farms Using Doppler Principle

Waseem Hassan, Martin Føre, Magnus Oshaug Pedersen, and Jo Arve Alfredsen

***Abstract*—A novel Doppler shift based technique for measurement of free-swimming fish speed in marine farms using acoustic telemetry tags was developed and evaluated in this study. The proposed method can potentially augment current telemetry systems with a new biologically relevant measurement without significantly changing the size and energy constrained tag-side of the telemetry systems. For speeds in the range of 20cm s^{-1}-110cm s^{-1} an overall relative rms error of less than 10% in measured speed based on the proposed Doppler method was achieved in the tests conducted at a fully stocked commercial fish cage, with an rms error of 7.85cm s^{-1} (std. dev. 7.5cm s^{-1}). The study thus demonstrates the feasibility of measuring the swimming speeds of individual free-ranging fish using this method.**

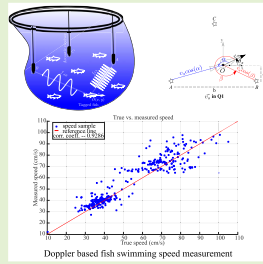

***Index Terms*—Acoustic signal processing, acoustic telemetry, Doppler measurement, fast Fourier transform, marine aquaculture, sensor phenomena & characterization.**

I. Introduction

FISH swimming is a coordinated function of various body systems and is a key behavioural parameter for understanding how fish cope with the environment and respond to external factors, and how this affects their energy consumption, stress and hunger levels. Swimming speed is particularly interesting in aquaculture, as studies have shown that sustained exposure to speeds that exceed the critical swimming speeds of the fish may lead to negative welfare impacts [12], [13], [20]. This is particularly relevant in light of the present industrial trend in moving fish farming to more remote and environmentally exposed locations [2] where fish may experience higher water velocities [14]. The ability to monitor swimming speeds could thus be an important component in future farm management methods and operations that take animal welfare conditions at exposed sites into account [15]. However, unlike laboratory studies or other small scale settings, where fish swimming speeds may be manually assessed, measuring individual fish swimming speeds in marine fish farms is a challenging task that requires technological tools [8]. In addition, the large variability in swimming abilities between individuals suggest that swimming speed should first be studied on an individual level before using aggregated measures of swimming speeds as a cage management parameter in aquaculture [13].

Individual fish swimming speeds have previously been assessed using split beam sonars [17] and camera solutions coupled with machine vision techniques [19]. Such methods can provide precise estimates on swimming speeds, for individual fish that are within their observation volume (i.e. the sonar beam or visual field) at any given time. However, evaluating the ultimate welfare impacts of being exposed to sustained strong currents requires data describing the individual histories of swimming speed over time. Since neither hydro-acoustic or camera-based methods can provide such data, this highlights the need for new tools for observing fish speed.

At present, bio-telemetry, where individual animals are equipped with miniature electronic devices, is the only viable option for obtaining individual data on free-ranging fish over time. Such devices, commonly known as electronic tags, often

Manuscript received February 18, 2020; revised April 21, 2020; accepted April 21, 2020. This work was supported by the Norwegian Research Council through the Centre for Research-based Innovation in Exposed Aquaculture Technology under Grant 237790. This article was presented at the 2019 IEEE Sensors Conference Proceedings [24]. The associate editor coordinating the review of this article and approving it for publication was Prof. Kazuaki Sawada. *(Corresponding author: Waseem Hassan.)*

Waseem Hassan, Martin Føre, and Jo Arve Alfredsen are with the Department of Engineering Cybernetics, Norwegian University of Science and Technology (ITK-NTNU), 7491 Trondheim, Norway (e-mail: waseem.hassan@ntnu.no; martin.fore@ntnu.no; jo.arve.alfredsen@ntnu.no).

Magnus Oshaug Pedersen is with SINTEF Ocean AS, 7052 Trondheim, Norway.

Digital Object Identifier 10.1109/JSEN.2020.2991294

contain sensors for sensing some property in or near the fish, and may be realised as either data loggers that store data internal storage mediums or as transmitter devices that transmit data using radio or acoustic signals [23]. Since radio signals are heavily attenuated by salt water, acoustic telemetry represents the only practical option for marine applications of transmitter devices.. The tags then contain an acoustic modem for wireless underwater data transmission of the tag ID and eventual data derived from the sensor measurements. In addition to tags, a typical acoustic telemetry system includes one or more matching acoustic receivers, which are specialised hydrophone devices that receive and decode the acoustic signals emitted by acoustic tags.

Acoustic telemetry has previously been used to observe individual fish behaviour both in wild and full-scale marine aquaculture applications [7], [21] and has been proven as an effective tool to quantify various fish behaviour parameters such as variations in swimming depth and activity [6], muscle activity via Electromyography (EMG) [4] and 3D position [10]. However, there exist no acoustic telemetry solutions able to directly measure instantaneous swimming speeds of individual fish. Indirect methods where speed is derived from consecutive position measurements tend to yield conservative estimates, and are strongly biased to the sampling rate and precision of the positioning system [4].

The first step in developing tools for measuring new parameters is to identify sensor principles able to measure the value of interest, in this case movement speed. Movement speed of objects in water is often measured using either impeller/turbine-based or acoustic methods. Although impellers have previously been applied to marine mammals [9], such solutions need to be mounted externally on the fish which could impair swimming ability and cause welfare issues due to skin abrasion.It is thus more likely that a viable solution can be found by applying acoustic principles.

Most acoustic methods exploit the Doppler effect, i.e. that the frequency of an acoustic signal received by a receiver will differ from the frequency of the signal emitted by the transmitter if there is relative movement between these. This Doppler Shifted Frequency (DSF) will be lower than the transmitted frequency when source and transmitter are moving away from each other, and conversely, higher if they are approaching. Examples of previous studies using this principle includes measuring aeroplane speed using the DSF of the acoustic tone generated by the propeller [5], and the calculation of fish tail beat rate using the DSF in a continuous acoustic signal [22]. Existing solutions using the Doppler effect for speed measurement include Acoustic Doppler Current Profilers (ADCPs) and Acoustic Doppler Velocimeters (ADVs) that could be used to measure current speeds in fish farms [16]. However, these devices are typically designed for stationary placement at the seabed or structural components, or to be mounted at vehicles, and are thus not suited to be mounted on or inside fish.

Although it might be possible to make an ADCP-like sensor small enough to fit inside an acoustic tag, this could prove difficult as the signal processing required to find the DSF might be beyond the capacity of the tag, both in terms of computation and power. Moreover, such a sensor would need to emit a dedicated acoustic signal to sense the DSF caused by the relative movement between the fish and the surrounding water, further increasing both power consumption and technical complexity. Using the DSF induced by tag movement upon the already existing carrier wave used to transfer data may therefore pose a more elegant and practical solution. This would move the effort of computing the Doppler shift to the receiver side, and not consume acoustic bandwidth, enabling the tag to simultaneously transmit other data types. Essentially, this means that movement speed would "piggyback" on other sensor data, enabling the collection of more diversified data-sets without increasing the number of fish tagged. A similar approach has previously been explored in laboratory experiments, where Doppler shift was employed to calculate fish tail beat frequency by using a continuous wave acoustic signal [22]. However, many present day solutions for acoustic telemetry use energy saving pulse interval modulation schemes rather than continuous signals to encode data from acoustic tags, with both encoding and processing being done in the time domain. A burst of pulses is then transmitted from the tag with the time interval between consecutive pulses being varied or kept constant to encode ID and sensor data [18]. Although this prohibits the possibility of obtaining continuous Doppler shift measurements, it is conceivable that modern signal processing methods can be used to obtain enough data from such pulses.

In this study, we developed and tested a fish swimming speed measurement technique based on the Doppler shift observed in the acoustic carrier wave transmitted by a telemetry tag. The technique is based on a commercially available acoustic telemetry system and extends the capabilities of this system by additional signal processing done in the acoustic receivers. The measurement technique was tested in a series of experiments ranging from speed extraction in a simple 1D laboratory setup, through a meso-scale experiment to evaluate 2D effects, to a full scale setup with multiple acoustic receivers in a commercial fish cage. The technique was evaluated for accuracy bounds and resolution of the measured speed using a signal frequency of 69 kHz, which is within the frequency range typically used in marine acoustic telemetry applications, and for speed ranges relevant for farmed Atlantic salmon. The sensitivity of the method towards inaccurate positioning was explored through a theoretical computer simulation study.

II. Materials and Methods

A. Theory and Method of Approach

Fig. 1 illustrates the proposed method. The DSF of a signal (f_d) represents a frequency shift in the received frequency (f_r) relative to the frequency transmitted by the source (f_s) and is found as:

$$f_d = f_s - f_r \tag{1}$$

A positive value of f_d means that the transmitter is moving towards the receiver, whereas a negative value implies that the transmitter is moving away from a receiver. The speed of transmitter v is related to f_d as:

$$v = \frac{c f_d}{f_s} \tag{2}$$

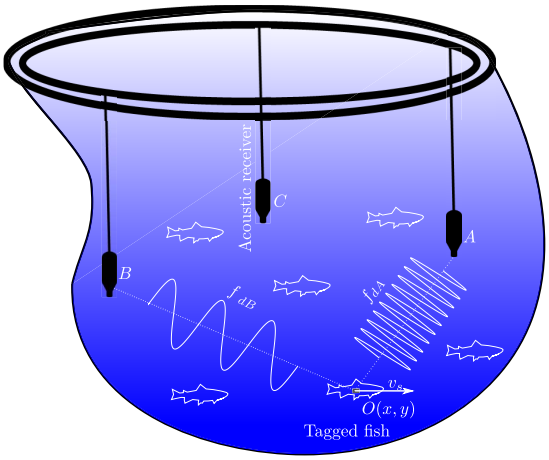

Fig. 1. Conceptual illustration of a tagged fish swimming inside a fish cage at a position O with swimming velocity $\vec{v_S}$ in the horizontal plane. The acoustic wave is compressed or stretched when received by receiver A, B and C depending on whether the fish movement is towards or away from the receivers.

where c is the speed of the acoustic signal in the propagation medium. The Doppler effect only applies to the velocity component along the axis between the receiver and transmitter, hence the angle θ between the velocity vector ($\vec{v}$) and this axis needs to be considered. This component is found as the cosine speed component of the transmitter's speed:

$$v = \frac{cf_d}{f_s cos\theta} \tag{3}$$

Reference [3] explained the use of the Doppler effect to determine the position and speed of a moving source in 3D using multiple sensor nodes, and highlighted the challenges using the method in that no closed-form solution exists and that non-linear equations are involved in the calculations. However, the authors also pointed out that by knowing the transmitted signal's frequency (f_s) and the position of a transmitter it is possible to achieve an exact solution. Most commercially available telemetry systems for marine applications use fixed known frequencies (f_s) ranging between 10 kHz and 100 kHz. Moreover, Time Difference of Arrival (TDoA) based positioning systems have been successfully used to position acoustic transmitter tags in marine aquaculture [10]. In TDoA based acoustic telemetry positioning, position in 3D (x, y, z) coordinates can be obtained directly using the difference in arrival times of an acoustic signal from a transmitter tag on four different acoustic receivers placed at known positions. A setup using three hydrophones can also be sufficient when using depth-sensing tags as TDoA then only needs to to locate the tag in the horizontal plane (xy-coordinates). When using TDoA, all receivers used in the calculations need to be synchronised to a common clock source, usually by using Global Navigation Satellite Systems (GNSS) [18].

This means that exact speed solutions are possible to achieve by extending existing acoustic telemetry systems with additional signal processing methods and frequency analysis at the receiver end. The likelihood of the proposed method functioning under the farm relevant conditions increases by employing the existing acoustic systems that have been extensively tested in the marine environment since the proposed method does not introduce significant modifications.

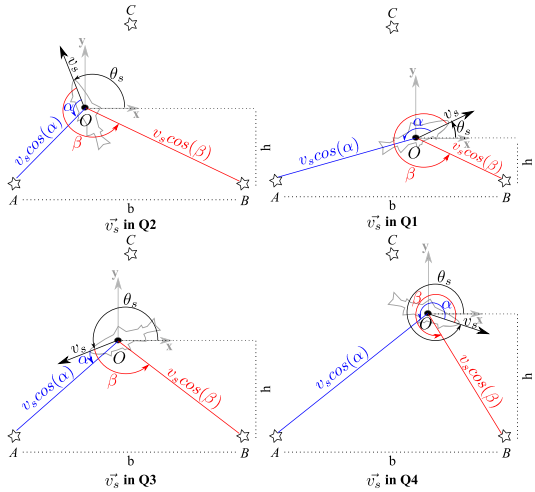

Fig. 2. Orientation of transmitter tag located at O moving with a velocity $\vec{v_S}$ in the four quadrants Q1-Q4 (horizontal plane). The Doppler shift measured at receiver locations A and B will be proportional to the components of the transmitter speed v_S along the lines AO and BO, respectively, defined by the angles α and β. A third receiver at location C enables TDoA based transmitter localisation.

B. Speed Computation Algorithm

The algorithm for computing movement speed was based on combining (3) with a geometric setup that would be reasonable to apply in a fish cage. A 2D (xy-plane) example of such a setup with three acoustic receivers A, B and C is shown in Fig. 2. The movement velocity vector $\vec{v_s}$ of an acoustic tag placed at O with coordinates (x_O, y_O) would then make an angle θ_s with respect to the x-axis.

For all values of θ_s, the DSFs observed at receivers A (f_{dA}) and B (f_{dB}) are given by:

$$f_{dA} = \frac{f_s v_s cos\alpha}{c} \tag{4}$$

$$f_{dB} = \frac{f_s v_s cos\beta}{c} \tag{5}$$

where α and β are the angles between $\vec{v_s}$ and the axes between O and receivers A and B respectively, and $v_s cos\alpha$ and $v_s cos\beta$ are the velocity components along these lines. Dividing (4) by (5) yields:

$$\frac{cos\alpha}{cos\beta} = \frac{f_{dA}}{f_{dB}} \tag{6}$$

Estimating f_{dA} and f_{dB} through Fast Fourier Transform (FFT) or similar frequency analysis enables finding the two unknown angles (i.e. α and β) using TDoA positioning methods and system geometry.

Assuming that the coordinates (x_O, y_O) of the tag and receivers A and B are known, the angle $\angle AOB$ can be calculated from $\triangle AOB$ since all three sides of the triangle are then known. $\angle AOB$ relates to the two unknown angles

as:

$$\angle AOB = \beta - \alpha \tag{7}$$

Deriving β from (7) and inserting it into (6) then yields:

$$\frac{cos\alpha}{cos(\angle AOB + \alpha)} = \frac{f_{dA}}{f_{dB}} \tag{8}$$

Inverting and solving (8) for α yields:

$$\frac{cos(\angle AOB + \alpha)}{cos\alpha} = \frac{f_{dB}}{f_{dA}} \tag{9}$$

$$\frac{cos(\angle AOB)cos\alpha - sin(\angle AOB)sin\alpha}{cos\alpha} = \frac{f_{dB}}{f_{dA}} \tag{10}$$

$$cos(\angle AOB) - \frac{sin(\angle AOB)sin\alpha}{cos\alpha} = \frac{f_{dB}}{f_{dA}} \tag{11}$$

$$cos(\angle AOB) - sin(\angle AOB)tan\alpha = \frac{f_{dB}}{f_{dA}} \tag{12}$$

$$tan\alpha = \frac{cos(\angle AOB) - \frac{f_{dB}}{f_{dA}}}{sin(\angle AOB)} \tag{13}$$

$$\alpha = atan(\frac{cos(\angle AOB) - \frac{f_{dB}}{f_{dA}}}{sin(\angle AOB)}) \tag{14}$$

Equations (6) and (7) can be written similarly in terms of angle β:

$$\frac{cos(\beta - \angle AOB)}{cos\beta} = \frac{f_{dA}}{f_{dB}} \tag{15}$$

or

$$\beta = atan(\frac{\frac{f_{dA}}{f_{dB}} - cos(\angle AOB)}{sin(\angle AOB)}) \tag{16}$$

Once angles α and β are found using either (14) and (7) or (16) and (7), the unknown speed v_s of the acoustic transmitter can be calculated using (3) in terms of α:

$$v_s = \frac{f_{dA}c}{f_s cos\alpha} \tag{17}$$

or in terms of β:

$$v_s = \frac{f_{dB}c}{f_s cos\beta} \tag{18}$$

To relate v_s to the $xy-$plane defined in Fig. 2, a right angle triangle $\triangle BOX$ can be defined using the $y-$component of O, y_O, as the height h of the triangle. The base of this triangle can then be calculated by subtracting x_O from the known distance b between A and B. The angle $\angle BOX$ can then be calculated and used to derive an expression for the angle between $\vec{v_s}$ and the $x-$axis, θ_s:

$$\theta_s = 360^\circ - \beta - \angle BOX \tag{19}$$

Equations to calculate angles θ_s, α and β when the velocity vector lies in one of the four different quadrants are shown in Fig. 2. When defining all angles in anticlockwise direction with respect to the x-axis, this yields the same set of equations for all quadrants except the 4th quadrant (Q4) where θ_s is calculated as a negative value. The present quadrant can easily be determined using the sign of the DSF (f_d) value on both receivers. Equations (4)-(19) can be applied to any pair of receivers (i.e. A and B, B and C or A and C).

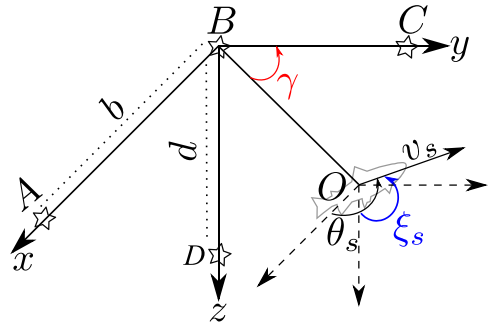

Fig. 3. Conceptual description of determining 3D fish velocities using three acoustic receivers. Receivers A and B are used to derive the direction of v_S in the plane spanned between them and O (θ_S), while receivers B and D are used to derive the angle in the plane BDO (ξ_S). The fourth receiver C is present to enable TDoA based localisation of the tag's position O. Angle γ accounts for scaling of the velocity vector $\vec{v_S}$ with tag's depth variation.

For simplicity, the above mentioned equations are derived in a 2D (x, y) plane assuming a fixed depth. However, since (4)-(19) can be applied to any geometric plane defined between a pair of receivers and O, it is possible to find 3D-velocities by using three hydrophones. The 3D velocity vector would then be projected onto two 2D planes e.g. $xy-$ and $yz-$planes, which could be solved independently. The equations would then be used to find the angles between the velocity vector and the $x-$ (θ_s) and $z-$axes (ξ_s). To accommodate this, (17) and (18) would be expanded to account for depth variation as:

$$v_s = \frac{f_{dA}c}{f_s cos\alpha sin\xi_s cos\gamma} \tag{20}$$

$$v_s = \frac{f_{dB}c}{f_s cos\beta sin\xi_s cos\gamma} \tag{21}$$

where γ is the angle between the receivers A, B and C and tag's depth planes. For 3D speed measurement, using only two acoustic receivers in $xy-$plane and accounting for the tag's depth variation, i.e. the angle γ, will result in measurement of $v_s sin\xi_s$ which is the cosine $z-$component of the original speed. An additional receiver at z-axis along with the receiver at y-axis then can be used in the $yz-$plane to measure ξ_s, hence speed in 3D.

C. System Requirements

Calculating speeds using (4)-(21) requires the acoustic receivers to perform FFT frequency analysis to determine the DFS. In addition, the source frequency (f_s) used by the acoustic tag and its position must be known. If TDoA algorithms are used to acquire position, at least three (if the tags measure depth) or four synchronised acoustic receivers are required. Three acoustic receivers are required to execute FFT frequency analysis for 3D speed measurement, whereas two acoustic receivers are required for speed measurement in 2D.

D. Experimental Testing, Verification and Validation

A series of experiments were executed to verify and validate the method and to assess the error bounds on the resulting speed values. Experiments were conducted in three different

environments: controlled lab, meso-scale in nearshore waters and a full scale fish farm. A custom made acoustic tag with a centre frequency of 68.968 kHz was used as the transmitter in the setup, while up to three broad spectrum hydrophones (Ocean Sonics Ltd., Nova Scotia, Canada) were used to collect acoustic data. The acoustic signal emitted by the tag was generated by a microcontroller based embedded system and designed to resemble the signal used in typical acoustic telemetry systems (i. e. a burst of pulses similar to those used in pulse interval encoding approaches). Eight pulses were used in a single burst and each pulse was set up with a longer duration (128 ms) than that typically used by commercial Pulse Position Modulation (PPM) protocols (10 ms) to improve the velocity resolution of the system [11]. The pulse bursts were spaced by a longer time interval (seconds) than the pulses in each burst (150 ms) to distinguish the separate bursts.

The basic principle in all experiments was to move the acoustic tag in a predefined motion pattern while monitoring the positions and speeds accurately using auxiliary positioning and speed measurement systems. Measured positions were used as input to the DSF speed algorithms, while the measured speeds were used as ground truth for validation of the speed computations. The target speeds used in the experiment varied from $5\,\mathrm{cm\,s^{-1}}$ to $20\,\mathrm{cm\,s^{-1}}$ for lab experiments and from $25\,\mathrm{cm\,s^{-1}}$ to $110\,\mathrm{cm\,s^{-1}}$ for sea based experiments, covering a range of swimming speeds typical for Atlantic salmon [13]. The embedded system transmitted acoustic bursts periodically, and logged the start times of each burst and the speed and position measured by the auxiliary system at these times. This resulted in a data-set on position and speed that was fully synchronised with the emitted pulses, enabling validation of the results from the DSF computations.

The goal of the initial 1D lab trials was to verify that the DSF speed extraction technique was feasible to apply for systems of this scale, and to evaluate the accuracy of the method. The experiment was conducted in a tank filled with water ($4.3\,\mathrm{m} \times 1.5\,\mathrm{m} \times 2.0\,\mathrm{m}$). A cart-on-rail mechanical setup driven by a geared DC motor (maxon RE 35) was used to move an acoustic tag mounted on an adjustable rod protruding down into the water. The embedded system controlled the speed of the DC motor and logged the reference speed measured by an encoder. The system was programmed to move back and forth in line with a hydrophone, meaning that the tag was either moving directly towards or away from the receiver (Fig. 4a). Position logging was therefore not required in this experiment.

The next step towards enabling 2D speed calculations was to evaluate if the method could estimate movements that are not in line with a hydrophone. This was done in an experiment in a fjord very close to shore. The acoustic tag was then attached to a rod fastened to a remotely controlled catamaran (Fig. 4b) placing the tag at a depth of 1 m. Burst start time, speed and position of the vehicle were measured using an on-board Real Time Kinematics (RTK) GPS, while the catamaran was driven in a straight line. Two hydrophones were placed such that one was in line with the tag/vehicle movement (i.e. with the tag moving directly from or toward it as in the 1D trials), while the other hydrophone was placed such that the angle between the tag movement direction and the line between the tag and the receiver varied between $-45°$ and $60°$.

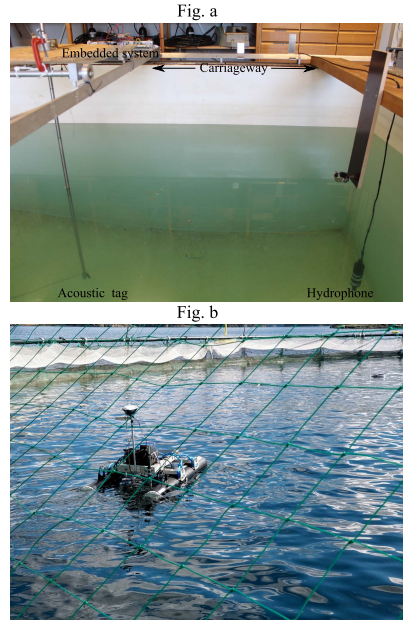

Fig. 4. (**Fig. a**) Electromechanical setup used for in lab experiments. Acoustic tag, hydrophone and direction of motion are highlighted with text. (**Fig. b**) Catamaran used to move the acoustic tag in the sea based experiments.

The final experiment aimed to test the ability of the method to measure 2D movement speeds in a relevant acoustic environment, and was thus conducted in a commercial sea-cage stocked with fish (approximately 200,000 animals). The catamaran was then driven in a circular path, meaning that the angles between the tag movement direction and the line from the hydrophones to the tag position varied continuously. This also served to demonstrate and test the algorithm for a more realistic range of speeds and angles (α and β in Fig. 2).

E. Collection and Processing of Acoustic Data

Through all experiments, the hydrophones stored acoustic data in waveform audio format (.wav) using a sampling frequency of $256\,\mathrm{kS\,s^{-1}}$ and a recording time of 10 min for each data-set. The data-set were analysed using Matlab (The MathWorks, Inc., Natick, Massachusetts, USA), finding peak frequency and DSF values for individual pulses by employing FFT. Average and modal values for eight DSF peaks (i.e. a single burst) were used for speed calculations (hereafter referred to as the averaging method and modal method, respectively). Since the trial in the sea cage was closest to a real world application, the data from this experiment was used in subsequent analyses to assess the error levels of the method.

F. Position Sensitivity Analysis

The sensitivity of the DSF speed calculation algorithm to errors in tag position was tested through theoretical simulations where a known error in tag position was introduced into

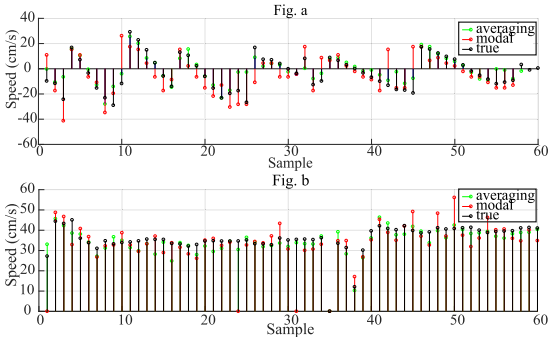

Fig. 5. (**Fig. a**) Fjord based experiments: Comparison of reference speed (true) with Doppler shift for both averaging and modal based speed measurements at hydrophone placed at angular orientation. (**Fig. b**) In fish cage experiments: Comparison of reference speed (true) with Doppler based speed measurements.

the computation of the cosine value of angle $\angle AOB$. Typical Circular Error Probability (CEP) values for the TDoA based positioning methods, (i.e. an error of metres [18]) were used in the simulations.

III. Results

A. Lab Experiments

The rms error between computed and real speeds achieved in the lab experiments was found to be around 5 cm s^{-1} (std. dev. < 2 cm s^{-1}) when using the averaging method and 6 cm s^{-1} (std. dev. <4 cm s^{-1}) when using the modal method, respectively.

B. Fjord Based Experiments

The rms error when using the averaging method was found to be about 7 cm s^{-1} (std. dev. <7 cm s^{-1}) for speeds <50 cm s^{-1} and 23 cm s^{-1} (std. dev. <23 cm s^{-1}) for speeds >50 cm s^{-1}. The rms errors were slightly higher when using the modal method, and were 12 cm s^{-1} and 31 cm s^{-1} for speeds <50 cm s^{-1} and >50 cm s^{-1} respectively (see Fig. 5a for excerpts of data from the fjord experiments).

C. Fish Cage Experiments

Since the modal method yielded slightly higher errors, speeds found using the averaging method were used in the further analyses (Fig. 5b). The correlation coefficient between measured speed and true speed was 0.9286 for complete speed range (i.e. 20 cm s^{-1}-110 cm s^{-1}) with a sample count of N = 357 (Fig. 6). The rms error for the averaging method was 7.85 cm s^{-1} (std. dev. <7.5 cm s^{-1}, mean <−2.35 cm s^{-1}) for the entire speed range (Fig. 7).

D. Position Sensitivity

When assuming a CEP of 1.5 m, simulations implied that the absolute error in the speed computation was highest near the hydrophone position (Fig. 8).

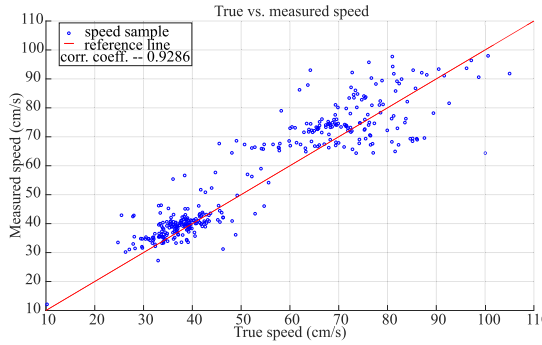

Fig. 6. Scatter plot of measured (averaging method) speed and true speed for fish cage experiments. A correlation coefficient of 0.9286 was achieved for measured and true speed with a sample count of N = 357. Reference line (1:1) is shown in red colour.

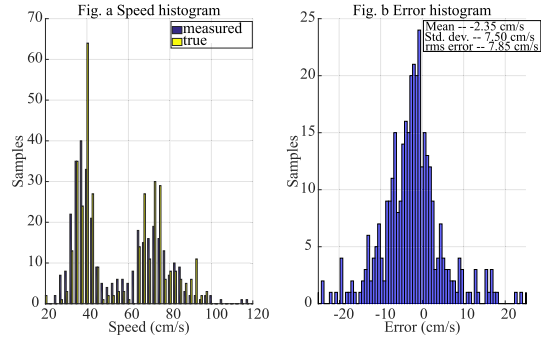

Fig. 7. (**Fig. a**) Histograms for true speed and Doppler based measured (averaging method) speed. (**Fig. b**) Histogram for error in measured (averaging method) speed. Sample count N = 357 for both plots.

IV. Discussion

The results from this study suggest that the Doppler based speed measurement method presented here is feasible for tracking individual fish speeds in commercial fish farms. The low errors compared with ground truth speed measurements obtained with independent methods in all three experiments thus served to validate the method through incremental stages. Moreover, the acceptable results achieved at full scale also showed that this method is applicable under realistic environmental conditions (i.e. the prevailing soundscape at a fish farm), and with arbitrary directions of movement.

For the fjord and fish cage based trials, the data were grouped into low (25 cm s^{-1}-50 cm s^{-1}, sample count N = 190) and high (50 cm s^{-1}-110 cm s^{-1}, sample count N = 167) speed data-sets. The two sub speed data-sets were analysed separately to capture possible differences in the assessment of the method's performance between low (sustained swimming speed of Atlantic salmon for longer duration) and high (critical swimming speed of Atlantic salmon for shorter duration) movement speeds [13]. The rms error using the averaging method was 5 cm s^{-1} (mean −1.9 cm s^{-1}, std. dev. <4.7 cm s^{-1}) for low and 10.1 cm s^{-1} (mean −2.9 cm s^{-1}, std. dev. <9.7 cm s^{-1}) for high speed data-sets respectively, implying that the error in measured speed for Atlantic salmon's sustained speed range was relatively lower than the overall

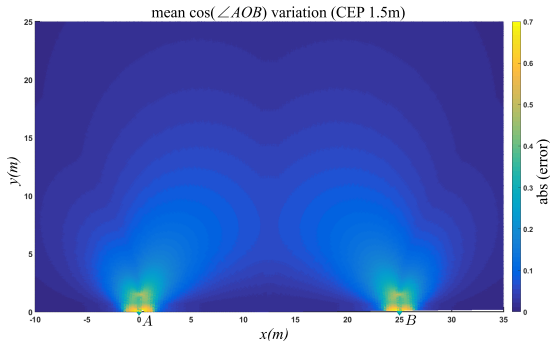

Fig. 8. Error in cosine value of $\angle AOB$ due to simulated variations in tag position. The error is relatively high close to the acoustic receivers (*A* and *B*), whereas it approaches to zero as the distance from the tag to the receivers increases.

speed range. Although the absolute error values were generally larger for higher than for lower movement speeds, the relative error vs speed ratio was almost constant at approximately 10% across all speeds. This implies that the method is consistent in deriving movement speeds and a robust approach for assessing underwater movement speeds. For low speed ranges, the averaging and modal methods had comparable error levels, while the modal method had larger errors for higher speed ranges. The averaging method therefore appeared to be most suitable for use in applications in sea-cages as it was acting as a filter, filtering out unwanted peaks at higher speeds. Both methods led to larger errors in the lab experiments than in the field trials. This can be attributed to very strong reflections and hence poor acoustic conditions, which are typical in tanks of relatively small volume [1].

The error was lower in the fish cage experiments than in the fjord based experiments for all speeds. This is probably because acoustic reflections had a larger impact during the fjord experiments than in the sea-cages. When applying the Doppler shift based technique, it is ideal to use only the first pulse arriving after signal emission for speed measurements, as this reduces the chance that multipathing will affect the results. In a real-world scenario such as a fjord or sea-cage environment, additional pathways of signal arrival may arise due to acoustic reflections from the surface, the seabed and other structures in the water column. This can potentially cause errors in the speed calculations [5]. Surface reflections can generally not be avoided when applying acoustic telemetry in aquaculture, as fish production is predominantly conducted in the upper parts of the water column, and will thus be a constant source of error. However, it is possible to avoid or reduce the impacts of bottom reflections and reflections from other structures by simply increasing the depth and the distance to those other structures, respectively. Increased distances will result in reflections that are both heavily attenuated and arrive more delayed at the receiver. While the fjord based experiments were conducted very close to shore at a depth of around 8 m, the fish cage experiments were conducted in a cage located several hundred meters from shore with a water depth of 75 m to 100 m under the farm. These conditions are typical for marine fish farming sites, and were probably instrumental in reducing the effects of reflections from the bottom and the coastline.

Apart from the surface, bottom and nearby structure reflections, the acoustic signal would also reflect from the fish/biomass present in the sea-cage. The fish cage experiments were performed inside a sea-cage stocked with approximately 200,000 animals. The 10% relative error in measured speed for the fish cage experiments implies that the Doppler principle works reliably under the realistic scenarios it is targeted for. The experiments in this study were performed by using only one acoustic tag at a given time. In a practical fish behaviour monitoring study, multiple fish would be tagged in a single fish cage. In such a multi-tag situation, the acoustic receivers would differentiate the overlapping signals by first processing the received signals in time domain to decode ID. Afterwards, the receivers would perform FFT to measure speed of the tagged fish corresponding to the decoded tag ID using the Doppler principle.

The duration of the individual pulses comprising a signal burst is an important parameter in determining the resolution of the DSF method ([11] Eq. 24). By inserting the typical pulse duration of commercial off the shelf acoustic tags (10 ms) into this equation, a maximum speed resolution of 100 cm s^{-1} is predicted. This means that it is impossible to monitor common swimming speeds of farmed fish using a 10 ms pulse length, as these are predominantly lower than 100 cm s^{-1}. By using a pulse duration of 128 ms (as used in these experiments) in the same equation, a resolution of 8 cm s^{-1} is obtained. Based on these theoretical observations and the outcomes from the present study, it is thus reasonable to conclude that the pulse duration should be at least 100 ms when aspiring to use DSF to measure the swimming speeds of farmed fish.

The simulated speed errors when positioning was subjected to a known error were relatively high when the simulated tag was placed closer to acoustic receivers but reached to zero for tag positions further away from the receivers (Fig. 8). This suggests that it might be reasonable to use the receivers furthest away from the current tag position to compute speeds, implying that it might be useful to have more receivers than strictly needed in a particular setup. For instance, this can be realised for the 2D-speed case, by using three receivers for both TDoA positioning and frequency, as the acoustic receiver pair furthest away from the tag could then be used for speed computations.

V. Conclusion

The proposed Doppler shift based speed measurement technique was proven to be a promising method for measuring fish swimming speed in a marine aquaculture environment. An rms error of 5 cm s^{-1} for Atlantic salmon's sustained swimming speed i.e. <50 cm s^{-1} makes the proposed technique a highly relevant tool for measuring fish speeds, while rms errors less than 10 cm s^{-1} for speeds up to 100 cm s^{-1} proved that the technique can be used to reliably monitor fish close to their critical swimming speed. Experiments conducted inside a fully stocked fish cage also proved that the technique can be used for

speed measurements on Atlantic salmon during commercial aquaculture production.

Acknowledgment

The authors would like to thank the NTNU-ITK mechanical workshop for their help on the mechanical setup of the experiments.

References

[1] T. Akamatsu, T. Okumura, N. Novarini, and H. Y. Yan, "Empirical refinements applicable to the recording of fish sounds in small tanks," *J. Acoust. Soc. Amer.*, vol. 112, no. 6, pp. 3073–3082, Dec. 2002.

[2] H. V. Bjelland *et al.*, "Exposed aquaculture in norway," in *Proc. Oceans*, Oct. 2015, pp. 1–10.

[3] Y. T. Chan and J. J. Towers, "Passive localization from Doppler-shifted frequency measurements," *IEEE Trans. Signal Process.*, vol. 40, no. 10, pp. 2594–2598, Oct. 1992.

[4] S. J. Cooke, E. B. Thorstad, and S. G. Hinch, "Activity and energetics of free-swimming fish: Insights from electromyogram telemetry," *Fish Fisheries*, vol. 5, no. 1, pp. 21–52, Mar. 2004.

[5] B. G. Ferguson, "Doppler effect for sound emitted by a moving airborne source and received by acoustic sensors located above and below the sea surface," *J. Acoust. Soc. Amer.*, vol. 94, no. 6, pp. 3244–3247, Dec. 1993.

[6] M. Føre, J. A. Alfredsen, and A. Gronningsater, "Development of two telemetry-based systems for monitoring the feeding behaviour of atlantic salmon (Salmo Salar L.) in aquaculture sea-cages," *Comput. Electron. Agricult.*, vol. 76, no. 2, pp. 240–251, May 2011.

[7] M. Føre, K. Frank, T. Dempster, J. A. Alfredsen, and E. Háy, "Biomonitoring using tagged sentinel fish and acoustic telemetry in commercial salmon aquaculture: A feasibility study," *Aquacultural Eng.*, vol. 78, pp. 163–172, Aug. 2017.

[8] M. Føre *et al.*, "Precision fish farming: A new framework to improve production in aquaculture," *Biosyst. Eng.*, vol. 173, pp. 176–193, Sep. 2018.

[9] J. Gabaldon *et al.*, "Integration, Calibration, and experimental verification of a speed sensor for swimming animals," *IEEE Sensors J.*, vol. 19, no. 10, pp. 3616–3625, May 2019.

[10] W. Hassan, M. Føre, H. A. Urke, T. Kristensen, J. B. Ulvund, and J. A. Alfredsen, "System for real-time positioning and monitoring of fish in commercial marine farms based on acoustic telemetry and Internet of fish (IoF)," in *Proc. 29th Int. Ocean Polar Eng. Conf.*, Jul. 2019, pp. 1496–1503.

[11] J. M. Hovem, "Underwater acoustics: Propagation, devices and systems," *J. Electroceram.*, vol. 19, no. 4, pp. 339–347, Dec. 2007.

[12] M. Hvas *et al.*, "Assessing swimming capacity and schooling behaviour in farmed atlantic salmon salmo salar with experimental push-cages," *Aquaculture*, vol. 473, pp. 423–429, Apr. 2017.

[13] M. Hvas and F. Oppedal, "Sustained swimming capacity of atlantic salmon," *Aquaculture Environ. Interact.*, vol. 9, pp. 361–369, Sep. 2017.

[14] K. Jónsdóttir *et al.*, "Fish welfare based classification method of ocean current speeds at aquaculture sites," *Aquaculture Environ. Interact.*, vol. 11, pp. 249–261, Jun. 2019.

[15] D. Johansson *et al.*, "The interaction between water currents and salmon swimming behaviour in sea cages," *PLoS ONE*, vol. 9, no. 5, 2014, Art. no. e97635.

[16] P. Klebert, O. Patursson, P. C. Endresen, P. Rundtop, J. Birkevold, and H. W. Rasmussen, "Three-dimensional deformation of a large circular flexible sea cage in high currents: Field experiment and modeling," *Ocean Eng.*, vol. 104, pp. 511–520, Oct. 2015.

[17] J. Pedersen, "Hydroacoustic measurement of swimming speed of north sea saithe in the field," *J. Fish Biol.*, vol. 58, no. 4, pp. 1073–1085, Apr. 2001.

[18] D. G. Pincock and S. V. Johnston, "Acoustic telemetry overview," in *Telemetry Techniques: A User Guide for Fisheries Research*, N. S. Adams, J. W. Beeman, J. H. Eiler, Eds. Bethseda, MD, USA: American Fisheries Society, 2012, pp. 305–308.

[19] T. H. Pinkiewicz, G. J. Purser, and R. N. Williams, "A computer vision system to analyse the swimming behaviour of farmed fish in commercial aquaculture facilities: A case study using cage-held atlantic salmon," *Aquacultural Eng.*, vol. 45, no. 1, pp. 20–27, Jul. 2011.

[20] M. Remen *et al.*, "Critical swimming speed in groups of atlantic salmon salmo salar," *Aquaculture Environ. Interact.*, vol. 8, pp. 659–664, Dec. 2016.

[21] C. Rillahan, M. Chambers, W. H. Howell, and W. H. Watson, "A self-contained system for observing and quantifying the behavior of Atlantic cod, gadus morhua, in an offshore aquaculture cage," *Aquaculture*, vol. 293, nos. 1–2, pp. 49–56, Aug. 2009.

[22] A. B. Stasko and R. M. Horrall, "Method of counting tailbeats of free-swimming fish by ultrasonic telemetry techniques," *J. Fisheries Res. Board Canada*, vol. 33, no. 11, pp. 2596–2598, Nov. 1976.

[23] E. B. Thorstad, A. H. Rikardsen, A. Alp, and F. økland, "The use of electronic tags in fish research—An overview of fish telemetry methods," *Turkish J. Fisheries Aquatic Sci.*, vol. 13, no. 5, pp. 881–896, 2013.

[24] W. Hassan, M. Fore, M. O. Pedersen, and J. Arve Alfredsen, "A novel Doppler based speed measurement technique for individual free-ranging fish," in *Proc. IEEE SENSORS*, Oct. 2019, pp. 1–4.

Waseem Hassan received the B.E. degree in electronics from PNEC-NUST, Pakistan, in 2012, and the M.Sc. degree in embedded systems jointly from NTNU Norway and TU Kaiserslautern, Germany (Erasmus Mundus EMECS Program, 2016). He is currently pursuing the Ph.D. degree with the Department of Engineering Cybernetics, Norwegian University of Science and Technology (NTNU), Norway. His main research area is real-time acoustic fish telemetry for marine aquaculture applications. He has been working with the development of new sensing principles for measuring fish behavior and embedded systems for providing real-time support to the existing acoustic telemetry systems.

Martin Føre received the M.Sc. degree from NTNU in 2006 and the Ph.D. degree in individual-based modeling and monitoring of fish in sea-cages in 2011. He is currently an Associate Professor with the Department of Engineering Cybernetics, Norwegian University of Science and Technology (NTNU). His main research area is the application of cybernetic methods (e.g., instrumentation, control theory, modeling, simulation, and estimation) to challenges in the aquaculture industry. Some of the highlights of his research career thus far are his work on fish modeling and instrumentation, and his role in defining the Precision Fish Farming (PFF) concept.

Magnus Oshaug Pedersen received the bachelor's degree in instrumentation with HIST in 2014. He is currently working as a Senior Engineer with SINTEF Ocean AS. During his career at SINTEF Ocean AS, he has played an important role in development of instrumentation solutions for the full-scale ACE test facility in Norway. He has prepared and performed instrumentation assignments at several locations, both for open and closed fish farming systems. He has in this way contributed to the development of methodology for data collection, which has been important to the researchers in their work. In this particular article, he developed the catamaran which was used during the experiments.

Jo Arve Alfredsen received the M.Sc. and Ph.D. degrees in engineering cybernetics in 1992 and 2000, respectively. He worked several years in the Maritime industry developing ship control systems. He is currently an Associate Professor in engineering cybernetics with the Department of Engineering Cybernetics, Norwegian University of Science and Technology (NTNU), with specialization in embedded systems design and applications to ocean biomonitoring and aquaculture control systems. His research interests are currently focused towards sensors, instrumentation and remote monitoring technology for observing processes and living resources in the ocean, and automation and control systems for aquaculture production.

New concept for swimming speed measurement of free-ranging fish using acoustic telemetry and Doppler analysis

Waseem Hassan*, Martin Føre*, Henning Andre Urke†, John Birger Ulvund‡, Eskil Bendiksen§ and Jo Arve Alfredsen*
*Department of Engineering Cybernetics-NTNU Trondheim, Norway
Email: waseem.hassan, martin.fore, jo.arve.alfredsen @ntnu.no
†INAQ AS Trondheim, Norway
Email: henning.urke@inaq.no
‡Nord University Bodø, Norway
Email: john.b.ulvund@nord.no
§Bjørøya AS Flatanger, Norway
Email: eskil@bjoroya.no

References

F. Adelantado, X. Vilajosana, P. Tuset-Peiro, B. Martinez, J. Melia-Segui, and T. Watteyne. Understanding the Limits of LoRaWAN. *IEEE Communications Magazine*, 55(9):34–40, 2017. ISSN 0163-6804. doi: 10.1109/MCOM.2017.1600613.

F. Arrhenius, B. J. Benneheij, L. G. Rudstam, and D. Boisclair. Can stationary bottom split-beam hydroacoustics be used to measure fish swimming speed in situ? *Fisheries Research*, 45(1):31 – 41, 2000. ISSN 0165-7836. doi: https://doi.org/10.1016/S0165-7836(99)00102-2. URL http://www.sciencedirect.com/science/article/pii/S0165783699001022.

F. Asche. Farming the sea. *Marine Resource Economics*, 23(4):527–547, 2008. ISSN 07381360, 23345985. URL http://www.jstor.org/stable/42629678.

F. Asche and T. Bjørndal. *The Economics of Salmon Aquaculture*. John Wiley & Sons, Ltd, 2011. ISBN 9781119993384. URL https://onlinelibrary.wiley.com/doi/abs/10.1002/9781119993384.

F. Asche, K. H. Roll, H. N. Sandvold, A. Sørvig, and D. Zhang. Salmon aquaculture: Larger companies and increased production. *Aquaculture Economics & Management*, 17(3):322–339, 2013. doi: 10.1080/13657305.2013.812156. URL https://doi.org/10.1080/13657305.2013.812156.

A. Augustin, J. Yi, T. Clausen, and W. M. Townsley. A Study of LoRa: Long Range & Low Power Networks for the Internet of Things. *Sensors*, 16(9), 2016. ISSN 1424-8220.

E. Baras and J.-P. Lagardère. Fish telemetry in aquaculture: review and perspectives. *Aquaculture International*, 3:77 – 102, 1995. ISSN 1573-143. doi: https://doi.org/10.1007/BF00117876.

Z. Biesinger, B. M. Bolker, D. Marcinek, T. M. Grothues, J. A. Dobarro, and W. J. Lindberg. Testing an autonomous acoustic telemetry positioning system for fine-scale space use in marine animals. *Journal of Experimental Marine Biology and Ecology*, 448:46 – 56, 2013. ISSN 0022-0981.

H. V. Bjelland, M. Føre, P. Lader, D. Kristiansen, I. M. Holmen, A. Fredheim, E. I. Grøtli, D. E. Fathi, F. Oppedal, I. B. Utne, and I. Schjølberg. Exposed Aquaculture in Norway. In *OCEANS 2015 - MTS/IEEE Washington*, pages 1–10, 2015. doi: 10.23919/OCEANS.2015.7404486.

J. W. Brownscombe, E. J. I. Lédée, G. D. Raby, D. P. Struthers, L. F. G. Gutowsky, V. M. Nguyen, N. Young, M. J. W. Stokesbury, C. M. Holbrook, T. O. Brenden, C. S. Vandergoot, K. J. Murchie, K. Whoriskey, J. M. Flemming, S. T. Kessel, C. C. Krueger, and S. J. Cooke. Conducting and interpreting fish telemetry studies: considerations for researchers and resource managers. *Reviews in Fish Biology and Fisheries*, 29:369–400, 2019. doi: https://doi.org/10.1007/s11160-019-09560-4.

G. Buttazzo, G. Lipari, L. Abeni, and M. Caccamo. *Soft Real-Time Systems: Predictability vs. Efficiency*. Springer US, Boston, MA, 2005. ISBN 978-0-387-28147-6. doi: 10.1007/0-387-28147-9_1. URL https://doi.org/10.1007/0-387-28147-9_1.

Y. T. Chan and J. J. Towers. Passive localization from Doppler-shifted frequency measurements. *IEEE Transactions on Signal Processing*, 40(10):2594–2598, Oct 1992. ISSN 1053-587X. doi: 10.1109/78.157301.

S. J. Cooke, E. B. Thorstad, and S. G. Hinch. Activity and energetics of free-swimming fish: insights from electromyogram telemetry. *Fish and Fisheries*, 5(1):21–52, 2004. doi: 10.1111/j.1467-2960.2004.00136.x. URL https://onlinelibrary.wiley.com/doi/abs/10.1111/j.1467-2960.2004.00136.x.

S. J. Cooke, G. H. Niezgoda, K. C. Hanson, C. D. Suski, F. J. Phelan, R. Tinline, and D. P. Philipp. Use of CDMA Acoustic Telemetry to Document 3-D Positions of Fish: Relevance to the Design and Monitoring of Aquatic Protected Areas . *Marine Technology Society Journal*, 39(1):31–41, 2005.

S. J. Cooke, S. G. Hinch, M. C. Lucas, and M. Lutcavage. *Biotelemetry and Biologging*, chapter 18, pages 819–881. American Fisheries Society, 2012. ISBN 978-1-934874-29-5.

S. J. Cooke, J. W. Brownscombe, G. D. Raby, F. Broell, S. G. Hinch, T. D. Clark, and J. M. Semmens. Remote bioenergetics measurements in wild fish: Opportunities and challenges. *Comparative Biochemistry and Physiology Part A: Molecular & Integrative Physiology*, 202:23 – 37, 2016. ISSN 1095-6433. doi: https://doi.org/10.1016/j.cbpa.2016.03.022. URL http://www.sciencedirect.com/science/article/pii/S1095643316300769. Ecophysiology methods: refining the old, validating the new and developing for the future.

Z. D. Deng, M. A. Weiland, T. Fu, T. A. Seim, B. L. LaMarche, E. Y. Choi, T. J. Carlson, and M. B. Eppard. A Cabled Acoustic Telemetry System for Detecting and Tracking Juvenile Salmon: Part 2. Three-Dimensional Tracking and Passage Outcomes. *Sensors*, 11(6):5661–5676, 2011. ISSN 1424-8220. doi: 10.3390/s110605661.

M. Espinoza, T. J. Farrugia, D. M. Webber, F. Smith, and C. G. Lowe. Testing a new acoustic telemetry technique to quantify long-term, fine-scale movements of aquatic animals. *Fisheries Research*, 108(2):364 – 371, 2011. ISSN 0165-7836. doi: https://doi.org/10.1016/j.fishres.2011.01.011.

B. T. Fang. Simple solutions for hyperbolic and related position fixes. *IEEE Transactions on Aerospace and Electronic Systems*, 26(5):748–753, Sept 1990. ISSN 0018-9251.

FAO. *The State of World Fisheries and Aquaculture*. Food and Agricultural Organisation of the United Nations, 2020. ISBN 978-92-5-132692-3.

FAOSTAT. Food and Agricultural Organisation of the United Nations Statistics. http://www.fao.org/faostat/en/#data/, 2018. Accessed: 2020-09-20.

B. G. Ferguson. Doppler effect for sound emitted by a moving airborne source and received by acoustic sensors located above and below the sea surface. *The Journal of the Acoustical Society of America*, 94(6):3244–3247, 1993. doi: 10.1121/1.407230. URL https://doi.org/10.1121/1.407230.

M. Føre, J. A. Alfredsen, and A. Gronningsater. Development of two telemetry-based systems for monitoring the feeding behaviour of Atlantic salmon (Salmo salar L.) in aquaculture sea-cages. *Computers and Electronics in Agriculture*, 76(2):240 – 251, 2011. ISSN 0168-1699.

M. Føre, K. Frank, T. Dempster, J. Alfredsen, and E. Høy. Biomonitoring using tagged sentinel fish and acoustic telemetry in commercial salmon aquaculture: A feasibility study. *Aquacultural Engineering*, 78:163 – 172, 2017. ISSN 0144-8609. doi: https://doi.org/10.1016/j.aquaeng.2017.07.004. URL http://www.sciencedirect.com/science/article/pii/S0144860917300432.

M. Føre, K. Frank, T. Norton, E. Svendsen, J. A. Alfredsen, T. Dempster, H. Eguiraun, W. Watson, A. Stahl, L. M. Sunde, C. Schellewald, K. R. Skøien, M. O. Alver, and D. Berckmans. Precision fish farming: A new framework to improve production in aquaculture. *Biosystems Engineering*, 173:176 – 193, 2018. ISSN 1537-5110. doi: https://doi.org/10.1016/j.biosystemseng.2017.10.014. URL http://www.sciencedirect.com/science/article/pii/S1537511017304488.

J. Gabaldon, E. L. Turner, M. Johnson-Roberson, K. Barton, M. Johnson, E. J. Anderson, and K. A. Shorter. Integration, Calibration, and Experimental Verification of a Speed Sensor for Swimming Animals. *IEEE Sensors Journal*, 19(10): 3616–3625, May 2019. ISSN 1530-437X. doi: 10.1109/JSEN.2019.2895806.

T. M. Grothues. *A Review of Acoustic Telemetry Technology and a Perspective on its Diversification Relative to Coastal Tracking Arrays*, pages 77–90. Springer Netherlands, Dordrecht, 2009. ISBN 978-1-4020-9640-2. doi: 10.1007/978-1-4020-9640-2_5.

D. Halliday, R. Resnick, and J. Walker. *"Fundamentals of Physics"*. John Wiley & Sons, Ltd, 10 edition, 2013. ISBN 978-1-118-23072-5.

W. Hassan, M. Føre, M. O. Pedersen, and J. A. Alfredsen. A novel Doppler based speed measurement technique for individual free-ranging fish. In *2019 IEEE SENSORS*, pages 1–4, Oct 2019a. doi: 10.1109/SENSORS43011.2019.8956870.

W. Hassan, M. Føre, J. B. Ulvund, and J. A. Alfredsen. Internet of Fish: Integration of acoustic telemetry with LPWAN for efficient real-time monitoring of fish in marine farms. *Computers and Electronics in Agriculture*, 163:104850, 2019b. ISSN 0168-1699. doi: https://doi.org/10.1016/j.compag.2019.06.005. URL http://www.sciencedirect.com/science/article/pii/S0168169918314121.

E. E. Hockersmith and J. W. Beeman. *A History of Telemetry in Fishery Research*, chapter 2, pages 7–19. American Fisheries Society, 2012.

J. P. Hoolihan, J. Luo, F. J. Abascal, S. E. Campana, G. De Metrio, H. Dewar, M. L. Domeier, L. A. Howey, M. E. Lutcavage, M. K. Musyl, J. D. Neilson,

E. S. Orbesen, E. D. Prince, and J. R. Rooker. Evaluating post-release behaviour modification in large pelagic fish deployed with pop-up satellite archival tags. *ICES Journal of Marine Science*, 68(5):880–889, 03 2011. ISSN 1054-3139. doi: 10.1093/icesjms/fsr024. URL https://doi.org/10.1093/icesjms/fsr024.

J. M. Hovem. Underwater acoustics: Propagation, devices and systems. *Journal of Electroceramics*, 19(4):339–347, Dec 2007. ISSN 1573-8663. doi: 10.1007/s10832-007-9059-9. URL https://doi.org/10.1007/s10832-007-9059-9.

N. E. Hussey, S. T. Kessel, K. Aarestrup, S. J. Cooke, P. D. Cowley, A. T. Fisk, R. G. Harcourt, K. N. Holland, S. J. Iverson, J. F. Kocik, J. E. Mills Flemming, and F. G. Whoriskey. Aquatic animal telemetry: A panoramic window into the underwater world. *Science*, 348(6240), 2015. ISSN 0036-8075. doi: 10.1126/science.1255642.

M. Hvas and F. Oppedal. Sustained swimming capacity of Atlantic salmon. *Aquaculture Environment Interactions*, 9:361–369, 2017. doi: 10.3354/aei00239. URL https://www.int-res.com/abstracts/aei/v9/p361-369/.

M. Hvas, O. Folkedal, D. Solstorm, T. Vågseth, J. O. Fosse, L. C. Gansel, and F. Oppedal. Assessing swimming capacity and schooling behaviour in farmed Atlantic salmon Salmo salar with experimental push-cages. *Aquaculture*, 473:423 – 429, 2017. ISSN 0044-8486. doi: https://doi.org/10.1016/j.aquaculture.2017.03.013. URL http://www.sciencedirect.com/science/article/pii/S0044848616308699.

IBM. IBM LMIC Git repository. https://github.com/mcci-catena/ibm-lmic, 2018. Accessed: 2018-05-24.

Ø. Jensen, T. Dempster, E. B. Thorstad, I. Uglem, and A. Fredheim. Escapes of fishes from norwegian sea-cage aquaculture: causes, consequences and prevention. *Aquaculture Environment Interactions*, 1(1):71–83, 2009. ISSN 1869215X, 18697534. URL http://www.jstor.org/stable/24864019.

D. Johansson, F. Laursen, A. Fernö, J. E. Fosseidengen, P. Klebert, L. H. Stien, T. Vågseth, and F. Oppedal. The Interaction between Water Currents and Salmon Swimming Behaviour in Sea Cages. *PLOS ONE*, 9(5):1–4, 05 2014. doi: 10.1371/journal.pone.0097635. URL https://doi.org/10.1371/journal.pone.0097635.

K. E. Jónsdóttir, M. Hvas, J. A. Alfredsen, M. Føre, M. O. Alver, H. V. Bjelland, and F. Oppedal. Fish welfare based classification method of ocean current speeds at aquaculture sites. *Aquaculture Environment Interactions*, 11: 249–261, 2019. doi: 10.3354/aei00310. URL https://www.int-res.com/abstracts/aei/v11/p249-261/.

K. E. Jónsdóttir, Z. Volent, and J. A. Alfredsen. Current flow and dissolved oxygen in a full-scale stocked fish-cage with and without lice shielding skirts. *Applied Ocean Research*, 108:102509, 2021. ISSN 0141-1187. doi: https://doi.org/10.1016/j.apor.2020.102509. URL https://www.sciencedirect.com/science/article/pii/S0141118720310683.

P. Klebert, Ø. Patursson, P. C. Endresen, P. Rundtop, J. Birkevold, and H. W. Rasmussen. Three-dimensional deformation of a large circular flexible sea cage in high currents: Field experiment and modeling. *Ocean Engineering*, 104:511 – 520, 2015. ISSN 0029-8018. doi: https://doi.org/10.1016/j.oceaneng.2015.04.045. URL http://www.sciencedirect.com/science/article/pii/S0029801815001262.

B. Koeck, J. Pastor, G. Saragoni, N. Dalias, J. Payrot, and P. Lenfant. Diel and seasonal movement pattern of the dusky grouper Epinephelus marginatus inside a marine reserve. *Marine Environmental Research*, 94:38 – 47, 2014. ISSN 0141-1136. doi: https://doi.org/10.1016/j.marenvres.2013.12.002.

R. Lhermitte and R. Serafin. Pulse-to-Pulse Coherent Doppler Sonar Signal Processing Techniques. *Journal of Atmospheric and Oceanic Technology*, 1(4):293 – 308, 1984. URL https://journals.ametsoc.org/view/journals/atot/1/4/1520-0426_1984_001_0293_ptpcds_2_0_co_2.xml.

R. A. Light. Mosquitto: server and client implementation of the MQTT protocol. *Journal of Open Source Software*, 2(13), May 2017. doi: doi:10.21105/joss.00265.

Y. Liu, J. Olaf Olaussen, and A. Skonhoft. Wild and farmed salmon in Norway—A review. *Marine Policy*, 35(3):413 – 418, 2011. ISSN 0308-597X. doi: https://doi.org/10.1016/j.marpol.2010.11.007. URL http://www.sciencedirect.com/science/article/pii/S0308597X10002125.

G. Macaulay, F. Warren-Myers, L. T. Barrett, F. Oppedal, M. Føre, and T. Dempster. Tag use to monitor fish behaviour in aquaculture: a review of benefits, problems and solutions. *Reviews in Aquaculture*, 13(3):1565–1582, 2021. doi: https://doi.org/10.1111/raq.12534. URL https://onlinelibrary.wiley.com/doi/abs/10.1111/raq.12534.

G. Niezgoda, M. Benfield, M. Sisak, and P. Anson. Tracking acoustic transmitters by code division multiple access (CDMA)-based telemetry. *Hydrobiologia*, 483: 275–286, 2002. URL https://doi.org/10.1023/A:1021368720967.

F. Oppedal, T. Dempster, and L. H. Stien. Environmental drivers of Atlantic salmon behaviour in sea-cages: A review. *Aquaculture*, 311(1):1 – 18, 2011. ISSN 0044-8486. doi: https://doi.org/10.1016/j.aquaculture.2010.11.020. URL http://www.sciencedirect.com/science/article/pii/S0044848610007933.

J. Pedersen. Hydroacoustic measurement of swimming speed of North Sea saithe in the field. *Journal of Fish Biology*, 58(4):1073–1085, 2001. doi: 10.1111/j.1095-8649.2001.tb00556.x. URL https://onlinelibrary.wiley.com/doi/abs/10.1111/j.1095-8649.2001.tb00556.x.

D. G. Pincock and S. V. Johnston. Acoustic Telemetry Overview. In *Telemetry Techniques: A User Guide for Fisheries Research*, pages 305–308. American Fisheries Society, Bethseda, Maryland, 2012. ISBN 978-1-934874-26-4.

T. Pinkiewicz, G. Purser, and R. Williams. A computer vision system to analyse the swimming behaviour of farmed fish in commercial aquaculture facilities: A case study using cage-held Atlantic salmon. *Aquacultural Engineering*, 45(1):20 – 27, 2011. ISSN 0144-8609. doi: https://doi.org/10.1016/j.aquaeng.2011.05.002. URL http://www.sciencedirect.com/science/article/pii/S014486091100029X.

U. Raza, P. Kulkarni, and M. Sooriyabandara. Low Power Wide Area Networks: An Overview. *IEEE Communications Surveys Tutorials*, 19(2):855–873, 2017. doi: 10.1109/COMST.2017.2652320.

A. J. Read. T - telemetry. In *Encyclopedia of Marine Mammals*, pages 1153 – 1156. Academic Press, London, second edition, 2009. ISBN 978-0-12-373553-9. doi: https://doi.org/10.1016/B978-0-12-373553-9.00265-0. URL http://www.sciencedirect.com/science/article/pii/B9780123735539002650.

M. Remen, F. Solstorm, S. Bui, K. Pascal, T. Vågseth, D. Solstorm, M. Hvas, and F. Oppedal. Critical swimming speed in groups of Atlantic salmon Salmo salar. *Aquaculture Environment Interactions*, 8:659–664, 2016. doi: 10.3354/aei00207. URL https://www.int-res.com/abstracts/aei/v8/p659-664/.

C. Rillahan, M. Chambers, W. H. Howell, and W. H. Watson. A self-contained system for observing and quantifying the behavior of Atlantic cod, Gadus

morhua, in an offshore aquaculture cage. *Aquaculture*, 293(1):49 – 56, 2009. ISSN 0044-8486. doi: https://doi.org/10.1016/j.aquaculture.2009.04.003. URL http://www.sciencedirect.com/science/article/pii/S0044848609003330.

P. Rundtop and K. Frank. Experimental evaluation of hydroacoustic instruments for ROV navigation along aquaculture net pens. *Aquacultural Engineering*, 74:143 – 156, 2016. ISSN 0144-8609. doi: https://doi.org/10.1016/j.aquaeng.2016.08.002. URL http://www.sciencedirect.com/science/article/pii/S0144860916300012.

C. Rutz and G. C. Hays. New frontiers in biologging science. *Biology Letters*, 5(3):289–292, 2009. doi: 10.1098/rsbl.2009.0089. URL https://royalsocietypublishing.org/doi/abs/10.1098/rsbl.2009.0089.

D. Schoeppler, H.-U. Schnitzler, and A. Denzinger. Precise Doppler shift compensation in the hipposiderid bat, *Hipposideros armiger*. *Scientific Reports*, 8 (4598), 2018. doi: https://doi.org/10.1038/s41598-018-22880-y.

O. T. Skilbrei, J. C. Holst, L. Asplin, and M. Holm. Vertical movements of "escaped" farmed Atlantic salmon (Salmo salar L.)—a simulation study in a western Norwegian fjord. *ICES Journal of Marine Science*, 66(2):278–288, 2009. doi: 10.1093/icesjms/fsn213.

E. Soliveres, P. Poveda, V. Estruch, I. Pérez-Arjona, V. Puig, P. Ordóñez, J. Ramis, and V. Espinosa. Monitoring fish weight using pulse-echo waveform metrics. *Aquacultural Engineering*, 77:125 – 131, 2017. ISSN 0144-8609. doi: https://doi.org/10.1016/j.aquaeng.2017.04.002. URL http://www.sciencedirect.com/science/article/pii/S0144860916301224.

Stephen Riter. Underwater Acoustic Telemetry. In *Offshore Technology Conference*, pages 1–4, 1970. doi: https://doi.org/10.4043/1174-MS.

E. B. Thorstad, A. H. Rikardsen, A. Alp, and F. Økland. The Use of Electronic Tags in Fish Research – An Overview of Fish Telemetry Methods. *Turkish Journal of Fisheries and Aquatic Sciences*, 13(5):881–896, 2013. ISSN 1303-2712. doi: 10.4194/1303-2712-v13_5_13. URL http://www.trjfas.org/abstract.php?id=141.

S. Tilseth, T. Hansen, and D. Møller. Historical development of salmon culture. *Aquaculture*, 98(1):1 – 9, 1991. ISSN 0044-8486. doi: https://doi.org/10.1016/0044-8486(91)90367-G. URL http://www.sciencedirect.com/science/article/pii/004484869190367G. Interactions between Cultured and Wild Atlantic Salmon.

P. S. Trefethen. Sonic Equipment for Tracking Individual Fish. Special Scientific Report 179, U.S. Fish and Wildlife Service, June 1956.

H. A. Urke, T. Kristensen, J. V. Arnekleiv, T. O. Haugen, G. Kjærstad, S. O. Stefansson, L. O. E. Ebbesson, and T. O. Nilsen. Seawater tolerance and post-smolt migration of wild Atlantic salmon Salmo salar × brown trout S. trutta hybrid smolts. *Journal of Fish Biology*, 82(1):206–227, 2013.

D. M. Webber, R. G. Boutilier, S. R. Kerr, and M. J. Smale. Caudal differential pressure as a predictor of swimming speed of cod (Gadus morhua). *Journal of Experimental Biology*, 204(20):3561–3570, 10 2001. ISSN 0022-0949. doi: 10.1242/jeb.204.20.3561. URL https://doi.org/10.1242/jeb.204.20.3561.

M. A. Weiland, Z. D. Deng, T. A. Seim, B. L. LaMarche, E. Y. Choi, T. Fu, T. J. Carlson, A. I. Thronas, and M. B. Eppard. A Cabled Acoustic Telemetry System for Detecting and Tracking Juvenile Salmon: Part 1. Engineering Design and Instrumentation . *Sensors*, 11(6):5645–5660, 2011. ISSN 1424-8220.

R. Williams, T. Lambert, A. Kelsall, and T. Pauly. Detecting Marine Animals in Underwater Video: Let's Start with Salmon. In *AMCIS 2006 Proceedings*, number 191, 2006.

D. W. Wright, L. H. Stien, T. Dempster, and F. Oppedal. Differential effects of internal tagging depending on depth treatment in Atlantic salmon: a cautionary tale for aquatic animal tag use. *Current Zoology*, 65(6):665–673, 12 2018. ISSN 2396-9814. doi: 10.1093/cz/zoy093. URL https://doi.org/10.1093/cz/zoy093.